University of Nevada, Reno

Identification of a first in-class integrin enhancing small molecule for the treatment of Duchenne Muscular Dystrophy

A dissertation submitted in partial fulfillment of the requirements for the degree of
Doctor of Philosophy in Cell and Molecular Biology

By

Apurva Sarathy

Dr. Dean J. Burkin/Dissertation Advisor

December, 2015

THE GRADUATE SCHOOL

We recommend that the dissertation
prepared under our supervision by

APURVA SARATHY

Entitled

**Identification of a first in-class integrin enhancing small molecule
for the treatment of Duchenne Muscular Dystrophy**

be accepted in partial fulfillment of the
requirements for the degree of

DOCTOR OF PHILOSOPHY

Dean J. Burkin, Advisor

Patricia Berninsone, Committee Member

Maria Valencik, Committee Member

Josh Baker, Committee Member

Thomas Kidd, Graduate School Representative

David W. Zeh, Ph. D., Dean, Graduate School

December, 2015

ABSTRACT

Duchenne muscular dystrophy (DMD) is a catastrophic X-linked neuromuscular disease that affects 1 in every 5000 males. DMD is caused by mutations in the dystrophin gene which results in the loss of dystrophin protein, an essential link between the extracellular matrix and the actin cytoskeleton. This leads to weakened sarcolemmal integrity in the muscle fibers thereby making them susceptible to damage. There is currently no cure for DMD and limited treatment options exist for patients. The α7β1 integrin is an additional laminin-binding heterodimeric protein at the sarcolemma that is elevated in the skeletal muscle of DMD patients and the *mdx* mouse model. Previous pharmacological and transgenic mouse studies have demonstrated that the α7β1 integrin is a major modifier of disease progression in mouse as well as the Golden retriever dog models of muscular dystrophy. Therefore, we hypothesized that drugs that promote α7β1 integrin expression in muscle could be therapeutic in the treatment of DMD. Utilizing a high-throughput drug discovery chemical screen, we identified SU9516, an adenosine mimetic, as an enhancer of ITGA7 expression, the gene encoding integrin α7. We found SU9516 increased α7B integrin protein levels in C2C12 and immortalized human DMD myotubes. Preclinical studies with oral delivery of 5mg/kg/day SU9516 treatments in the *mdx* mouse model ameliorated the dystrophic pathology and improved muscle force and function at 10 weeks of age. This thesis presents the therapeutic benefits of a first in-class integrin enhancing small molecule therapeutic SU9516, for the treatment of DMD.

DEDICATION

To my parents Raghavan and Stanila Sarathy

To my brother Akhil Sarathy

my constants

ACKNOWLEDGEMENTS

I would like to thank my advisor Dr. Dean Burkin for providing me with the opportunity to work in the exciting field of therapeutics for muscular dystrophy. His guidance, encouragement and expertise in the field was invaluable towards my progress in the laboratory and for that I am extremely grateful. Thank you for being the best advisor a graduate student could ever ask for.

I would like to thank Dr. Ryan Wuebbles for being a wonderful mentor and colleague. His input and advice towards various aspects of my project were extremely beneficial.

I would like to thank members of my thesis committee Dr. Thomas Kidd, Dr. Maria Valencik, Dr. Patricia Berninsone and Dr. Josh Baker for agreeing to mentor me and participating in my thesis committee. I would like to specifically thank Dr. Ian Buxton and Dr. Heather Burkin for mentoring me during my first rotation as a graduate student in the Molecular Biosciences program. It was truly a wonderful and very enriching start to my career here at the University of Nevada Reno.

I would like to thank Dr. Dante Heredia, Dr. Grant Hennig and Dr. Thomas Gould for all their help with the phrenic nerve stimulation and neuromuscular kinetic experiments that were critical for the completion of my project.

I would like to thank the past and present members of the Burkin lab, who made coming in to work every day so enjoyable. There was never a dull moment in the lab thanks to my lab mates; Ryan Wuebbles, Pam Van Ry, Paul Brewer, Andreia Nunes,

Table of Contents

List of Figures

Chapter 1

Chapter 2

Chapter 3

Chapter 4.

List of Tables

CHAPTER 1

INTRODUCTION

DUCHENNE MUSCULAR DYSTROPHY AND PROMISING THERAPIES

TARGETING THE SARCOLEMMAL ADHESIVE COMPLEXES

INTRODUCTION: A BRIEF HISTORY OF DUCHENNE MUSCULAR DYSTROPHY

The association between skeletal muscle fibers and the components of the extracellular matrix (ECM) allows for maintenance of the skeletal muscle during daily activities. The loss of critical connections between the muscle fiber and the ECM results in many forms of muscular dystrophy and muscle-wasting disorders. One of the most common muscular dystrophies and the main focus of this thesis is a disease known as Duchenne Muscular Dystrophy (DMD). DMD was first described by a French neurologist Guillaume Benjamin Amand Duchenne. In 1986, researchers identified a gene on the X chromosome that when mutated leads to DMD. In 1987, the protein associated with this gene was identified and named *dystrophin*. Dystrophin is a large 427 kDa protein responsible for the critical link between the ECM-laminin and the intracellular actin cytoskeleton. In DMD, the loss of the dystrophin protein in muscle cells disrupts this critical link and causes fibers to become fragile and susceptible to damage. It has been almost 30 years since the discovery of the dystrophin gene; however, there is currently no effective cure for this fatal disease.

The research conducted in this study focuses on the idea that small molecules that can enhance proteins and/or protein complexes in the muscle fiber may act as surrogates for the missing dystrophin, thereby ameliorating the dystrophic pathology. Some protein complexes that perform a similar functional role to dystrophin and its associated proteins (i.e. the dystrophin glycoprotein (DGC) complex) are **the utrophin–glycoprotein complex (UGC) and the α7β1 integrin**. This work focuses specifically on the α7β1 integrin and its potential as a therapeutic target for the treatment of DMD.

THE ETIOLOGY AND PROGNOSIS OF DUCHENNE MUSCULAR DYSTROPHY

Duchenne Muscular Dystrophy (DMD) is an X-linked neuromuscular disease and one of the most common forms of muscular dystrophy with a prevalence of one in every 3500 male births[1]. DMD is a progressive muscle wasting disorder in which the muscle regeneration program is overcome by the high level of muscle degeneration which is accompanied by an infiltration of collagen and adipose deposits. DMD patients suffer from progressive muscle weakness, impaired mobility and premature death[2]. DMD is caused by reading frame mutations in the large *Dmd* gene (locus Xp21.2) which prevent the normal expression of the dystrophin protein[3–5]. 65% of *Dmd* mutations are intragenic deletions, 6–10% are intragenic duplications and 30–35% are point mutations[6]. Becker Muscular Dystrophy (BMD) is the milder version of DMD, usually caused by in-frame mutations which leads to a shorter, but functional dystrophin protein[7]. Children affected with DMD are clinically normal at birth and diagnosed at an average age of five years, but several motor deficits, such as difficulty sitting, transitioning from a supine to standing position, climbing and walking, as well as deficits in cognitive development display much earlier[8,9]. Untreated children eventually become constrained to the wheelchair in their teenage years. At 18 years of age or so, most DMD patients experience severe respiratory, orthopedic, and cardiac complications and require ventilation support at night[10,11]. DMD patients usually die in their third decade of life from cardiac and respiratory complications [10].

There is no cure for DMD. One of the major impediments in developing therapeutics is the inability to target all muscles in the human body, especially, the

cardiac and respiratory muscles for all patients. Symptoms of the disease can be managed utilizing a multidisciplinary care approach that includes the use of corticosteroids as well as appropriate respiratory, cardiac, orthopedic and rehabilitative interventions that addresses the more severe complications of the disease [8,10]. Corticosteroids attenuate the progression of muscle weakness and delay some of the complications, but do not treat or correct the underlying causes of DMD [8]. Additionally, the continued use of corticosteroids leads to significant detrimental side effects such as weight gain, osteoporosis, stunted growth and delayed puberty. Hence, the rapid advancement of clinical research for other DMD therapeutics is warranted.

1.3 COMMON ANIMAL MODELS OF DUCHENNE MUSCULAR DYSTROPHY

Researchers across the globe have utilized various animal models to study DMD. The most common animal model used to study therapeutics for DMD is the *mdx* mouse owing to its low cost and easy accessibility. The *mdx* mouse, has a nonsense mutation in exon 23 of the *Dmd* gene that leads to complete loss of the dystrophin protein [12, 13]. The *mdx* mouse model of DMD is not considered an ideal model for understanding the pathogenesis of DMD owing to significant differences in physiology from humans and display of milder phenotypes compared to DMD patients. The diaphragm muscle of the *mdx* mouse however, exhibits a pattern of degeneration, fibrosis and severe functional deficit comparable to that of human DMD limb muscle[14] and is often the muscle of choice to evaluate the functional and histopathological characteristics of disease progression and translate basic research findings into preclinical studies within the laboratory. Four additional strains, *mdx*[2cv–5cv] were generated with chemical

mutagenesis, utilizing N-ethylnitrosourea, that resulted in point mutations which lead to loss of full-length dystrophin isoforms [15]. In *mdx*[3cv] mice, a point mutation in intron 65 caused aberrant splicing thereby abolishing dystrophin expression [16] while in *mdx*[4cv] mice, a nonsense point mutation in exon 53 led to premature termination of dystrophin translation [17]. In the *mdx*[5cv] mice, a mutation in exon 10 selectively disrupted expression of dystrophin [17]. Among all the generated strains, the *mdx*[4cv] and *mdx*[5cv] strains displayed a 10-fold lower level of dystrophin-containing revertant fibers compared to the *mdx* mutant, making them well suited as animal models for preclinical testing of DMD therapies [18]. Additionally, recent studies have shown that the *mdx*[5cv] mouse strain exhibited more severe pathology, as well as muscle function deficits compared to the *mdx* mutant strains [19,20].

The canine X-linked model of muscular dystrophy is considered valuable for testing the efficacy and scalability of therapeutics. The Golden Retriever Muscular Dystrophy dog (GRMD) was the first and currently, the most widely used canine model for DMD. In the GRMD dog, a point mutation was found in intron 6 of the dystrophin gene [21] generating a single base pair change in the 3′ consensus splice site of intron 6, resulting in the skipping of exon 7 during mRNA processing and an out-of-frame transcript with a stop codon. The resulting transcript predicts termination of the dystrophin reading frame within its N-terminal domain in exon 8[21,22]. The GRMD is considered a more appropriate animal model for evaluating promising therapeutics because it closely mimics the human disease pathophysiology[23] exhibiting features such as increased sarcolemmal fragility, muscle force deficits, larger force decrement with eccentric contractions, alterations in pelvic and limb joint angles owing to muscle

hypertrophy and atrophy, infiltration of fibrotic tissue in the muscle, loss of ambulation and premature death [22,24–31]. The lifespan of the affected dogs is usually 3 years which is an ~75% reduction in lifespan [32] in contrast to the *mdx* mouse model in which the lifespan is reduced by 25% [33,34]. In addition, treatment of GRMD dogs with corticosteroids such as prednisone, which prolonged ambulation in human DMD patients [35], yielded improvement in muscle outcome measures in the GRMD dogs [36]. Thus, GRMD dogs are generally thought to be a very good model that mirror the severe progression of DMD pathophysiology in human patients and therefore potentially more appropriate for testing DMD therapies.

Another animal model currently being explored especially for screening large chemical and drug libraries is the *sapje* zebrafish model of DMD. The sapje locus was identified as *dmd*, the zebrafish orthologue of the human DMD gene and mutations at the sapje locus abolish the dystrophin orthologue in zebrafish [37, 38]. Sapje zebrafish mutants have a recessive, lethal, nonsense mutation that results in a premature stop codon in the dystrophin gene (on chromosome 1). The resulting phenotype is the embryonic-onset, progressive degeneration of skeletal muscle in the sapje homozygous zebrafish. Embryonically, the mechanism of degeneration occurs due to the detachment of somitic myofibers from the myosepta, the tendon-like sheets of ECM. In the zebrafish larvae, this muscle fiber detachment is visible at the myotendinous junctions and is accompanied by extensive degeneration, fibrosis, inflammatory responses and activation of muscle fiber regeneration, reminiscent of the severe pathological phenotype observed in human DMD [39]. This makes the zebrafish animal model a powerful tool that can be used to assess the effect of therapeutics for DMD. There are several benefits of using zebrafish

for highthroughput whole-organism screening of chemical libraries. Firstly, the mutant zebrafish progeny are easy to obtain in large numbers and can be easily treated with different chemicals in multi-well plates to determine if disease progression can be attenuated.

Secondly, chemical compounds can bind to proteins and generate non-heritable phenotypic changes in the zebrafish. Additionally, the transparency of the zebrafish larvae allows its usability in muscle development studies. A commonly used structural assay to characterize skeletal muscle defects in zebrafish is the birefringence assay. Birefringence is a physical property in which light rotates as it passes through organized matter, such as muscle sarcomeres in the zebrafish [40]. Wild-type zebrafish with highly ordered myofibers appear very bright when visualized between two polarized light filters, whereas zebrafish modeling muscular dystrophies like the *sapje* mutants exhibit degenerative dark patches in skeletal muscle under polarized light and an overall reduction in birefringence, reflecting the disorganization of sarcomeres. Recently, a drug called Ataluren which is currently in clinical trials for DMD was shown to improve muscle function significantly after two days of treatment in the *sapje* zebrafish [41], thereby corroborating the positive effects of the drug seen in human patients. Hence, in the near future, the zebrafish animal model has the potential to become a more widespread tool for the development of therapeutics for DMD.

LAMININS IN SKELETAL MUSCLE

Laminins are a family of large (400-900 kDa) heterotrimeric, multidomain, extracellular matrix glycoproteins composed of α-, β-, and γ-chains. These large proteins are localized to basement membranes underlying epithelial cells, nerve cells and muscle fibers. Laminin is a major constituent of the basal lamina together with type IV collagen. Currently, it is known that five α-, β-, γ-chains give rise to 16 different protein isoform combinations that vary in tissue distribution [42]. These isoforms are not only crucial for cell extracellular matrix integrity but also play roles in epithelial proliferation, adhesion, migration, differentiation and survival [43]. While laminin α1 and α5 chains are crucial for early embryonic development and organogenesis, postnatal development relies on the laminin α2, α3, and α4 chains [44]. Laminin-211 (previously called merosin) is the predominant laminin isoform in the basement membrane of adult skeletal muscle [45,46] along with Laminin-221 the primary laminin found in neuromuscular and myotendinous junctions [47]. In skeletal muscle, Laminin-211 has two major receptors namely αdystroglycan which is a major component of the dystrophin glycoprotein complex (DGC), and the integrin α7β1 which is a heterodimeric transmembrane protein. Laminin-211 also directly interacts with other components of the extracellular matrix such as agrin, nidogen and perlecan and interacts indirectly with type IV collagen. All laminins are ligands to cell-surface receptors with most binding interactions occurring at the five laminin-type G domains (LG1–5) at the C-terminus of the laminin α chain [48,49]. However, mapping studies of the laminin α2 chain have identified LG1–3 as the domains responsible for laminin-211 interactions with integrin α7β1 [50]. Reports have shown that the coiled-coil domain of laminin α chains has an indirect effect on integrin binding,

wherein it is required to form a stable contact between LG1 and LG2-3, which are the domains that directly bind integrin[51,52]. Laminin-211 binding to α-dystroglycan is mediated through the domains LG1–3 and 4–5 [48,53]. The interactions of Laminin-211 with various proteins are depicted in Figure 1.

Laminin-111 is an isoform of laminin that is currently being investigated as a potential therapeutic for DMD. It is an embryonic isoform of laminin-211/221 and is found in the tissues of the placental, kidneys, ovaries, liver, testis and blood vessels [54]. Recently, it was shown that myoblast transplantation is more efficient in a laminin rich microenvironment [55]. Laminin-111 as a protein therapeutic injectable in *mdx* mice, showed improvements in pathological markers of disease progression such as creatine kinase and centrally located nuclei and also offered protection from exercise induced muscle damage [56]. It was observed that Laminin-111 therapy increased the levels of α7 integrin in the skeletal muscle of the *mdx* mice [56]. Additionally, it was also demonstrated that Laminin-111 coadjuvant therapy enhanced myoblast transplantation in the *mdx* mouse model of DMD [57]. The development of Laminin-111 as a therapeutic for DMD is currently in the pre-clinical stage.

THE DYSTROPHIN GLYCOPROTEIN COMPLEX

The human dystrophin gene is 2.4-Mb long and encodes a ~14-kb cDNA that comprises 79 exons [58]. The full-length protein contains four functional domains: 1: Nterminal 2: rod, 3: cysteine-rich and 4: C-terminal domains. Dystrophin associates transmembrane proteins such as dystroglycan, sarcoglycan and sarcospan as well as cytosolic proteins such as syntrophin, dystrobrevin and neuronal nitric oxide synthase

(nNOS) to assemble the dystrophin glycoprotein complex (DGC) at the sarcolemma of muscle fibers [59]. Together, the various components of the DGC form a structural link between the ECM and the intracellular cytoskeleton, in addition to serving a critical role in signal transduction. Dystrophin is a large 427 kDa protein that is a critical component of the DGC. At its N-terminal end as well as in the spectrin like repeats of its central rod domain, dystrophin binds to cytoskeletal, filamentous γ-actin, while the cysteine rich carboxyl-terminus domain of dystrophin interacts with the transmembrane protein βdystroglycan which helps localize dystrophin to the sarcolemma [60]. The β-dystroglycan forms a strong link with the α-dystroglycan. The highly glycosylated α-dystroglycan interacts with laminin α2, a major component of the of muscle fiber basement membrane. Together the dystrophin, dystroglycans and laminin-α2 comprise a transmembrane complex that directly links the actin cytoskeleton to the ECM [59]. The extreme end of the carboxyl-terminal dystrophin is α-helical in nature and interacts with syntrophins [61,62].

The α, ε, γ, δ sarcoglycans in the DGC are transmembrane glycoproteins proteins, that together form a distinct complex in the DGC. The sarcoglycan complex is known to form a tight association with dystroglycans, α-dystrobrevin, syntrophins, neuronal nitric oxide synthase (nNOS) and sarcospan [63–67]. The sarcoglycan complex, excluding γsarcoglycan, associates with α-dystroglycan [64] via an extracellular proteoglycan, biglycan [68]. The intracellular tail of β- and δ-sarcoglycan associates directly with the C-terminus of dystrophin [69] whereas the N-terminal region of α-dystrobrevin allows the association of sarcoglycans and dystrophin [65]. Through its numerous associations with various components of the DGC, the sarcoglycan complex is able to stabilize the DGC

structure at the sarcolemma. The glycosylation of specific sarcolemmal proteins is critical for proper muscle development and function. Dystroglycanopathies, which comprise over fifty percent of all known congenital muscular dystrophies (CMDs), occur due to the hypoglycosylation of α-DG [70].

α-Dystrobrevin shares significant homology with the cysteine-rich and carboxyl terminal domains of dystrophin but lacks the actin binding and rod domains [71]. Alternative splicing gives rise to three isoforms of α-dystrobrevin that assemble with other components of the skeletal muscle DGC. Dystrobrevin binds to the intermediate filament protein syncoilin, which links desmin to the DGC thereby maintaining mechanical strength and structural integrity required for muscle contractions [72]. The coiled coil motif of α-dystrobrevin interacts directly with dystrophin while an upstream syntrophin binding site allows α-dystrobrevin to interact with the syntrophins [73]. Syntrophin is a 58 kDa protein that interacts directly with the carboxyl-terminus of both full-length and truncated forms of dystrophin [74,75]. The dystrophin complex also associates with the GLGF motif bearing N-terminal of nNOS at the sarcolemma of muscle fibers [64]. nNOS is a downstream signaling mediator of α-dystrobrevin and has also been shown to bind to syntrophin [76]. nNOS synthesizes nitric oxide (NO) that is critical for the opposition of contractile forces in active muscle. Dystrophin also plays a critical role in signaling; it interacts with and localizes neuronal nitric oxide synthase (nNOS) to the DGC. nNOS is a protein that also directly interacts with syntrophin. nNOS regulates skeletal muscle blood flow according to its metabolic needs [77]. Loss of dystrophin in DMD is accompanied by a loss of nNOS at the sarcolemma which is believed to exacerbate the muscle fiber damage in DMD. Another important component

of the DGC is Sarcospan (SSPN), a quadruple transmembrane, 25kDa protein with both N- and C-termini on the cytosolic side, that is localized to cardiac and skeletal muscle sarcolemma. SSPN is capable of forming higher order oligomers [78,79] which contribute to the formation of a lattice network, as observed in structurally similar proteins. It has been proposed that the partial function of SSPN is to hold the components of the DGC in tight proximity [78]. The various components that assemble to form the DGC are depicted in the schematic in Figure 2.

Localization of dystrophin within the muscle cells is consistent with its role in linking myofibers to the ECM to aid in muscle contraction. Enrichment of dystrophin is observed around the sarcolemma at costameres [80,81], myotendinous junctions and neuromuscular junctions in healthy muscle. In DMD patients, despite the continued transcription and translation of the aforementioned proteins that comprise the DGC (at reduced levels) the absence of dystrophin leads not only to muscular dystrophy but also causes the destabilization of the entire DGC complex.

CURRENT THERAPEUTIC STRATEGIES FOR SARCOLEMMAL DYSTROPHIN REPLACEMENT

Exon skipping of the *Dmd* gene. Gene therapies seek to restore dystrophin to the sarcolemma. One modality of genetic therapy is utilizing antisense oligonucleotides (AONs) that facilitate exon skipping and splicing of the dystrophin pre-mRNA, in order that the dystrophin reading frame be restored. The result is the generation of a partially functional albeit truncated dystrophin protein as observed in BMD. This therapeutic

modality can address the majority of DMD mutations that are partial dystrophin gene out of frame mutations [82]. Recent trials in DMD patients have been conducted with two types of AON molecules; 2′O-methylribooligonucleoside-phoshophorothioate (Drisapersen) and phosphorodiamidate morpholino oligomers (PMOs/morpholinos) (Eteplirsen). Drisapersen is marketed by Glaxo-Smith-Kline/Prosensa [83] and Eteplirsen is marketed by Sarepta Therapeutics [84], respectively. Each AON targets exon skipping at exon 51, a *DMD* gene hot spot involved in approximately 13% of cases. Clinical trials with the aforementioned AONs showed production of variable amounts of dystrophin protein and hence this therapeutic strategy holds great promise. Several Phase2/3 trials with both compounds are currently underway with both Etilpersen and Drisapersen. Recently, a new class of AONs namely tricyclo-DNA that showed improved bio-distribution compared to Etilpersen and Drisapersen, targeting skeletal muscle, the heart and the brain [85]. Additionally, tcDNA targeted exon 23 and showed greater efficacy in restoring dystrophin expression than etilpersen and drisapersen. tcDNA AON was also successful in improving respiratory function, benefits the CNS and improved cognitive functions.

Approximately 15% of the DMD patient population present with nonsense mutations [86] that result from single nucleotide DNA polymorphisms that give rise to inframe stop codons UAA, UAG, or UGA codons in mRNA coding regions. These stop codons lead to premature termination of protein translation, with resultant truncated, nonfunctional dystrophin protein. An antibiotic Gentamicin was initially shown to suppress premature stop codons thereby allowing translational dystrophin read-through, increasing dystrophin expression in the *mdx* mouse, a study first verified *in vitro* in

cultured myotubes as well. Treated mice expressed dystrophin in muscle and had functional improvement [87]. Clinical trials with gentamicin treatment of DMD patients harboring stop codons have generated ambiguous results, with one study failing to demonstrate expression of the full-length dystrophin protein or any functional improvement [88] and others demonstrating increased dystrophin protein expression [89] up to 15% [90]. Owing to concerns regarding potential toxicity of higher dose or longer duration gentamicin regimens, a highthroughput chemical assay was designed to identify compounds with equal potency and minimal toxic profiles. This screen led to the identification of PTC124, currently known as Ataluren. Ataluren suppressed *DMD* gene nonsense mutations in *mdx* myogenic cell lines and systemic treatment of *mdx* mice with the drug led to dystrophin expression and functional improvement in mice [91]. These positive results paved the way for DMD trials with Ataluren, initiated with healthy volunteers participating in Phase 1 trials, who showed no toxicity and subsequently to Phase 2 trials in DMD patients. The results from the DMD trials have been inconclusive. While the initial Phase 2a study showed restoration of dystrophin expression in approximately one-third of the treated DMD patients, the report on the larger Phase 2b study showed minimal benefits in the 6 minute walk test (MWT) and did not include dystrophin protein expression data [92,93]. The downside of exon skipping strategies is that they cannot be applied to all DMD patients universally as they are mutation specific.

AAV mediated *Dmd* restoration: AAV delivery of AONs is a therapeutic strategy that stems from the promising results obtained from the aforementioned clinical trials that described the use of synthetic AONs to restore the dystrophin open reading

frame. A variety of vectors for *Dmd* gene delivery such as nonviral, retroviral, adenoviral, herpes simplex viral and AAV vectors have been used with the aim of introducing a functional dystrophin gene in skeletal muscle fibers of animal models. The candidate gene can be the full-length *Dmd* cDNA or a synthetic truncated gene. For AAV mediated restoration of dystrophin, there are currently two strategies progressing towards clinical trials; the first is AAV delivery of antisense oligonucleotides (AON) to facilitate exon-skipping of specific complementary pre-mRNA sequences in order that the dystrophin reading frame be restored [94–98]. A recent study showed that AAV8 mediated exon-skipping was applied intramuscularly in the forelimbs of a large cohort of dogs and the technique successfully restored moderate to high levels of dystrophin [99]. The second strategy is AAV-mediated mini-/micro-dystrophin expression cassettes that have been administered in the *mdx* mouse [100,101] and the GRMD dog model [102–104] where sustained dystrophin expression was reported in the skeletal muscle of these animal models. Microdystrophin genes are also termed miniature dystrophin genes because although they bear the major protein interaction domains of dystrophin, they are missing a large portion of the central rod and the C-terminal domain. A drawback of viral mediated therapy is the potential for immunologic rejection via T-cell mediated immune response either to the viral capsid antigens and/or dystrophin recognized as a neoantigen[24]. Adverse events can be countered with transient immunosuppression. Recently, a novel technique for the delivery of the full-length dystrophin utilizing a triple-AAV trans-splicing vector system was developed, which may result in better functional improvement[105]. Current work involving AAV therapeutics seeks to develop methods for systemic delivery, increase the production of virus titers, improve viral

transduction efficiency and reduce innate and acquired immune responses so as to allow for multiple dose delivery of the AAV-dystrophin [106].

Cell based therapies for dystrophin replacement: Cell transplantation therapy has the same goal as genetic approaches, cell based-therapies seek to restore dystrophin to the sarcolemma of muscle fibers. Satellite cell or myoblast transplantation proved to be futile owing to the low efficiency of dystrophin production in the muscle fibers of DMD patients and children did not show improvements in functional or clinical parameters [107]. Embryonic stem cell (ESC) derived progenitors have excellent self-renewal capacity and are a strong candidate for stem cell transplantation in dystrophic muscle. There is a lot of optimism surrounding the idea that ESCs provide a versatile source for the treatment of a variety of diseases. ESC-based therapy has many advantages, owing to ESCs being a more primitive cell type with a higher proliferative potential. The issue of immune rejection can be circumvented by utilizing patient specific ESCs induced from adult somatic cells. However, ethical, logistic and economic concerns surrounding ESC based transplantation require attention before any possible future clinical applications human ESCs.

Cell replacement therapies also address the loss of muscle mass associated with muscular dystrophies [108]. For clinical implementation, adult stem cells harvested from tissue of DMD patients could be genetically manipulated *ex vivo* and restored to the donor through intra-arterial delivery, thereby allowing the cells to distribute throughout the patient musculature. This technique can be used to treat patients who have experienced severe loss of body mass owing to muscular dystrophy. Induced pluripotent

stem cells (iPSCs) bear most of the characteristics of ESCs but are reprogrammed from adult somatic cells such as dermal fibroblasts, by the transient expression of a defined set of factors [109]. Unlike ESCs, iPSCs bypass the ethical issues that surround the use of embryos and allow for autologous production of the pluripotent cells. iPSCs could serve as a viable source of myogenic donors for muscle regeneration owing to their indefinite replicative capacity and their ability to differentiate into myoblast-like cells *in vitro*. iPSC myogenic progenitors can also be used for *in vitro* drug testing/screening and disease modeling for genetic muscular conditions. The field of human satellite cell (huSC) biology for muscle diseases is in a very incipient stage of development. Researchers are only just beginning to characterize the huSC transcriptome to identify factors that will allow *ex vivo* expansion and efficient engraftment of the cells prior to utilization in the clinic [110]. Based on current findings the most promising therapy would be a combinatorial approach to obtain the benefits of multiple therapeutics strategies combined into a unified approach for e. g. cellular therapy in conjunction with gene therapy or pharmacologic treatments.

UTROPHIN AND THE SKELETAL MUSCLE

Utrophin is the autosomal homolog of dystrophin. In the adult, dystrophin is expressed solely in the muscle and brain tissue however utrophin is expressed in various adult tissues. Utrophin is present in vascular smooth muscle and the endothelium with the highest levels of mRNA and protein expressed in lung and kidney tissue [111,112]. Mouse development studies have demonstrated that utrophin transcripts are first

detectable in the neural groove at embryonic day 8.5 which is an early stage of development [112]. As development progresses, utrophin expression becomes abundant in a subset of neural crest derived tissues such as peripheral nerve assembled in a complex with dystroglycan and other dystrophin-associated protein homologues [113]. Once skeletal muscle has attained adulthood, utrophin becomes localized at the neuromuscular and myotendinous junctions [114]. It is also normally expressed in the sarcolemma of developing and regenerating myofibers [114–116]. Dystrophin eventually replaces utrophin in the sarcolemma of maturing fibers but utrophin remains concentrated at the neuromuscular and myotendinous junctions in healthy muscle. Similar to dystrophin, utrophin has binding domains for both F-actin and β-dystroglycan [117,118]. Additionally, like dystrophin, utrophin has been shown to associate with a membrane-linked glycoprotein complex. The domain structure of utrophin is very similar to that of dystrophin which is why utrophin could function as the perfect surrogate for dystrophin in dystrophic muscle. Utrophin can via its COOH-terminal domain, bind to a membrane associated glycoprotein complex, similar to the complex that associates with dystrophin in healthy muscle [113]. Additionally, utrophin is capable of binding to actin via its NH2 terminus. Hence, utrophin can form a direct functional link between the actin cytoskeleton and via the dystrophin associated glycoprotein and laminin, the extracellular matrix [119]. Utrophin is physiologically upregulated in the skeletal muscle of DMD patients [120,121], the *mdx* mouse [122], and the GRMD [123,124] and German shorthaired pointer [125] canine models. The utrophin protein is found in extra junctional regions in dystrophic myofibers [116]. In muscle, there are two promoters A and B that regulate the expression of two fulllength transcripts of utrophin. Each transcript has unique 5′ exons,

and at exon 3 they splice into a single common RNA. Studies in *mdx* mice, have shown that post transcriptionally, A-utrophin is up-regulated in muscle fibers while B-utrophin localizes to endothelial cells [126]. Loss of both dystrophin and utrophin in the *mdx/utrn⁻ᐟ⁻* mice leads to more severe muscular dystrophy with animals dying prematurely by 20 weeks of age [76,127]. Alternatively, the exogenous expression of utrophin improved the dystrophic pathophysiology in *mdx* mice, indicating that utrophin has the ability to compensate for dystrophin when expressed at high levels [128]. Although utrophin and dystrophin are structurally homologous, they bind to F-actin through distinct sites [129,130] and only dystrophin contains nNOS binding sites [131]. It is thought that in DMD afflicted muscle ischemia occurs because nNOS is unable to anchor to the sarcolemmal membrane [131]. The utrophin glycoprotein complex (UGC) also differs from the DGC in the glycosylation of α-DG, which is important for the determination of the binding specificity of ECM ligands [132–135]. Nevertheless, utrophin is the functional and structural homolog of dystrophin and one of the top candidates for surrogate protein replacement therapy at the sarcolemma of dystrophic muscle.

CURRENT THERAPEUTIC STRATEGIES FOR UTROPHIN REPLACEMENT IN THE TREATMENT OF DMD

Functional and structural replacement of dystrophin at the sarcolemma with surrogates such as utrophin is a therapeutic modality that offers tremendous potential for DMD. There has been a lot of focus on utrophin (also known as dystrophin-related protein) because it is the structural and functional homolog of dystrophin[136] [136,137] and several studies have demonstrated that enhancing utrophin expression has therapeutic

benefit in the pathophysiology of DMD. Upregulation of utrophin, either genetically [128] or through treatment with the small molecule compound SMTC1100 [138] improved the pathophysiology in the *mdx* mouse. Several researchers are relentlessly pursuing the field of potent utrophin modulators for the treatment of DMD. High-throughput, cell-based screens were performed to identify potent drugs that upregulated utrophin [139]. Protein therapies that modulate utrophin expression include biglycan, an extracellular matrix protein that associates with the dystrophin-glycoprotein complex. Treatment of *mdx* mice with recombinant human biglycan, recruited utrophin to the sarcolemma and reduced histopathologic lesions and the extent of eccentric contraction decrement[140]. Recently, a protein therapeutic Galectin-1 when administered intraperitoneally into *mdx* mice showed improvement in function and alleviation of dystrophic pathology [141]. Galectin-1 is a small 14kDa, non-glycosylated protein encoded by a member of the Lectin family of genes, Galactoside-binding, soluble-1 (LGALS1) gene. Galectin-1 is found in the cell nuclei, cytoplasm and intracellular membranes and is known to be secreted in a number of cell types to the extracellular membrane and extracellular matrix [142–147]. Mice treated with recombinant mouse galectin-1 (rMsGal-1) exhibited reduced skeletal muscle pathology demonstrated by a reduction centrally located nuclei and Evans blue uptake. rMsGal-1 treatments resulted in elevated levels of the Utrophin glycoprotein Complex (UGC) [141].

Genetic introduction of micro-utrophin utilizing adenovirus-mediated delivery in *mdx/utr*^{-/-} mice and mini-utrophin GRMD dogs showed a significant amelioration of dystrophic phenotype in mice and reduced histopathologic lesions in GRMD dogs with sustained expression of utrophin for approximately 60 days [148,149]. Delivery of a fusion

protein called TAT-Utrophin circumvents the problems of immune rejection by the virus and the transgene behaving as a non-self-gene. Researchers have developed a fusion protein between utrophin and the Human Immunodeficiency virus (HIV) derived TAT sequence, which is used to transport molecules into cells, in order to facilitate utrophin replacement therapy in DMD. The TAT sequence signals for the internalization of utrophin in muscle cells. Once internalized, the utrophin can compensate the functional and structural absence of dystrophin thereby ameliorating the pathogenic effects of DMD[150].

Two therapies developed to upregulate the levels of utrophin in muscle are currently in or near Phase 1 clinical trials: SMTC1100/BMN195 (Summit plc) and biglycan (Trivorsan Pharmaceuticals). The chemical name of BMN195 is 5-(ethylsulfonyl)-2-(naphthalene-2yl) benzodoxazole. BMN195 was first identified in a screen for small molecules, which enhanced mRNA levels of utrophin by 25% in human myoblasts, increased utrophin protein levels by two-fold in DMD patient cells, and demonstrated efficacy in treatment of *mdx* mice [138]. In the *mdx* mouse, BMN195 reduced regeneration, inflammation, necrosis, serum CK levels, and fibrosis, improved functional calcium-dependent parameters and prevented eccentric contraction mediated muscle membrane damage in treated *mdx* mice [138]. BMN195/SMT C1100 was the first new chemical entity (NCE) with a design targeted at the utrophin-A promoter [151] which has progressed into clinical development. Although BMN195 was tolerated at all doses in a Phase 1 clinical trial conducted by BioMarin Pharmaceuticals, even at the highest doses, it did not achieve the plasma concentrations required to increase utrophin expression. Summit pharmaceuticals has since reformulated BMN195 to allow for better

absorption and the company has subsequently initiated Phase 1 clinical trials. SMT022357 was a second generation compound derived from the same family as SMTC1100 that showed significant improvements in the physicochemical properties and *in vivo* efficacy compared to its predecessor SMT C1100 [152].

Another protein that upregulates utrophin levels is biglycan; an extracellular protein that like utrophin is highly expressed in regenerating and developing muscle [153,154]. Injection of recombinant human biglycan protein improved muscle pathology in the *mdx* mouse and elevated the expression of utrophin and γ-SG at the cell membrane [155]. Furthermore, the inability of biglycan to alleviate the disease pathology in *mdx/utr*^{-/-} mice demonstrated that utrophin was a necessary component in order for biglycan therapies to have effect [155]. Biglycan is currently in Phase 1 clinical trials conducted by Trivorsan Pharmaceuticals. The aforementioned studies describe the therapeutic potential of utrophin upregulation as a disease modifying therapeutic strategy that can be applied universally to all DMD patients irrespective of their dystrophin mutation.

α7β1 INTEGRIN IN THE SKELETAL MUSCLE

Integrins are αβ heterodimeric transmembrane proteins that are critical to a variety of cellular processes such as adhesion, migration and differentiation [156]. The β1 subunit is the most common subunit for the majority of integrins that participate in cell-extracellular matrix adhesion. While both the α and β subunits can contribute to ligand binding, it is the α chain that mediates the specificity of the ligand interaction and the β subunit regulates cell signaling and integrin activation. Integrins can mediate both

"inside out" and "outside in" signaling [157,158]. Initiation of inside out signaling occurs within the cell. "Inside out" signals are necessary in order for integrins to switch between conformational states and become active[156]. Integrin activation specifically requires the binding of the cytoskeletal protein talin to the cytoplasmic domain of the β-subunit. This binding results in a conformational change which allows ligands in the extracellular domain to bind to the integrin complex [159]. This signaling event allows cells to interact with components of the extracellular matrix (ECM) and is capable of affecting ECM organization and assembly [43]. Outside-in cell signaling is downstream of integrin activation wherein signals are transduced from the outside of the cell to the intracellular compartments [160]. The apparent lack of enzymatic activity in the cytoplasmic domains of integrins enables the formation of distinct macromolecular complexes following the recruitment of different sets of proteins [160,161]. Upon binding, a conformational change in the integrin regulates interactions between the integrin cytoplasmic domain and cytosolic proteins and/or the cell cytoskeleton [156,159].

Integrins have a long extracellular domain, a single transmembrane domain and a relatively short cytoplasmic domain both of which bind to extracellular ligands. The α7 subunit has two alternatively spliced cytoplasmic domain variants namely α7A and α7B that are present in murine and human adult skeletal muscle, where they associate with the β1D subunit, an integrin β1 splice form [162]. α7β1 integrin is one of the major cell surface transmembrane receptors that links laminin-211 in the extracellular matrix to the intracellular cytoskeleton [163,164] (Figure 3). It is the predominant laminin receptor in skeletal, cardiac and smooth muscle fibers [165]. In skeletal muscle it is localized at the

neuromuscular junctions and the myotendinous junctions [166,167] as well as at the sarcolemma [168]. Additionally, in skeletal muscle cell lines, there is an increase in α7 integrin expression during myogenic differentiation [163]. Intracellularly, integrins bind to F-actin through a protein complex that includes the integrin-linked kinase (ILK), PINCH and α/β-parvin [169-171]. The ILK, PINCH and parvin protein complex is known to facilitate cell signaling through the Akt/PKB, GSK3β/β-catenin, JNK, and α-Pix/Rac1 pathways apoptotic and pro-autophagic signals such as FoxO, Bad and Bax[174]. Integrin α7β1 can also activate the Ras pathway resulting in upregulation of the pro-survival, proto-oncogene Bcl-2 expression[175]. Hence integrin α7β1 plays a critical role in mediating several signaling events.

In human and mouse tissues there exist two cytoplasmic and two extracellular splice variants of the α7 integrin subunits[176–178], the expression of which is regulated during development. While the cytoplasmic variant α7B is expressed in cardiac, smooth and in both embryonic and adult skeletal muscle, the α7A variant is expressed only in mature skeletal muscle fibers and not in cardiac muscle [179]. The extracellular variants of α7 integrin are α7X1 and α7X2, which result from the alternative splicing of exons that encode a region located in the β-propeller domain of α7 between the homology repeats III and IV[180]. This region represents a portion of the putative ligand binding site. While the α7X1 and α7X2 splice variants are expressed in equal amounts during early development in mouse skeletal myoblasts and adult heart, in adult skeletal muscle, the

α7X2 splice variant is predominant [176,177]. The α7X1 integrin is vital to muscle development and repair, whereas the α7X2 isoform is responsible for anchoring mature muscle to the ECM [181,182]. Both splice variants bind to laminin-1- and laminin-2-coated surfaces when expressed in HEK293 cells; however, α7X1B promoted cell migration only on laminin-2, and α7X2B stimulated motility on both substrates [183]. Further, the cell-specific environment has a critical impact on binding [180,183].

Like the α7 integrin chain, the β1 integrin subunit also has several cytoplasmic domain isoforms that arise from alternative RNA splicing events [161,184,185]. In early stages of muscle development, β1A integrin is the predominant isoform in myoblasts, whereas in adult muscle fibers β1D is the major form and mediates a stronger interaction with laminin[186, 187]. β1 integrin plays a vital role in regulating cell–extracellular matrix interactions during embryonic development and this is corroborated by the fact that β1 integrin deletion is embryonic lethal in mice [188,189]. The β1 subunit is the only integrin β chain that forms functional heterodimers with α7 integrin chains [157,162,163]. Under normal circumstances, both subunits of the integrin heterodimer are synthesized in the endoplasmic reticulum (ER) and later transported to the cell membrane after post-translational modifications in the Golgi[190–193]. However, when one subunit is in excess of the other, the extra subunits are retained in a premature form in the ER until the opportunity to dimerize with other subunits arises [190,192]. Therefore, the stoichiometry of the α and β subunits is important for the formation of integrin receptors on the cell surface in the right amounts.

α7β1 INTEGRIN IS A MAJOR MODIFIER OF DISEASE PROGRESSION IN DMD

The α7β1 integrin is a laminin receptor in skeletal muscle that serves to link laminin-211/221 in the basal lamina to the actin cytoskeleton of muscle fibers [165]. The α7β1 integrin has structural and signaling functions that contribute to muscle development and physiology and was originally identified as a marker for muscle differentiation [163][177]. Although normally concentrated at the myotendinous junction in postnatal muscle, α7 integrin is upregulated throughout the sarcolemma in DMD and the *mdx* mouse [194]. Studies have shown that enhanced transgenic expression of the α7 integrin in skeletal and cardiac muscle can ameliorate dystrophic pathology and extend the lifespan of *mdx/utr$^{-/-}$* mice more than three-fold [195]. Multiple mechanisms appear to contribute to α7 integrin mediated rescue of dystrophin deficient muscle including maintenance of myotendinous and neuromuscular junctions, enhanced muscle hypertrophy and regeneration, and decreased apoptosis and cardiomyopathy[196]. Enhanced α7 integrin also protects muscles against exercise-induced damage [197]. Conversely loss of the α7 integrin in *mdx* mice resulted in more severe muscle disease where *mdx/α7$^{-/-}$* mice experienced an early onset death between 2-4 weeks of age [198]. Additionally, the *mdx/α7$^{-/-}$* mice had a significant decrease in laminin-α2 which was one of the factors that exacerbated the pathology in the double knockout mice [198]. Recently, it was demonstrated that the AAV mediated overexpression of human α7 in *mdx* as well as *mdx/utr$^{-/-}$* mice led to histological and functional improvements as well as increased

survival in the dystrophic mice [199,200]. Recent evidence suggests that prednisone, the current front line treatment for DMD, may maintain muscle function by stabilizing the α7 integrin protein levels [201].

While transgenic overexpression and viral mediated delivery of α7 integrin rescued disease pathology in *mdx* mice, increasing the amount of the β1D chain by virus-mediated infection, protected the muscle fibers from developing membrane damage[202]. Additionally, the simultaneous enhancement of α7 and β1D chain levels provided even better protection to the *mdx* mice [202]. Hence developing a therapeutic that targets the level of both the α7 and β1 subunit of integrin would be optimally effective for the treatment of DMD. A schematic that proposes the mechanism by which integrin enhancement therapies may be beneficial for treating DMD is depicted in Figure 4. Together, these observations support the idea that the α7β1 integrin is a major disease modifier in DMD.

POTENTIAL THERAPIES THAT TARGET α7β1 INTEGRIN AS A SURROGATE REPLACEMENT PROTEIN IN DMD.

Although transgenic studies and AAV mediated delivery of ITGA7 have demonstrated the therapeutic benefit of enhancing integrin as a surrogate for dystrophin at the sarcolemma of myofibers in *mdx* and *mdx/utr*^{-/-} mice, there are currently no effective pharmacological small molecule therapeutics being developed that enhance the expression of the heterodimeric adhesive integrin protein complex at the sarcolemma. Recently, two protein therapeutics namely Laminin-111 and Galectin-1 when administered intraperitoneally into *mdx* mice showed improvement in function and

alleviation of dystrophic pathology [56,141]. Laminin-111 is the embryonic form of adult skeletal muscle laminin-211/221 and can be found in placenta, kidney, liver, testis ovaries and blood vessels [203]. Purified EHS laminin-111 can now be purchased commercially. Intramuscular injections with the readily available purified EHS laminin-111 into *mdx* muscle provided proof of principle that laminin-111 can be delivered throughout the treated muscle and can reestablish muscle repair and regeneration [57]. Systemic Laminin-111 treatments in *mdx* mice led to elevated levels of the α7β1 integrin complex at the sarcolemma of muscle fibers [56]. From a clinical trials perspective, delivering a protein like Laminin-111 for therapy could prove difficult owing to the fact that it is a large heterotrimeric protein (900kDa) that is glycosylated. Recently, recombinant mouse Galectin-1 (rMSGal-1) administered systemically to *mdx* mice showed significant improvements in the function and pathophysiology of the dystrophic mice and this was accompanied by elevated levels of the α7β1 integrin at the sarcolemma[141]. Galectin-1 being a much smaller protein than Laminin-111 could be a better candidate for protein delivery targeted at the α7β1 integrin. However, two disadvantages of protein therapeutics are 1. A possible immune response developed by the patients to the therapeutic and 2. Off-target effects of protein therapeutics may prove detrimental to the well-being of the patients in the long term. Hence, development of a targeted small molecule therapeutic that specifically elevates the α7β1 integrin complex at the sarcolemma of dystrophic myofibers could circumvent the problems associated with a viral mediated delivery or a protein therapeutic. This dissertation will discuss the identification of a first in-class α7β1 integrin enhancing compound for the treatment of DMD. Several functional differences exist between the three afore-discussed adhesion

complexes at the sarcolemma namely the DGC, the UGC and the α7β1 integrin. The

extent to which therapeutics that target the UGC and integrin, can fully replace the lost

DGC function in DMD and ameliorate pathology is a question that remains unanswered.

α7 INTEGRIN ENHANCING SMALL MOLECULE DRUG SCREEN

To translate transgenic mouse studies into potential therapies for DMD, we initiated a

drug discovery program to identify chemical probes that increase α7 integrin in skeletal

muscle. We have previously reported on the generation and characterization of an α7

integrin knockout line of mice[204] in which the LacZ gene is inserted into exon 1,

downstream of the endogenous α7 integrin promoter. Thus, β-galactosidase functions as

a reporter for α7 integrin expression in these animals. Primary myogenic cells were

isolated from a heterozygous mouse (α7βgal$^{+/-}$) so that the cells express α7 integrin and

also report for transcription of the integrin. The second *Itga7* gene allele had exon 1

replaced by the LacZ gene, providing a reporter for α7 integrin transcription and

maintaining the endogenous promoter, enhancer, and chromatin environment.

Undifferentiated α7$^{+/lacZ}$ myoblasts and differentiated myotubes were used to screen

compounds (48 hour treatment) and β-Galactosidase enzymatic activity was measured

using the Fluorescein di-β-Dgalactopyranoside (FDG) assay. FDG is an extremely

sensitive fluorogenic substrate that can be used for detecting the activity of β-

Galactosidase that cleaves non-fluorescent FDG to produce the fluorescent molecule

fluorescein. The identification of a first in-class α7β1 integrin enhancing drug, which is

the focus of this dissertation, provides further support for the utilization of this chemical

screen to identify promising integrin enhancing compounds with the potential to make it to clinical trials for DMD. The myogenic reporter cells were designated α7βgal$^{+/-}$ and were used to identify two molecules, valproic acid and laminin-111, in preliminary screens and have been successfully tested in mouse models of DMD[198,205].

To identify additional small molecules that increase α7 integrin in skeletal muscle, we used our muscle cell-based assay to screen 403,000 compounds, including FDA approved drugs and the large compound libraries at the National Chemical and Genomics Center (NCGC) now part of the National Institutes for Advancing Translational Sciences or NCATS. The four compound libraries that were screened using our muscle cell based assay were 1) Prestwick Chemical and Microsource Spectrum Libraries (BioFocus DPI, Leiden Netherlands with facilities in UK, Basel, Heidelberg) (Overington et al., 2006). 2) DIVERSet library (Chembridge Corp., San Diego, CA) and compounds from the ChemDiv library. 3) LOPAC library (Sigma-RPI) consists of 1280 pharmaceutically active compounds. 4) MLSMR-Molecular Libraries Small Molecule Repository (2011). We have identified several compounds that increase the α7 integrin with known mechanisms of action including iron chelators, microtubule inhibitors, cell cycle inhibitors and steroid-like molecules. Additionally, several small molecules with unknown biological activities were identified. Overall, our results identified novel small molecules that increase the α7 integrin in cultured muscle cells and may serve as molecular probes to further dissect signaling pathways that regulate the α7β1 integrin in skeletal muscle. These small molecules could potentially be developed as novel therapeutics in the treatment of Duchenne and other fatal muscular dystrophies.

One of the molecules identified as a potent inhibitor of α7 integrin through the chemical drug screen was a compound called SU9516. SU9516 is a three-substituted indolinone compound and was identified in a screen for cyclin dependent kinase 2 (cdk2) inhibitors, with the goal of developing a potential anti-cancer therapeutic [206]. SU9516 was identified as an extremely potent and highly selective inhibitor of cdk2 in RKO, SW80 and other colon carcinoma cell lines and was shown to potently induce apoptosis in association with pRb (tumor suppressor gene) dephosphorylation and cell cycle arrest in G_1 or G_2M [207]. Additionally it has been shown that SU9516 triggers cell death in human leukemia cells (e.g., U937, HL-60, and Jurkat) through 1) the potent induction of mitochondrial oxidative injury (i.e., cytochrome *c* release and Bax translocation), 2) the inhibition of phosphorylation on serine 2 of the carboxyl-terminal domain (CTD) of RNA Pol II, and 3) the pronounced down-regulation of Myeloid cell leukemia -1 (Mcl-1), an anti-apoptotic protein, through transcriptional repression combined with proteasomal degradation[208]. Thus, previous literature has identified SU9516 as an anti-neoplastic agent that can potentially be used in combination chemotherapy with other anti-cancer agents such as 5-fluorouracil (5-FU) [209]. This dissertation seeks to describe the development of SU9516 as a potential therapeutic for DMD that targets the α7β1 integrin heterodimer complex at the sarcolemma of dystrophic muscle fibers.

SUMMARY

The main hypothesis of this dissertation is that the development of an α7β1 integrin enhancing small molecule will be an important stride in the field of therapeutics for Duchenne Muscular Dystrophy. The data presented in this dissertation reinforces the

potential of α7β1 integrin as a therapeutic target for drug development in DMD. The results obtained from the investigation of a novel α7β1 integrin enhancing compound show that this group of therapeutics has the potential to improve the quality of life of patients suffering from DMD. The focus of this dissertation is the α7β1 integrin complex in skeletal muscle and the data generated from the studies presented in this dissertation corroborate the fact that α7β1 integrin is a major modifier of disease progression in DMD.

There are currently no definitive therapies available for DMD patients and the corticosteroids, prednisone and deflazacort are the only treatments available with limited positive effect [210–214]. Chapter 2 focuses on prednisone the current front line therapeutic for Duchenne muscular dystrophy. Using muscle cells cultured from mice or human DMD patients, it was shown that prednisone acts to increase protein levels of α7 integrin in a dose-dependent manner. Additionally, prednisone treatment in the well-established *mdx* mouse model of DMD and the GRMD canine model increased protein levels of α7β1 integrin, as well as those of laminin-α2, which is a critical component of the basement membrane. Finally it was demonstrated that GRMD dogs that had not been treated with prednisone exhibited reduced levels of laminin-α2 and α7 integrin proteins. This study showed that Prednisone acts in part to increase laminin-211/221 (composed of α2, β1 and γ1 chains) in the muscle basal lamina to stabilize protein levels of α7β1 integrin in skeletal muscle cells. These changes would lead to improvements in muscle fiber integrity in dystrophin-deficient muscle to slow the disease process. The results also suggest a shared mechanism for disease progression in GRMD dogs and humans,

reinforcing the view that the canine model provides a useful tool for studies of the human disease.

Our findings from the prednisone study and other studies suggested that targeting the α7 integrin could be a therapeutic strategy for DMD. This led us to translate this finding into a therapeutic approach for DMD. In order to do so, we initiated a program to identify small molecules that increase α7 integrin in skeletal muscle. Using myogenic cells from mice in which the LacZ reporter gene was inserted into exon 1 of the mouse α7 integrin gene, we screened 403,000 compounds and identified more than 1500 hits that increased the β-galactosidase reporter. Further evaluation identified 6 compounds that increased α7 integrin at least 1.5-fold in myotubes. Compounds were classified as iron chelating compounds, cell cycle inhibitors and compounds with undefined function. Compounds identified from this screen represent novel molecular probes that can be used to further elucidate regulation of α7β1 integrin expression and signaling in skeletal muscle and may serve as potential therapeutics for the treatment of DMD. One of the top compounds identified from this chemical drug screen is a molecule called SU9516.

Chapter 3 discusses the discovery of a novel α7 integrin enhancing drug called SU9516 for the treatment of DMD. The chemical name for SU9516 is (*Z*)-1,3-Dihydro-3(1*H*-imidazol-4-ylmethylene)-5-methoxy-2*H*-indol-2-one. The molecular structure is depicted in Figure 5. Although there is a vast amount of literature that suggests that developing pharmacological therapies targeted at the α7β1 integrin complex could be promising for the treatment of DMD, there is no effective drug being developed towards that end. This chapter discusses the identification, *in vitro* and *in vivo* on-target activity of a novel small molecule α7β1 integrin enhancing compound called SU9516 for the

treatment of DMD. In this translational study, it was demonstrated that SU9516 increases the levels of α7B in mice as well as human DMD patient myogenic cell lines. Pre-clinical trials were undertaken in the *mdx* mouse model of DMD, where mice were treated via oral gavage with a dose of 5 mg/kg/day, from 3 weeks to 4 weeks of age. The drug elevated the levels of α7B and β1D at the sarcolemma of *mdx* myofibers. These increases in α7β1 integrin were associated with significant functional improvements in the diaphragm of the *mdx* mice as well as forelimb grip strength assessments. Phrenic nerve stimulation of the diaphragm showed that treatment with the drug improved the neuromuscular kinetics and restored the resting membrane potential of the dystrophic myofibers. Finally, the SU9516 treatment regimen ameliorated the dystrophic histopathology with increased percentage of centrally nucleated fibers obtained in association with an increase in embryonic myosin heavy chain positive fibers. SU9516 treatment decreased fibrosis in the muscle and improved myofiber size distribution. This study presents for the first time the benefits of utilizing an α7β1 integrin enhancing small molecule drug in the *mdx* mouse-model of DMD.

Chapter 4 discusses the molecular targets of SU9516. SU9516 is a known kinase inhibitor and hence it was important to determine the kinases targeted by SU9516 in skeletal muscle in order for the drug to proceed towards clinical development. It was hypothesized that the inhibition of one or more specific kinases in skeletal muscle is what results in the increase in α7 integrin. It was determined that in mouse myogenic cell lines, SU9516 potently inhibited a kinase known as Mitogen activated protein kinase-4 (MAP4k4) and its inhibition led to enhanced fusion and differentiation of C2C12 telomerized mouse myoblasts to myotubes. Hence, we showed that SU9516

increased levels of α7B in myoblasts at least partially through the inhibition of MAP4k4, however this inhibition was not responsible for the increased levels of α7B integrin seen in differentiated myotubes. Through a KiNativ screen, we were able to screen for several kinases as potential targets of SU9516 in human patient myotubes. Three kinases that were robustly inhibited by SU9516 in human myotubes were PFTAIRE1, STK39 and OSR1.

SU9516 also decreased the levels of CD82/KAI-1 a tetraspanin membrane protein that is currently being investigated by collaborators at Harvard University as a marker of skeletal muscle satellite cells. Lastly, SU9516 was identified as an inhibitor of the p65NF-kB pathway that plays a role in the development of fibrosis and inflammation in DMD, secondary effects that lead to further muscle damage. In addition, to the α7β1 integrin as a therapeutic target, SU9516 also inhibits an inflammatory pathway that causes a lot of the secondary pathology that occurs owing to the loss of dystrophin.

Chapter 5 of this dissertation discusses the scope and future directions for SU9516 being further developed as a viable treatment of DMD. This chapter discusses the potential of a first in-class integrin enhancing compound for the treatment of DMD and provides further evidence that the α7β1 integrin could compensate for the loss of dytrophin in this fatal disease. SU9516 is toxic in mice at a dose of 10 mg/kg or higher and also has low absorption in skeletal muscle. Structure activity relationship studies are the next course of action for this drug, in order to improve the absorption and minimize the toxicity. However, after that point, preclinical trials with a modified compound will be assessed prior to transitioning the study in a larger model of DMD like the GRMD dog. Finally, experiments show that SU9516 improves the neuromuscular kinetics in the

diaphragm of the *mdx* mouse and it would be important to see whether the drug in fact improves calcium handling through the elevation of α7 integrin.
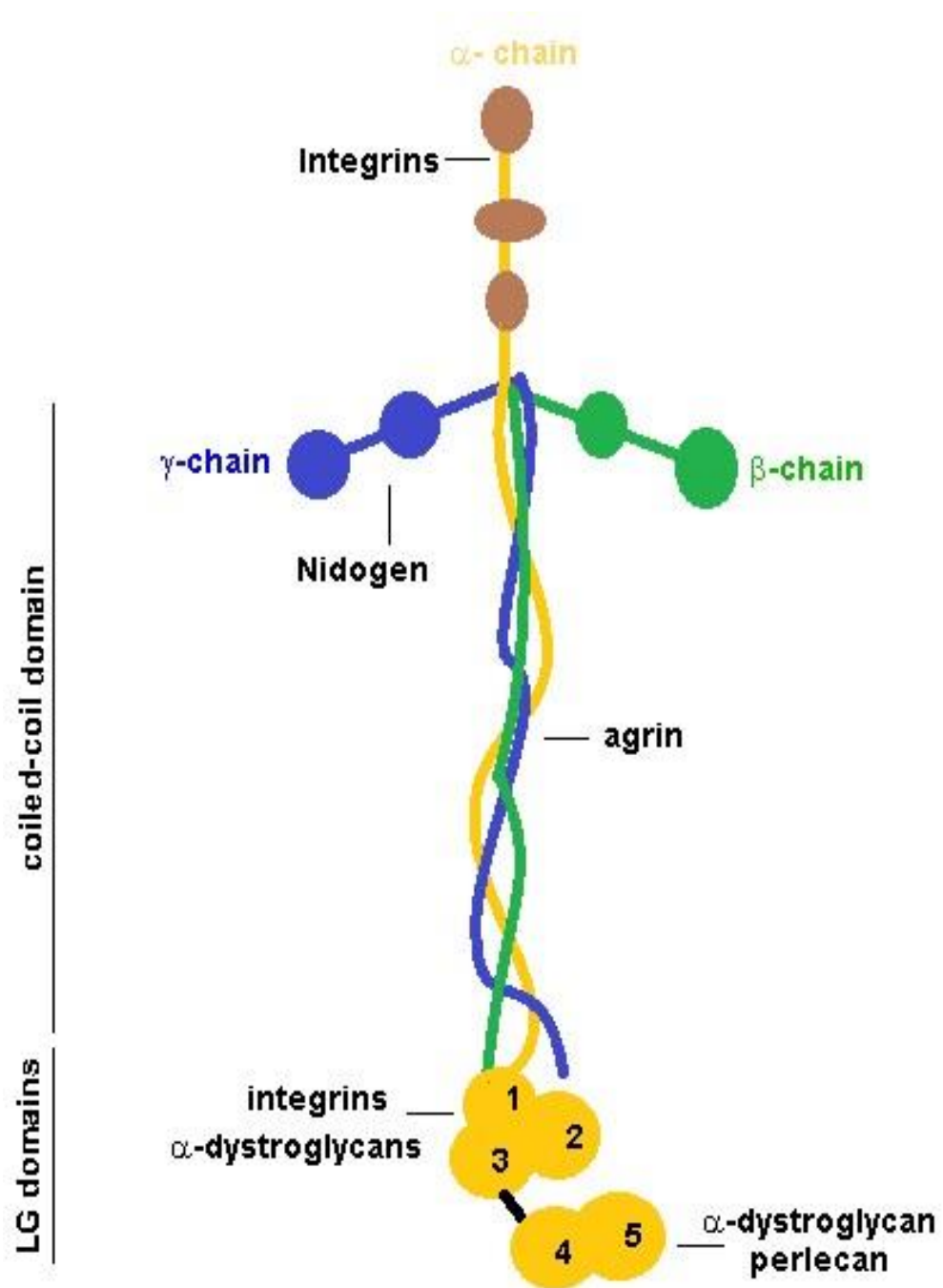
Figure 1- Laminin and its interactions- Laminins directly interact with agrin, nidogen and perlecan as depicted in the schematic above. All laminins are ligands to cell-surface receptors with most binding interactions occurring at the five laminin-type G domains (LG1–5) at the C-terminus of the laminin α chain. LG1–3 are the domains responsible for laminin interactions with integrins. Laminin binding to α-dystroglycan is mediated through the domains LG1–3 and 4–5. This schematic has been adapted from Holmberg and Durbeej, 2013 [215].
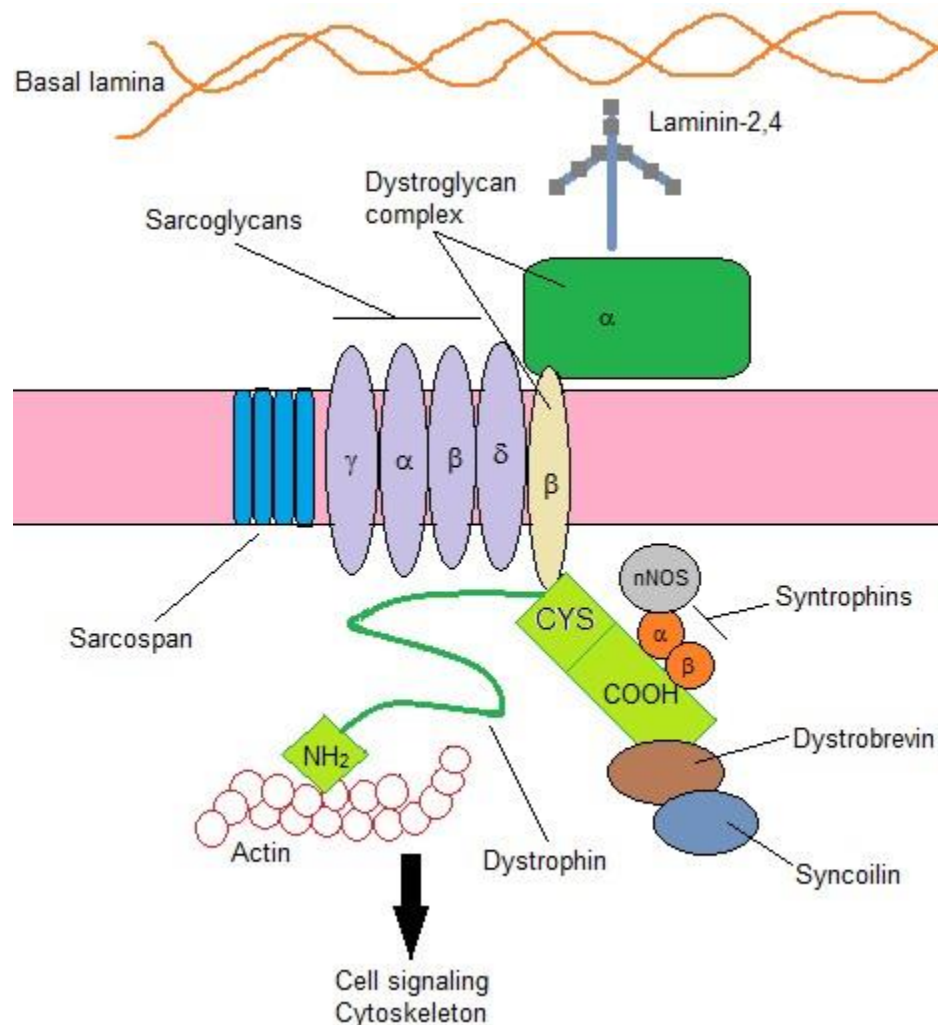
Figure 2- The Dystrophin Glycoprotein complex in normal adult muscle. Dystrophin assembles the members of the DGC at the sarcolemma of muscle fibers which together link the actin cytoskeleton to the extracellular matrix thereby providing stability to the sarcolemma. The central rod domain of dystrophin has 24 spectrin repeats interspersed with four hinges. The amino terminal domain binds the actin cytoskeleton and the cysteine rich C-terminal domain links dystrophin to the

sarcolemmal-bound β-dystroglycan. The dystroglycan complex is formed by the association of β-dystroglycan with α-dsytroglycan. The sarcoglycans, sarcospan and laminin-α2 at the extracellular matrix strengthen the existing complex. The CTD of dystrophin also binds to dystrobrevins and syntrophins. Syntrophins recruit nNOS to the sarcolemma via their PDZ domains. Additionally, the spectrin repeats 16/17 can also recruit nNOS to the sarcolemma. Dystrophin and its associated proteins play a critical mechanical role in stabilizing the sarcolemma during contraction thereby preventing contraction-induced injuries. Reproduced as an adaptation of Figure from Lisi and Cohn, 2007 [216].
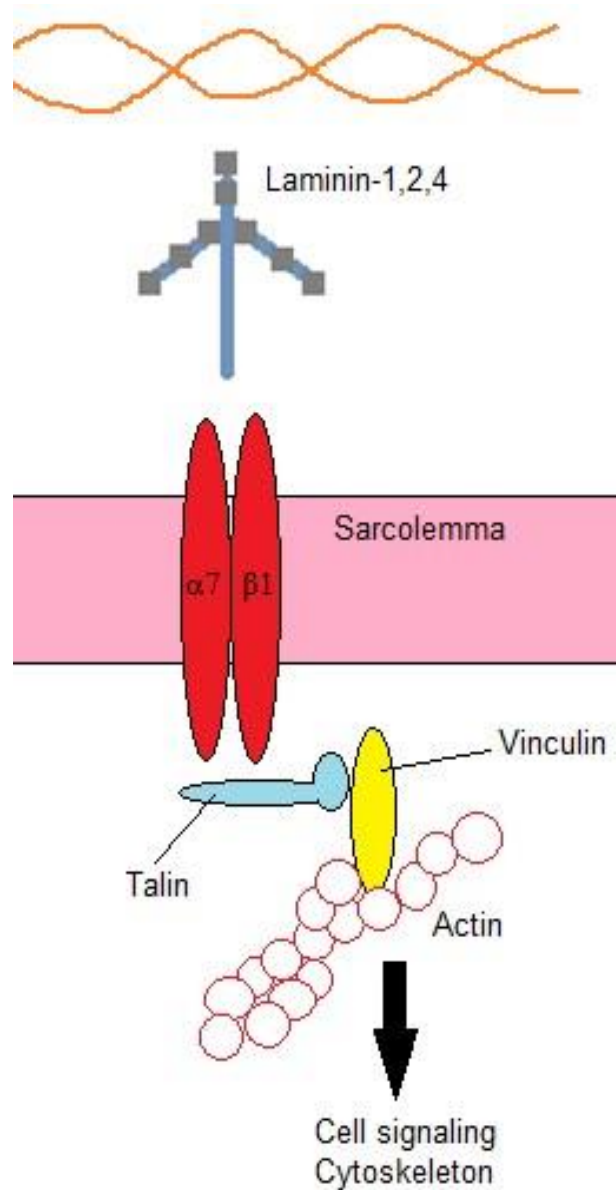
Figure 3- The α7β1 integrin complex at the sarcolemma of muscle fibers. The α7β1 integrin is a major laminin receptor in skeletal muscle fibers. It links laminin in the extracellular matrix to the actin cytoskeleton and is known to mediate cell signaling.

A. Normal muscle- Intact sarcolemma
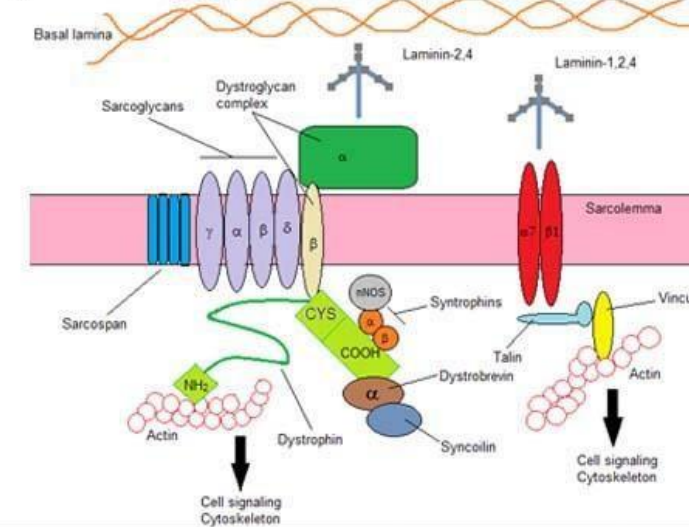
B. DMD/*mdx*/GRMD muscle- Abolished sarcolemma
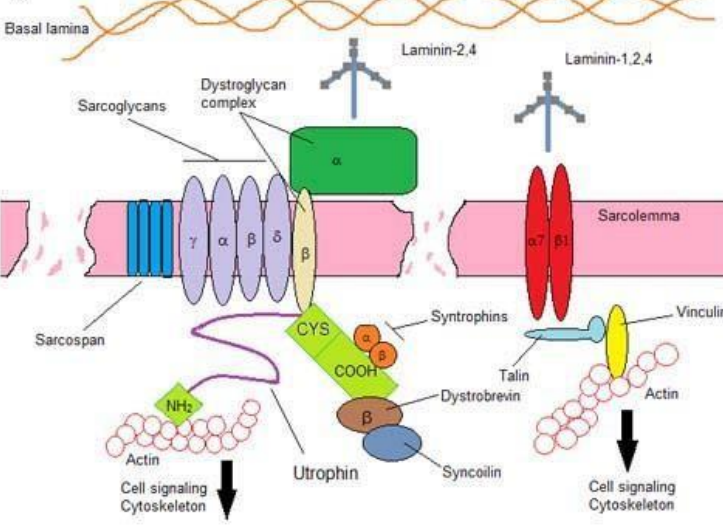
C. DMD/mdx/GRMD muscle + Integrin enhancement therapy- Restored sarcolemma
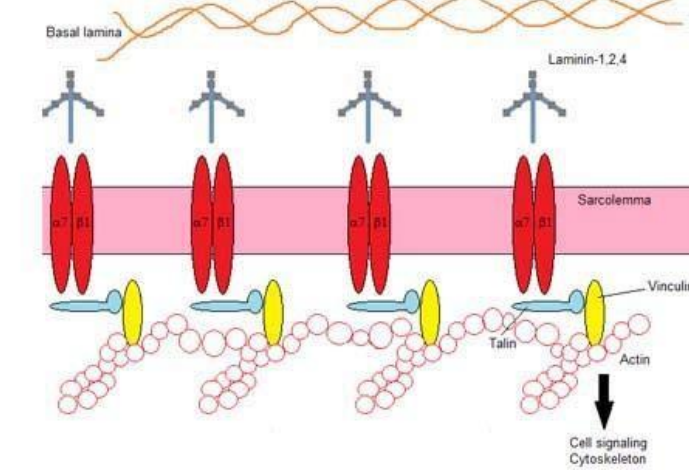
Figure 4- Integrin enhancement therapy for DMD. **(A)** Schematic of dystrophin and α7β1 integrin laminin binding complexes in healthy, normal skeletal muscle **(B)** Loss of dystrophin in DMD patients, *mdx* mice and the GRMD dog model leads to sarcolemmal damage and loss of muscle integrity. **(C)** Enhanced levels of the α7β1 integrin protects the sarcolemma from damage and improves muscle survival in dystrophin deficient muscle.
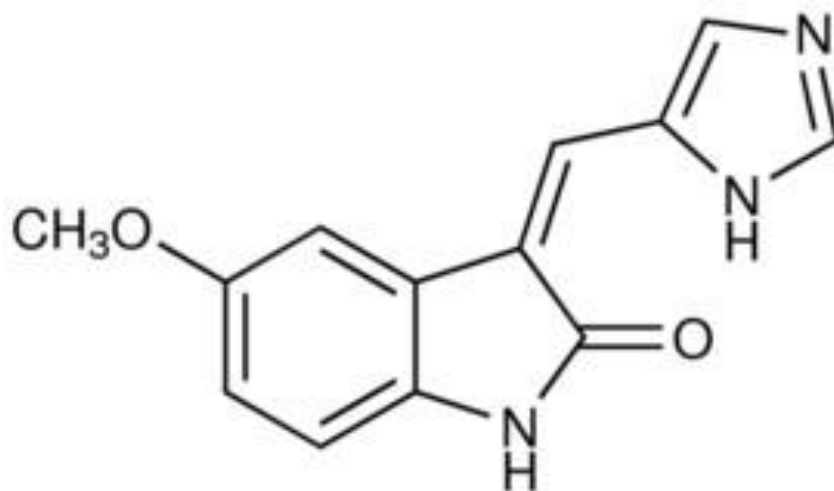
Figure 5- Molecular structure of SU9516. SU9516 is an indolinone with the chemical formula (*Z*)-1,3-Dihydro-3-(1*H*-imidazol-4-ylmethylene)-5-methoxy-2*H*-indol-2-one.

CHAPTER 2

PREDNISONE INCREASES α7 INTEGRIN AND LAMININ-α2 IN THE *MDX* MOUSE AND GRMD DOG MODELS OF DUCHENNE MUSCULAR DYSTROPHY

ABSTRACT

Duchenne muscular dystrophy (DMD) is a fatal neuromuscular disease for which there is no cure and limited treatment options. Prednisone is currently the first line treatment option for DMD and studies have demonstrated that prednisone improves muscle strength. Although prednisone has been used for the treatment of DMD for decades, the mechanism of action of this drug remains unclear and has been shown not to exclusively involve well known anti-inflammatory actions. Recent studies have shown that the α7β1 integrin is a major modifier of disease progression in mouse models of DMD, and drugs that promote α7β1 integrin levels in muscle may be therapeutic in the treatment of DMD. In this study we examined if prednisone increased α7β1 integrin levels in *mdx* and GRMD models and myogenic cells from DMD patients. Our results showed prednisone promotes an increase in α7 integrin protein in cultured myogenic cells and in the muscle of *mdx* and GRMD animal models of DMD. The increase in α7 integrin was associated with increased laminin-α2 transcript in prednisone treated dystrophin-deficient muscle. Together our results suggest that prednisone improves muscle strength in part through increased laminin211, laminin-221 and α7β1 integrin in dystrophin-deficient muscle. These results further confirm that drug-based therapies that target an increase in muscle α7β1 integrin, its signaling pathways and/or laminin may be therapeutic in DMD.

INTRODUCTION

   Duchenne muscular dystrophy (DMD) is a lethal X-linked neuromuscular disease that affects 1 in 3500 boys. Clinical symptoms are first detected at 2-5 years of age and DMD patients often die from cardiac or respiratory failure by the second or third decade of life. DMD is caused by mutations in the *Dmd* gene that lead to loss of the dystrophin protein [217,218]. Dystrophin and the associated protein complex link laminin in the extracellular matrix (ECM) to the cell cytoskeleton and serves as a structural and signaling platform in muscle. Loss of dystrophin in the *mdx* mouse, golden retriever muscular dystrophy (GRMD) dog and DMD patients result in a fragile sarcolemma prone to contraction induced muscle injury. Damaged muscle activates satellite cells to repair muscle damage and muscle degeneration followed by regeneration occurs. Regeneration eventually fails and muscle is replaced with fibrotic and fatty tissue [2]. There is currently no cure for DMD, however, improved medical care and treatment with corticosteroids, prednisone or deflazacort, have improved muscle strength and longevity of patients [210,213,214,219,220].

   The *mdx* mouse model has provided valuable insights into the functional role of dystrophin in muscle. While these mice exhibit muscle damage at the cellular level, outwardly they show little signs of muscle pathology [13]. Short term prednisone therapy in the *mdx* mouse has been shown to improve muscle strength [221]. The GRMD dog model develops progressive and fatal muscle disease and exhibits pathophysiological disease features similar to DMD, including progressive loss of muscle function, muscle membrane fragility, cardiomyopathy and premature death [22–24]. Studies indicate short term treatment with prednisone shows functional benefits to the GRMD model [36].

Although corticosteroids are the current front line treatment for DMD and show short term benefits in animal models of this disease, the mechanisms by which this drug improves short term clinical outcomes remains unknown.

The α7β1 integrin is the predominant laminin-binding integrin in cardiac and skeletal muscle [165]. The α7β1 integrin protein is localized at neuromuscular and myotendinous junctions and extrajunctional sites in skeletal muscle [165,167]. Within the α7β1 integrin heterodimer the α7 integrin chain specifies laminin isoform interactions while the β1 integrin chain determines signaling and actin cytoskeletal interactions [165,222,223]. In skeletal muscle, six isoforms of the α7 integrin chain are produced by developmentally regulated RNA splicing [177]. Mutations in the α7 integrin gene cause congenital myopathy in both humans and mice [204,224,225]. Enhanced transgenic expression of the α7 integrin in the skeletal muscle of severely dystrophic mice improves muscle pathology and increases lifespan[195,196]. Conversely, loss of the α7 integrin in dystrophin-deficient *mdx* mice results in a more severe dystrophic phenotype and reduced viability with mice dying prematurely by 4 weeks of age [198,226]. Together, these results support the idea that the α7β1 integrin is a modifier of muscle disease progression in DMD and a target for drug-based therapies. To investigate if glucocorticoids act to increase α7β1 integrin in muscle, we examined levels of the α7 integrin in myogenic cells from mouse and DMD patients as well as in *mdx* and GRMD animal models treated with prednisone. Our results show treatment with prednisone promotes a dose-dependent increase in α7 integrin in mouse myogenic cells. In addition, we show the skeletal muscle of *mdx* mice and GRMD dogs treated with prednisone exhibit elevated levels of laminin-α2 and α7

integrin. Our results show for the first time that prednisone promotes an increase in the α7β1 integrin in muscle, which may contribute to the mechanism of action of this important therapeutic agent for DMD.

MATERIALS AND METHODS

Tissue Culture

 C2C12 cells used in this study were purchased from ATCC and were grown in DMEM media (GIBCO, Grand Island, NY) supplemented with 20% Fetal Bovine Serum (FBS, Atlanta Biologicals, Lawrenceville, GA), 0.5% Chick-embryo extract (CEE, Seralab, West Sussex, UK), 1% L-Glutamine (GIBCO, Grand Island, NY), and 1% penicillin/streptomycin (PS), (GIBCO, Grand Island, NY). C2C12 myoblasts were differentiated to myotubes in DMEM supplemented with 1% horse serum (HS), 1% LGlutamine, and 1% PS. Human DMD myoblasts were a generous gift from Dr. Kathryn North and used under an approved IRB from the University of Nevada, Reno. DMD myogenic cells were grown in F10 media (GIBCO, Grand Island, NY) supplemented with 20% FBS, 1% CEE, 0.5mM $CaCl_2$, 1% L-Glutamine, and 1% PS. Human DMD myoblasts were differentiated to myotubes in F10 media supplemented with 1% HS, 1% L-Glutamine, and 1% PS.

Mice

The *mdx* mouse line (C57Bl10scsn-Dmdmdx) (Jackson Laboratories, Bar Harbor, ME) was used in these studies in accordance with an animal protocol approved by the University of Nevada, Reno, Institutional Animal Care and Use Committee. Mice were treated with 100μL of PBS or 100μL of a 200μg/mL solution prednisone (1 mg/kg) (Sigma, St. Louis, MO) by daily oral gavage for two weeks beginning at 3 weeks of age. At 5 weeks, mice were sacrificed and muscle tissues were surgically removed and frozen using standard procedures[56]. The tibialis anterior (TA) was used for immunofluorescence, the gastrocnemius was used for western blotting, and the tricep muscle was used for quantitative RT PCR.

Dog Tissue

All dogs were used and cared for according to principles outlined in the National Institutes of Health Guide for the Care and Use of Laboratory Animals. Archived vastus lateralis muscle samples from dogs included in a prednisone preclinical trial completed at the University of Missouri-Columbia were used. The Vastus lateralis muscle was surgically removed at 6 months of age from five untreated wild-type dogs, six untreated GRMD dogs, and four prednisone-treated GRMD dogs (two treated with 1 mg/kg/day and two treated with 2 mg/kg/day prednisone). GRMD prednisone treatment began at either 1 week or 2 months old and continued daily until tissue extraction (Liu et al., 2004)

Western Blotting

Protein was extracted from cell pellets or tissue powdered in liquid nitrogen as previously described [56]. Protein quantified using a Bradford assay and equal quantities were separated on SDS polyacrylamide gels and α7A and α7B integrin was detected as was previously described [56]. Protein loading was normalized to either α-Tubulin (1:1000 mouse-monoclonal, Abcam), GapDH (1:1000, goat-polyclonal, Santa Cruz Biotechnology, Santa Cruz, CA), or the entire lane stained with Ponceau-S or Swift Stain (G-Biosciences, St. Louis, MO). Quantitation was performed using Image J Software.

Immunofluorescence

10μm sections of TA muscles from mice and VL muscles from dog were removed using a Leica Cryostat and immunofluorescence was performed using antibodies against α7A integrin as previously described [177] or standard IF procedures using Laminin-α2 (1:100 goat-polyclonal, SC-16582 (C-20), Santa Cruz Biotechnology, Santa Cruz, CA) followed by FITC-Donkey-anti-Goat (1:1000, Jackson ImmunoResearch Baltimore, MD) and mounted using Hard-mount Vectashield w/DAPI (H-1500, Vector Laboratories, CA). IF images were taken using an Olympus Fluoview FV1000 Laser Confocal Microscope using consistent settings for all images, and intensity evaluation was performed using FV10-ASW3.1 software histogram function. Intensity counts were averaged across all images for each dog group and graphed using GraphPad Prism software.

Quantitative Real-time PCR

Total RNA from powdered mouse tricep muscle and sectioned canine *Vastus lateralis* was isolated using Trizol (Invitrogen, Grand Island, NY) followed by a R01 DNase treatment (Promega, Madison, WI), and cDNA was made with random hexamers (IDTDNA) and SuperscriptIII (Invitrogen, Grand Island, NY) using standard procedures. Quantitative Real-time was performed using Quanta Perfecta SYBR-Green with ROX Master Mix and were run and analyzed as previously described [227]. Mouse primers for *mItga7, mGapdh, mLama4, and mLama5* were used as previously described [227]. Mouse primers for *mLama2* were: F-ctgggagtcagcagtcagaagat and R-ctttatgccactgtccattgcaca. Primers against canine transcripts were as follows: cITGA7 F-actgtccgagccaatatcaccgt, *cITGA7* R-accagtagtcccgccagcaca, cGapDH F- ccccaatgtatcagttgtggatctga, cGapDH Rggtgtcactgttgaagtcacagga, cLAMA2 F-,tgggaatcagcagccagaaaatg, cLAMA2 Rgactttatgccactgtccatcaca, cLAMA4 F- ggggagtacctgaatgttcacatg, cLAMA4 Rctacatccaactgaaccacatttgaatctc, cLAMA5 F-atgaacttctcctactcgccgct, cLAMA5 R-taatagtaccggcgggtgacggt.

Statistical Analysis

All statistical analysis was performed using GraphPad Prism 5 software. Averaged data is reported as the mean +/- the standard error of the mean (SEM). Comparison for two groups was performed using a Students t-test and between multiple groups using Kruskal-Wallis one-way ANOVA on ranks for nonparametric data. $P < 0.05$ was considered statistically significant.

RESULTS

Prednisone increases α7 integrin levels in a mouse model and in DMD myogenic cells

Corticosteroids are used to treat many chronic diseases, including DMD. In many cases, the benefits of prednisone treatment are known to occur through anti-inflammatory effects. However, inflammatory suppression does not explain the short-term benefits to muscle strength in DMD patients and the overall delay of muscle degenerative symptoms. Previous studies have shown reduced muscle pathology and improved strength in transgenic *mdx/utr*$^{-/-}$ mice (lacking both dystrophin and utrophin) that overexpress α7B integrin [195]. We hypothesized that increased α7 integrin might be one of the mechanisms by which prednisone functions to improve muscle strength in DMD. In order to test this hypothesis, C2C12 mouse myoblasts and myotubes were treated with increasing concentrations of prednisone for 48 hours, and levels of α7B integrin protein were analyzed by western analysis and normalized to levels of α-tubulin (Figure 1A, B). In C2C12 myoblasts, treatment with prednisone had no significant effect on α7B integrin levels compared with DMSO-treated control cells (Figure 1A, quantified in 1C). In contrast, C2C12 myotubes showed a dose-dependent increase in α7B integrin compared with DMSO-treated control cells (Figure 1B, quantified in 1D). Prednisone treatments of 112 μM and 176 μM resulted in a 1.6- and 1.8-fold increase in α7B integrin protein in myotubes, respectively, compared with DMSO alone. The highest dose of prednisone the cells were exposed to was 176 μM, which also gave the largest α7 integrin increase (Figure 1D). This maximum dose was limited by both the solubility of prednisone in DMSO and cell toxicity, which was shown at >1% DMSO. These data indicate that

prednisone promotes an increase in α7B integrin protein in a dose-dependent manner in cultured mouse myotubes. Next, we examined whether prednisone treatment increased α7 integrin in human DMD myotubes. Western analysis showed that DMD myotubes treated with 112 μM prednisone had a 1.8-fold increase in α7B integrin protein compared with those treated with DMSO (Figure 1E, quantified in 1F). These results confirm that prednisone acts to increase α7 integrin in a conserved pathway in both mouse and human myotubes.

Prednisone increases α7 integrin in *mdx* mouse muscle

The *mdx* mouse model for DMD was used to examine the effect of prednisone treatment on α7 integrin levels in the muscle of mice. PBS (*n*=9) or 1 mg/kg prednisone in PBS (*n*=7) was given daily by oral gavage to 3-week-old *mdx* mice. Treatment was performed for 2 weeks, at which time the mice were sacrificed and tissues harvested for analysis. We then analyzed the protein levels of α7A integrin from both the tibialis anterior (TA) and gastrocnemius muscles in prednisone-treated versus control *mdx* mice (Figure 2A, B respectively). In the TA we found a non-significant trend of elevated α7A integrin protein levels (∼13% increase) by western analysis (Figure 2A); however, a significant increase (∼30% increase) was observed in prednisone-treated gastrocnemius muscles compared with controls (Figure 2B). Results were quantified and normalized to α-tubulin (Figure 2C, D). This differential effect is not completely surprising because previous work has shown that the TA muscle maintains lower levels of β1 integrin than the gastrocnemius muscle [228]. These results indicate that short-term treatment with prednisone increases α7A integrin in the muscle of *mdx* mice. Next, we examined the

distribution of α7A integrin in the TA muscle by immunofluorescence (IF; Figure 2E). Compared with PBS-treated mice, prednisone-treated animals showed an increase in α7A integrin at the sarcolemma, confirming western studies. These results suggest that short-term prednisone treatment within the *mdx* mouse model results in an increase in the α7A integrin protein levels at the sarcolemma.

Next, we assessed whether the prednisone-induced increase in α7A integrin protein levels in the *mdx* mouse was due to protein stabilization or increased transcription of the *Itga7* gene in muscle fibers. Quantitative real-time PCR was used to examine the transcript levels of *Itga7*, *Lama2*, *Lama4*, *Lama5* and *Utrn* relative to *GapDH* within the TA muscle of the PBS- and prednisone-treated mice (Figure 3A-E). A 30% increase in *Itga7* transcript levels was observed with prednisone treatment, but this value did not reach significance (Figure 3A). Similar results were obtained from triceps muscle, where prednisone treatment led to a 40% increase in *Itga7* transcript levels, albeit insignificant (supplementary material Figure S1). These results indicate that the increased level of α7 integrin that is observed in prednisone-treated *mdx* muscle likely occurs through a transcriptionally based mechanism.

To explore the mechanism by which prednisone increased α7 integrin protein levels in skeletal muscle, we examined the transcription of laminin isoforms and utrophin in PBS- and prednisone-treated *mdx* mice. Recent studies have demonstrated that deflazacort increases laminin-α2 levels in the muscle of *mdx* mice [229]. Our results show that, compared with PBS, prednisone promoted a significant increase in *Lama2* transcripts in the TA (Figure 3B) and triceps (supplementary material Figure S1) muscles of *mdx* mice. There was no significant change in the levels of *Lama4*, *Lama5* or *Utrn*

transcripts (Figure 3C– E) in prednisone-treated mice. Together, these results indicate that prednisone might act to alter the laminin composition of the myomatrix and promote an increase in laminin-211 and laminin-221 in *mdx* muscle. The presence of more laminin-211 and laminin-221 in skeletal muscle basal lamina would promote stabilization of the α7β1 integrin complex in skeletal muscle, thus improving the integrity of the dystrophin-deficient sarcolemma.

Prednisone increases α7A integrin in the muscle of GRMD dog model

We next examined whether prednisone treatment increased α7 integrin levels in the GRMD canine model of DMD. We began by examining α7A integrin protein levels in the vastus lateralis (VL) muscle of 6-month-old wild-type, untreated GRMD dogs and prednisone-treated GRMD dogs. Using western blotting and quantitation techniques, we found a 1.7-fold increase in the levels of α7A integrin protein in the prednisone-treated GRMD dogs compared with either wild-type or untreated GRMD dogs (Figure 4A, quantified in 4B). Although not significantly different, the average α7A integrin protein levels in untreated GRMD muscle were found to be 25% lower than that of the wild-type dogs (Figure 4A, quantified in 4B). Furthermore, we found increased sarcolemmallocalized α7A integrin within the VL muscle of GRMD animals by immunofluorescence (Figure 4C). We next examined *ITGA7* transcript levels in the VL muscle of dogs using quantitative real-time PCR (Figure 4D). Surprisingly, we found that the *ITGA7* transcript levels in prednisone-treated GRMD dogs were ⌣twofold lower than untreated wild-type levels (Figure 4D). Furthermore, although not statistically significant (*P*=0.08), the prednisone-treated GRMD dogs had average *ITGA7* transcript

levels that were threefold lower compared with the levels in untreated GRMD dogs (Figure 4D). Similar to previous findings from individuals with DMD [194], we found a twofold increase in the average *ITGA7* transcript levels in untreated GRMD dogs compared with wild-type dogs (Figure 4D), although again this difference was not statistically significant owing to the high variability of the transcript levels in the untreated GRMD dogs. This variability was not apparent in the *ITGA7* transcript levels of prednisone-treated GRMD dogs (Figure 4D). Together, these results along with western data in the dog model suggest that the improved α7 integrin protein stability caused by prednisone treatment results in a negative feedback loop on *ITGA7* transcriptional activity.

Prednisone maintains Laminin-a2 protein localization and levels in GRMD dogs

Next, we determined laminin-α2 protein levels and localization in the VL muscle of wild-type, untreated GRMD and prednisone-treated GRMD dogs using immunofluorescence. Laminin-α2 was clearly present surrounding the muscle fibers in both wild-type and prednisone-treated GRMD dogs, but was only weakly visible around untreated GRMD dog muscle fibers (Figure 5A). Levels were semi-quantified by performing intensity measurements on images from wild-type, untreated GRMD and prednisone-treated GRMD muscle (Figure 5A). Prednisone-treated GRMD dogs showed a 32% increase in peak relative intensity compared with wild-type muscle (Figure 5A). Both peak intensities were higher and had different curve distributions than that observed for the untreated GRMD dog images. Untreated and prednisone-treated GRMD dogs contained numerous intense fluorescence regions of unknown origin in the muscle

interstitial space that are likely to have affected measurements, especially in untreated GRMD dogs (Figure 5A and supplementary material Figure S2). Together, these results support that prednisone acts to increase laminin-α2 and α7 integrin protein levels in GRMD dogs.

Next, we determined whether the canine model showed differences in the transcript levels of *LAMA2*, *LAMA4*, *LAMA5* and *UTRN* (Figure 5B–E). Like the *ITGA7* transcript levels, untreated GRMD dogs showed a large amount of individual variability in relative levels of *LAMA2*, *LAMA4*, *LAMA5* and *UTRN* transcripts, which was not observed in prednisone-treated GRMD dogs (Figure 5B–E). *LAMA2* transcript levels were significantly increased in the VL muscle in prednisone-treated (twofold) and untreated (sixfold) GRMD dogs compared with untreated wild-type dog (Figure 5B). The *LAMA4* (P=0.6), *LAMA5* (P=0.08) and *UTRN* (P=0.4) transcript levels in the prednisone-treated GRMD dogs were not significantly different compared with untreated wild-type dogs, but the *LAMA5* average was around twofold lower (Figure 5C–E). *LAMA4* (P=0.051), *LAMA5* (P=0.03) and *UTRN* (P=0.13) transcript levels were around threefold lower in prednisonetreated GRMD dogs relative to the untreated GRMD dogs (Figure 5C–E). Together, this data suggests that prednisone treatment of GRMD dogs stabilizes the transcriptional levels of all genes that we examined.

We were curious as to whether lesion severity would also vary between untreated and prednisone-treated GRMD dogs, and examined muscle histology by hematoxylin and eosin (H&E) staining (Figure 5F). All GRMD dogs displayed increased myofiber size variation, fibrosis and inflammation compared with wild-type dogs. Changes in untreated GRMD dogs were more pronounced than in those treated with prednisone

(Figure 5F). Based on the overall histology, including fiber size, fibrosis and inflammation, we scored the VL sections between 1+ and 5+, with lower values suggesting greater lesion severity. These values were then summarized along with α7A integrin protein levels, laminin-α2 immunofluorescence peak intensity, and individual real-time fold-changes for *ITGA7*, *LAMA2*, *LAMA4*, *LAMA5* and *UTRN* transcripts for all dogs used in this study (Table 1). The prednisone-treated GRMD dogs had higher (more normal) lesion scores. Individual profiles from some dogs showed higher α7A integrin protein levels while exhibiting lower levels of *ITGA7* transcript and vice versa in both prednisone-treated and untreated GRMD dogs (Table 1). A similar inverse pattern was seen for the laminin-α2 protein:transcript ratio. Overall, the prednisone dose did not seem to affect protein or transcript levels in the GRMD dogs. Taken together, our data strongly suggest that a negative feedback loop exists between α7 integrin protein and *ITGA7* transcript levels in the GRMD dog model (Figure 6). Furthermore, elevated levels of *ITGA7* and/or *LAMA2* transcripts might be indicators of a more severe muscle disease phenotype in DMD.

DISCUSSION

 DMD is a devastating lethal genetic disease for which there is no cure and limited treatment options. Although corticosteroids have been used for the treatment of DMD for over 20 years, our understanding of the mechanism of action of these drugs remains unclear. The therapeutic benefits involve a complex combination of inflammatory inhibition and strength enhancement in muscle. In this study we identified a new potential strength inducing molecular benefit of prednisone treatment on dystrophin

deficient muscle, increased α7β1 integrin protein levels. We show that this benefit does not occur as a direct result of increased *ITGA7* transcription, but rather through a stabilization mechanism through increased and maintained laminin-211/221 protein. Finally, we have shown for the first time an inverse correlation between *ITGA7* transcript and protein levels in the GRMD model for DMD.

One of the most interesting aspects of this study was the comparison of α7 integrin levels between the *mdx* mouse and the GRMD dog. Previous work established that *ITGA7* transcript levels are elevated in the *mdx* mouse model and in DMD patients [194]. The 2-fold increase in the *mdx* mouse α7 integrin protein levels are well defined [194]; however, the only evidence of α7 integrin protein levels from DMD patients comes from non-quantitative immunofluorescence studies and *ITGA7* transcript analysis [194]. Here we examined α7 integrin protein and transcripts in the GRMD dog, which is phenotypically and histologically comparable to DMD. As with previous work from DMD patient tissue we found elevated levels of ITGA7 transcripts in the untreated GRMD dog muscle compared to wild-type dogs[194]. However, we also show that this is not indicative of an increase in protein levels. In fact we found an inverse correlation between the transcript and protein levels exists in the untreated GRMD dystrophic tissues. This raises the question of why this phenomenon is not present in the *mdx* mouse model. One possibility is that the mouse α7 integrin protein is more stable, lacking a secondary extracellular protease cleavage site conserved in rats, dogs and humans [230]. This non-cleavable mouse α7 integrin may enable the *mdx* mouse to stabilize their sarcolemma by reducing α7 integrin protein turnover, thus preventing the dystrophic progression. The severe pathology of the *mdx/α7⁻/⁻* double knockout mouse compared to the mild dystrophy in the

mdx or α7$^{-/-}$ knockout mouse lines is evidence that dystrophin and α7 Integrin have overlapping roles in maintaining sarcolemmal stability in mice [198]. The severe decrease in α7 integrin protein in several GRMD dogs suggest that in dystrophin-deficient dogs and humans, the α7 integrin protein may be less stable, than in *mdx* mice. Further, the histological appearance of dystrophindeficient dog muscle correlates with the levels of α7A integrin suggesting that α7 integrin protein levels alone may be a major determinant of dystrophic progression. Thus, prednisone confers a strength increase and muscle maintenance benefits to DMD patients through increased sarcolemmal stabilization of α7β1 integrin.

The inverse correlation between α7 integrin protein and transcript levels observed in the GRMD dog model also suggests a strong transcriptional feedback loop. Since the α7B integrin protein is an important signaling molecule in muscle[197,205,230]. Its loss could promote a large transcriptional change through downstream signaling. Interestingly the GRMD1 tissues, which had severely reduced α7 integrin protein levels also showed the highest transcript levels of the genes examined. Prednisone treatment helped stabilize the transcriptional levels in the GRMD dog and greatly reduced individual transcript level variation. Although we have clearly shown that the transcript levels of *ITGA7* and *LAMA2* are not indicative of protein levels in the GRMD dog, it is interesting that prednisonetreatment led to a lower level of all transcripts observed except *LAMA2* relative to Wildtype dog levels. This corresponds to the elevated laminin-α2 protein in our IF and is likely part of the mechanism through which prednisone stabilizes and increases the α7 Integrin protein levels. Previous data has shown that laminin-111 protein therapy increases α7 integrin in *mdx* mouse and DMD muscle cells [56]. These

results indicate that the elevated levels of laminin-211/221 in the myomatrix of dystrophic muscle caused by prednisone treatment helps stabilize the α7β1 integrin at the sarcolemma, providing mechanical stability and strength to dystrophin-deficient muscle.

Studies in *mdx* mice and GRMD dog suggest that although short term treatment with prednisone may temporarily improve muscle strength, long term treatment may have negative consequences on muscle histology and cardiac function [36,221]. Our findings suggest short term treatment with prednisone acts in part to increase Laminin-α2 and α7β1 integrin protein, a laminin receptor in muscle known to improve preclinical outcomes in transgenic mouse studies. Some key questions remain concerning the action of prednisone through the α7β1 integrin: (1) Why is this action of prednisone transient in dystrophindeficient muscle? (2) Does long term treatment with prednisone result in down-regulation of the α7β1 integrin receptor and/or laminin in muscle (3) Does prednisone have a similar mechanism of action on the α7β1 integrin in the dystrophic heart? (4) Does prednisone activate known α7β1 integrin signaling pathways in muscle? (5) Does prednisone increase integrin localization at myotendinous and neuromuscular junctions? and finally (6) Does prednisone's actions on the α7β1 integrin extend to other types of muscular dystrophies e.g. Merosin deficient congenital muscular dystrophy type 1A.

What is clear from this study is that Prednisone, a drug currently used in the treatment of DMD, acts in part through stabilization of Laminin-α2 and α7β1 integrin in muscle and our results suggest that molecules targeting or stabilizing these proteins are likely to be beneficial in the treatment of DMD.
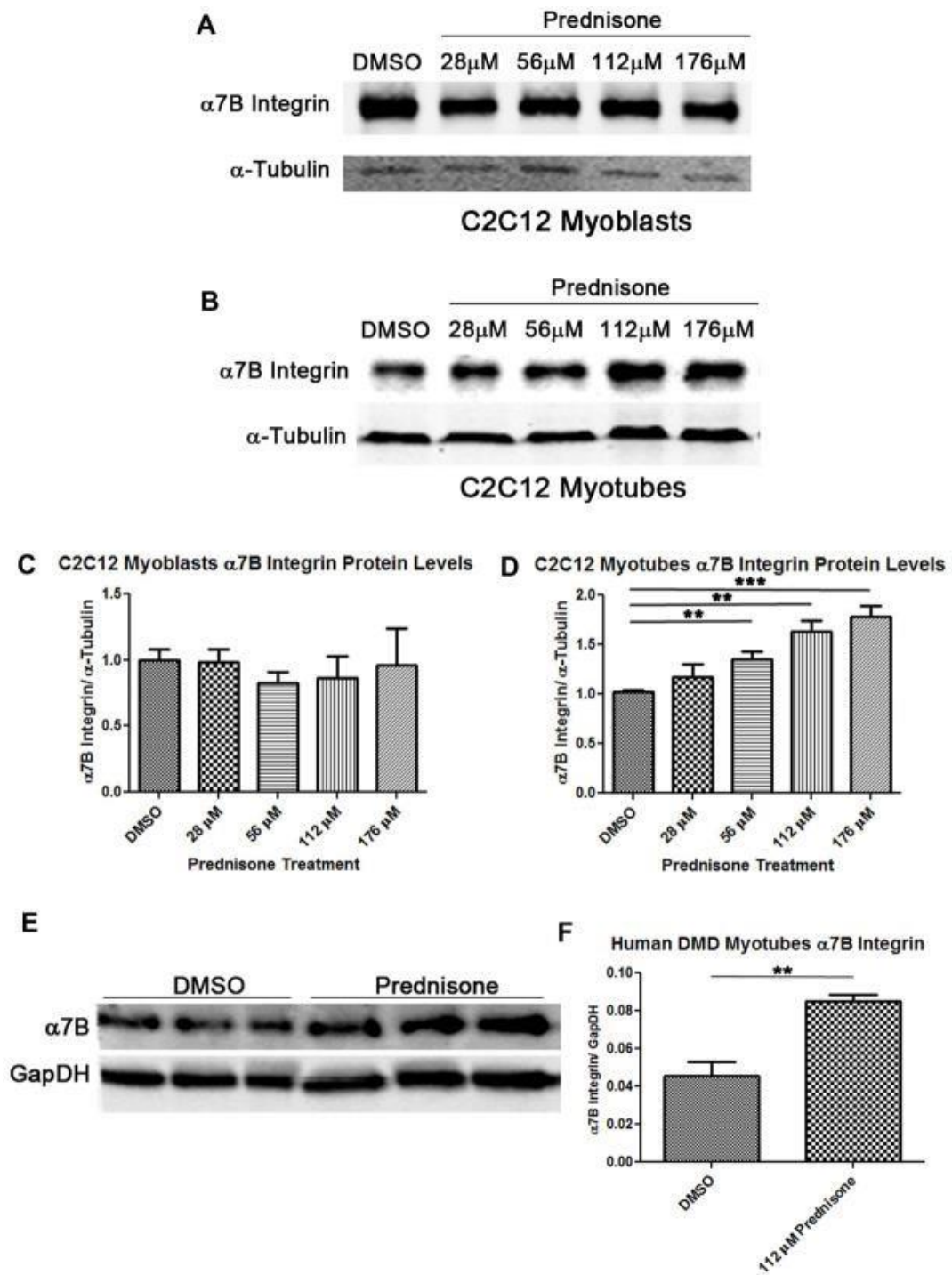
Figure 1: Effects of prednisone on α7 integrin levels in C2C12 mouse myoblasts and myotubes, and human DMD myotubes. (A, B) Western blot analysis of α7B integrin and α-tubulin from C2C12 myoblasts (A) or myotubes (B) treated with a DMSO control

or increasing amounts of prednisone. (C, D) Quantitation of α7B integrin levels normalized to α-tubulin was performed and graphed for the C2C12 myoblast (C) and myotube (D) treatments (*n*=4 per treatment group, **P<0.01, ***P=0.0005). (E) Western blot analysis of α7B integrin and GapDH from cultured human DMD myotubes. (F) Western results were quantified and graphed for α7B integrin normalized to GapDH (*n*=3 per treatment group, **P=0.0021).

A **TA Muscle**

PBS-Treated   Prednisone-Treated

α7A Integrin

α-Tubulin

B **Gastroc Muscle**

PBS-Treated   Prednisone-Treated

α7A Integrin

α-Tubulin

C *mdx* TA α7A Integrin Protein Levels

p = 0.07

D *mdx* Gastroc α7A Integrin Protein Levels

*

E   PBS-Treated   Prednisone-Treated
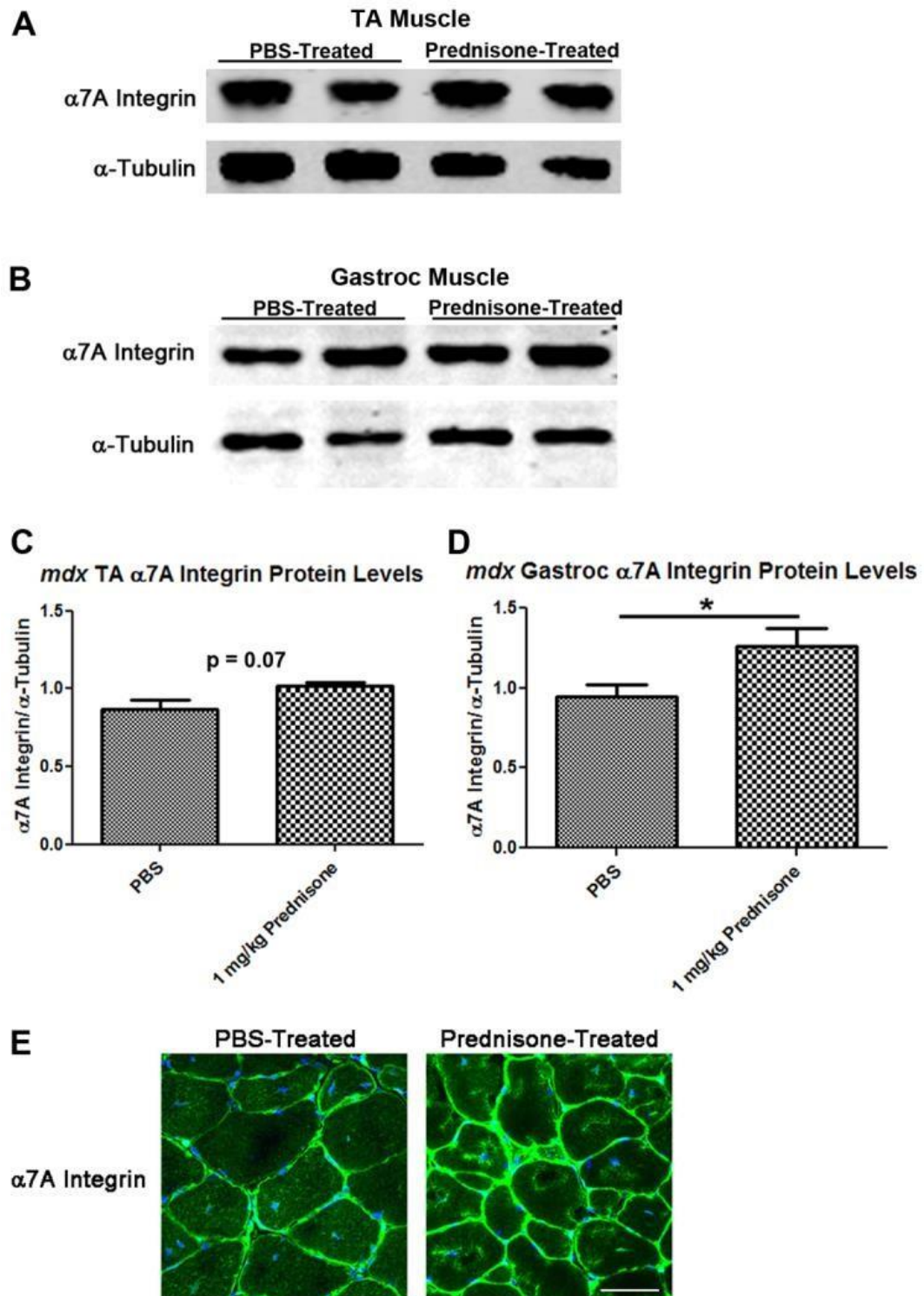
α7A Integrin

Figure 2: *Mdx* **mice treated with prednisone (1 mg/kg body weight/day) have**

increased α7A integrin in muscle. (A, B) PBS-control (*n*=9) or 1 mg/kg/day prednisone

(*n=7*)-treated *mdx* mouse TA (A) or gastrocnemius (B) muscle extracts analyzed for α7A integrin and α-tubulin protein levels using standard western blotting procedures. (C,D) Western blots were quantitated and graphed for α7A integrin normalized to α-tubulin for the TA (C) or gastrocnemius (*P=0.04) (D). (E) Immunofluorescence of α7A integrin from the TA of PBS-treated or 1 mg/kg/day prednisone-treated *mdx* mice. Scale bar: 50 μm.
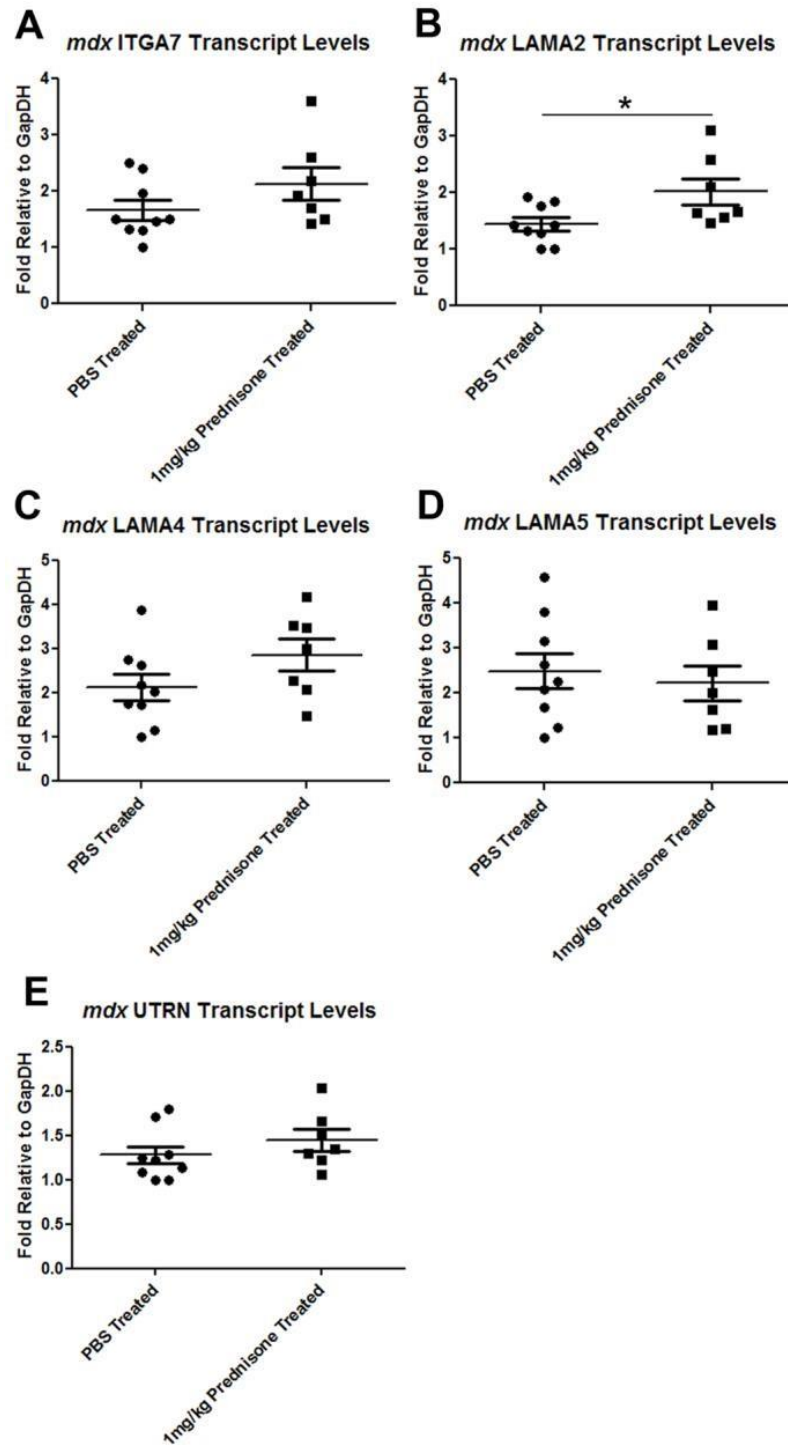
Figure 3: *Lama2* transcript levels are significantly elevated in prednisone-treated

***mdx* mouse muscle.** Quantitative real-time PCR was performed against *mdx* TA cDNA

from animals treated with PBS (*n*=9) or 1 mg prednisone/kg body weight/day (*n*=7),

using gene-specific primers against mouse *Itga7* (A), mouse *Lama2* (*P=0.03; B), mouse

Lama4 (C), mouse *Lama5* (D) and mouse *Utrn* (E).
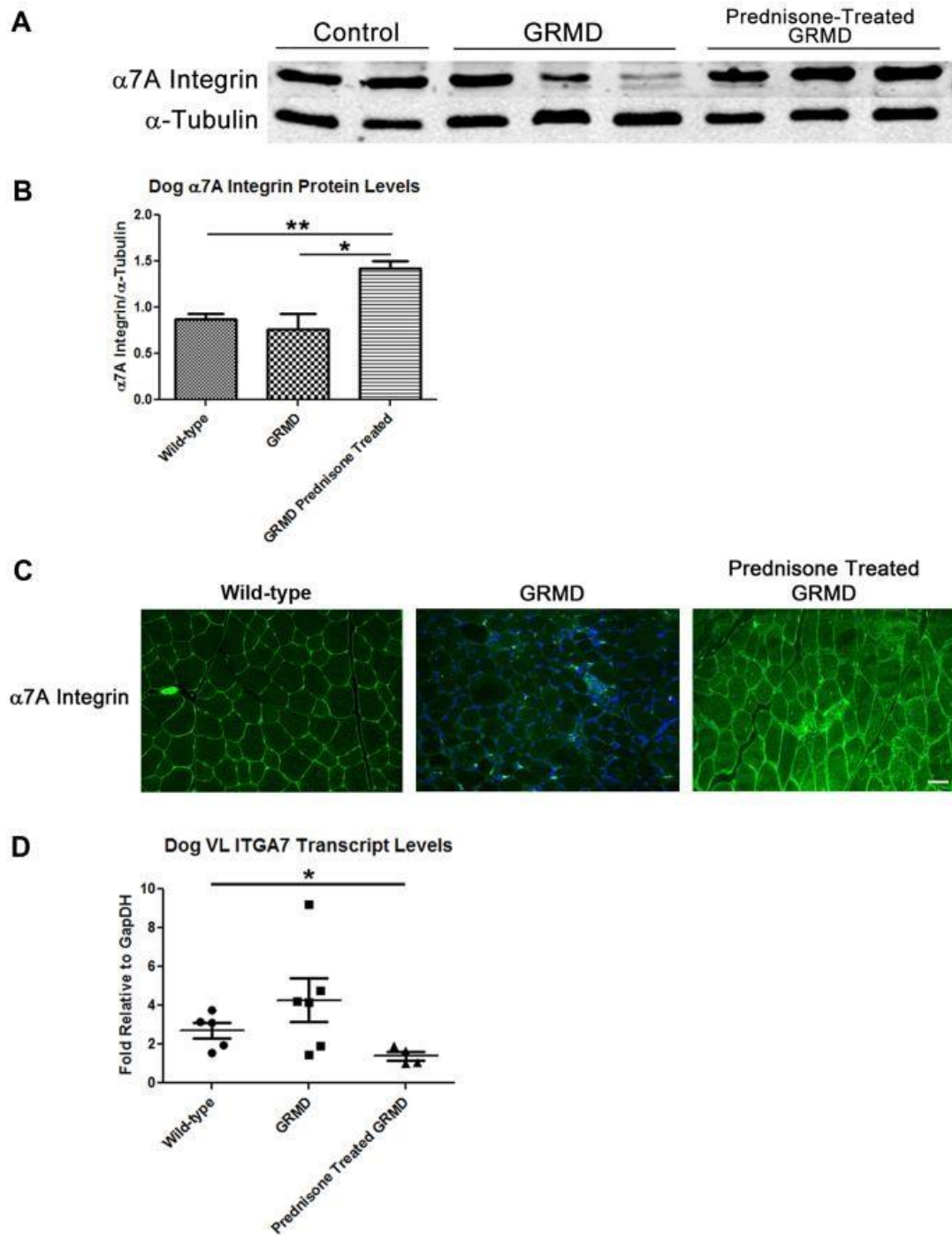
Figure 4: Prednisone treatment leads to elevated α7A integrin protein and reduced

ITGA7 **transcript levels in GRMD dog muscle.** (A) Representative western blot of α7A

integrin and α-tubulin protein levels from the VL of control (*n*=5), untreated GRMD

(n=6) and prednisone-treated GRMD (n=4) dogs. (B) Western results for α7A integrin normalized to α-tubulin were quantified and graphed (*P=0.019, **P=0.0023). (C) Immunofluorescence of α7A integrin in the VL of the three dog groups. (D) Quantitative real-time PCR of VL cDNA from wild-type (n=5), untreated GRMD (n=6) and prednisonetreated GRMD (n=4) dogs using primers against canine *ITGA7* (*P=0.037). Scale bar:

50μm.
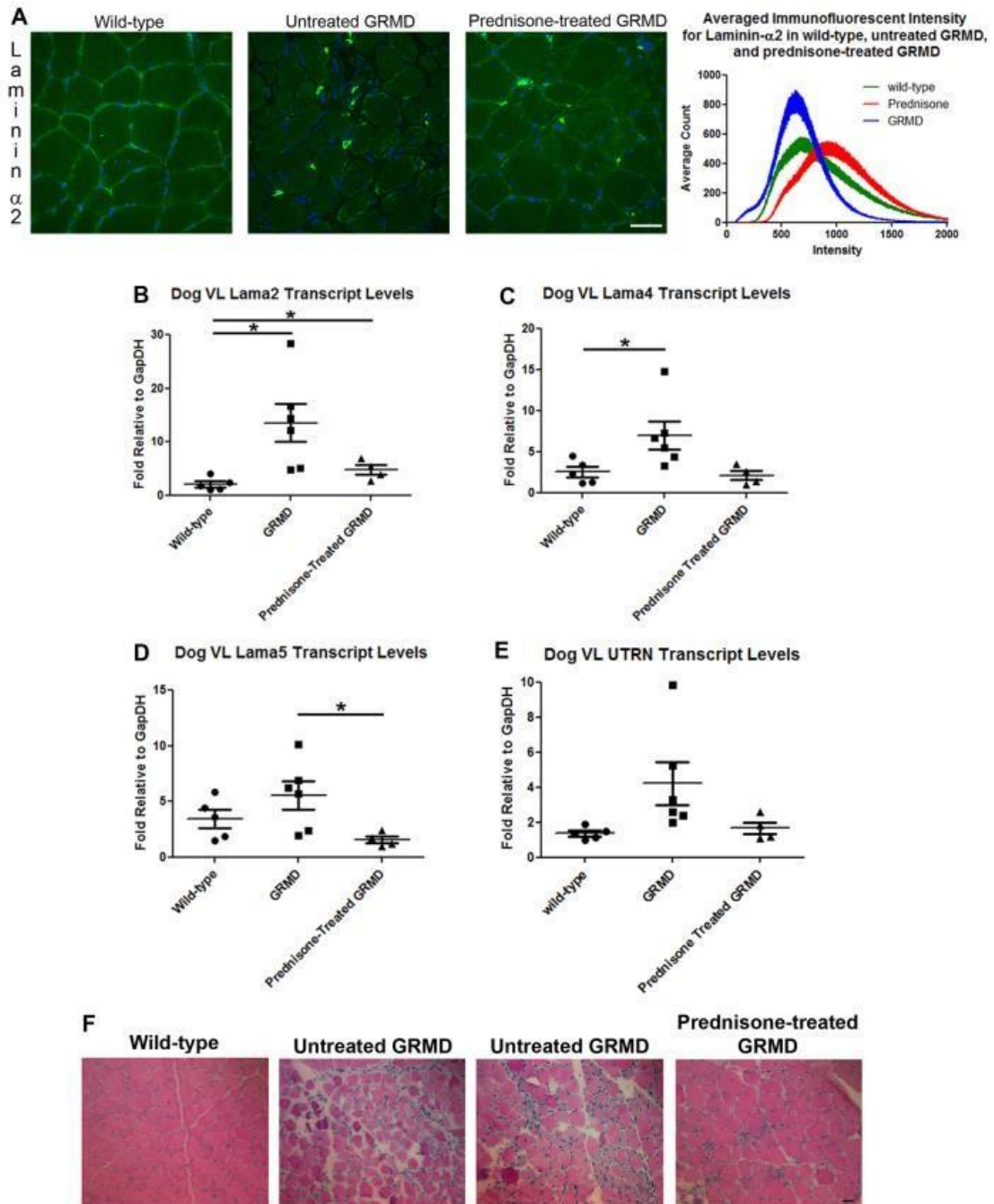
Figure 5: Prednisone restores laminin-α2 protein, stabilizes transcript levels and improves muscle pathology in the GRMD dog. (A) Immunofluorescence of laminin-α2 protein in wild-type, untreated GRMD and prednisone-treated GRMD dog VL muscle. The intensity values for two images per dog were counted, averaged by groups and

plotted (see supplementary material Fig. S2). Quantitative real-time PCR of VL cDNA from wild-type control (*n*=5), untreated GRMD (*n*=6) and prednisone-treated GRMD (*n*=4) dogs using primers against canine *LAMA2* (*P<0.035) (B), canine *LAMA4* (*P=0.047) (C), canine *LAMA5* (*P=0.035) (D) and canine *UTRN* (E). (F) H&E of the VL from control, untreated GRMD and prednisone-treated GRMD dogs. The VL sections were examined and graded (Table 1) for fibrosis, inflammation and muscle fiber hypotrophy. Prednisone-treated GRMD dog tissue had less fibrosis, inflammation and fiber size disparity than the untreated GRMD dog muscle, but slightly more than that observed in wild-type dogs. Scale bar: 50 μm.

Table 1. Analysis of VL muscles

Dog name	Gender	Pred	Dose (mg/kg/day)	Treatment duration	Normalized α7A integrin protein	Laminin-α2 IF peak intensity	Itga7	Lama2	Lama4	Lama5	Utrn	Histology grade
Untreated wild type												
Kip	M	N	n/a	n/a	0.85	771	3.14	2.45	3.41	4.43	1.49	+++++
Oregano	M	N	n/a	n/a	1.02	1179	3.12	4.06	4.56	5.87	1.89	+++++
Parsley	M	N	n/a	n/a	0.71	529	3.76	1.88	2.31	3.58	1.33	+++++
Pinkman	M	N	n/a	n/a	0.89	689	1.57	1.00	1.20	1.92	1.00	+++++
Tuco	M	N	n/a	n/a	0.87	524	1.94	1.18	1.35	1.52	1.11	+++++
Untreated GRMD (affected)												
Cosmo	M	N	n/a	n/a	0.76	649	4.74	12.16	5.56	5.72	5.25	++
Napoleon	M	N	n/a	n/a	0.81	476	4.21	14.39	7.32	6.22	3.30	++
Summer	F	N	n/a	n/a	0.23	631	4.15	16.67	6.67	6.93	2.39	+
Dorothy	F	N	n/a	n/a	0.21	551	9.21	28.31	14.84	10.15	9.82	+
Gaea	F	N	n/a	n/a	1.03	626	1.93	4.86	4.40	2.40	2.59	+++
Athena	F	N	n/a	n/a	1.11	726	1.45	5.18	3.29	1.97	1.97	+++
Prednisone-treated GRMD (affected)												
Elf	F	Y	1	2-6 months	1.49	1216	1.03	2.75	1.46	1.23	1.19	++++
Bam Bam	M	Y	1	2-6 months	1.49	1064	1.66	5.44	2.57	1.73	1.82	++++
Copper	M	Y	2	1 week to 6 months	1.54	611	1.00	3.91	1.00	1.00	1.07	++++
Romano	M	Y	2	2-6 months	1.15	839	1.91	6.98	3.48	2.39	2.57	++++

All dogs were aged 6 months. M, male; F, female; N, no treatment; Y, prednisone treated.

Table 1: Analysis of Vastus Lateralis muscles
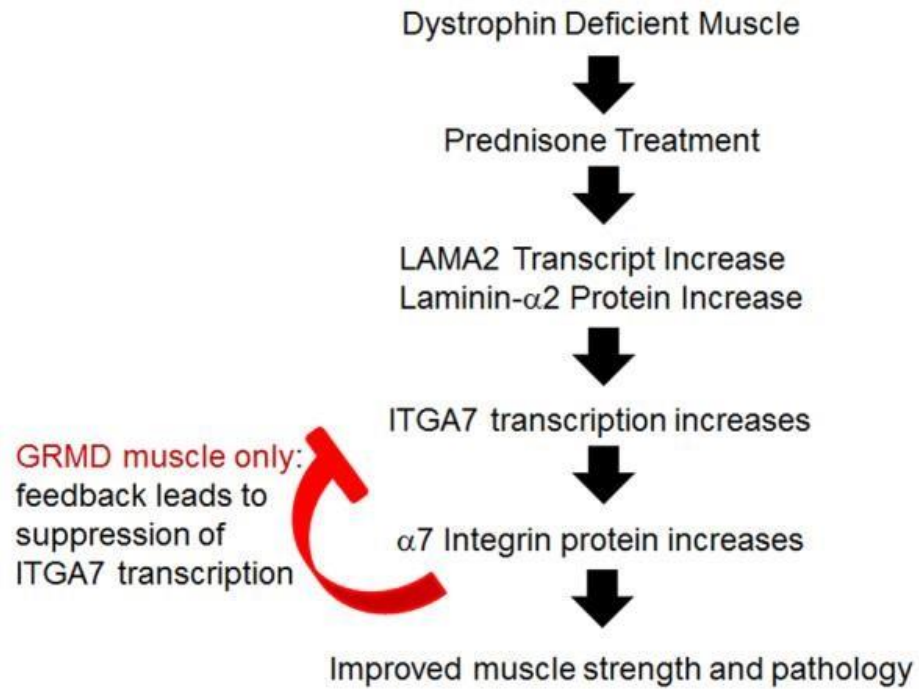
Figure 5: Model depicting the action of prednisone on laminin-α2 and α7 integrin in the muscle of the *mdx* mouse and GRMD dog models of DMD.
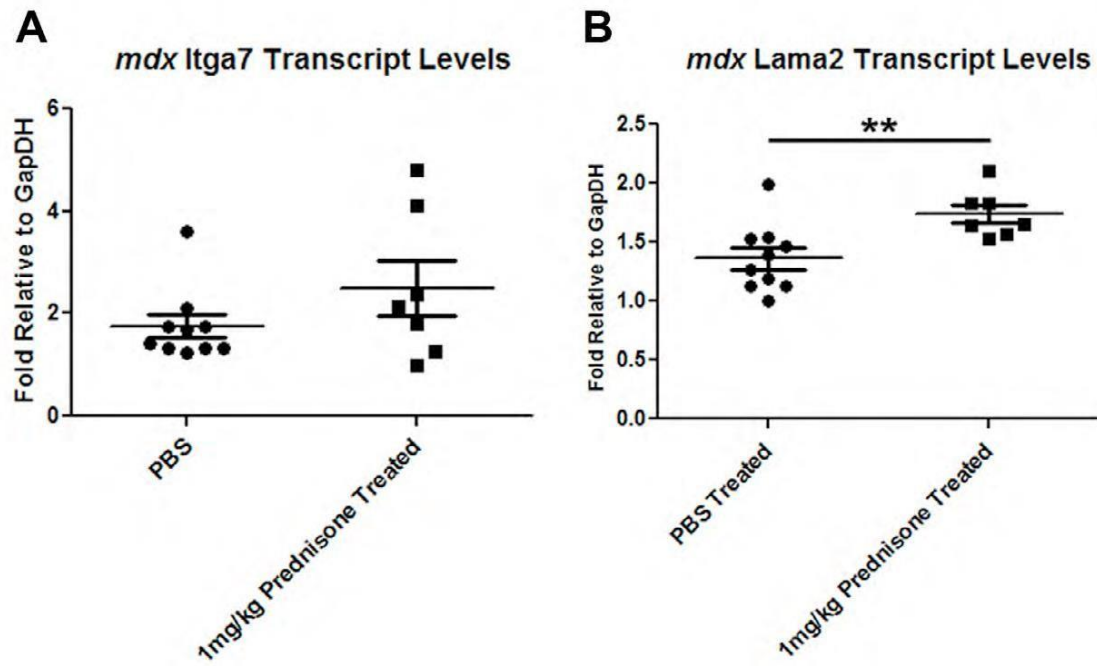
Figure S1. Quantitative real-time PCR of mouse *Itga7* (A) and mouse *Lama2* (**P=0.001) (B) from *mdx* triceps muscle.**
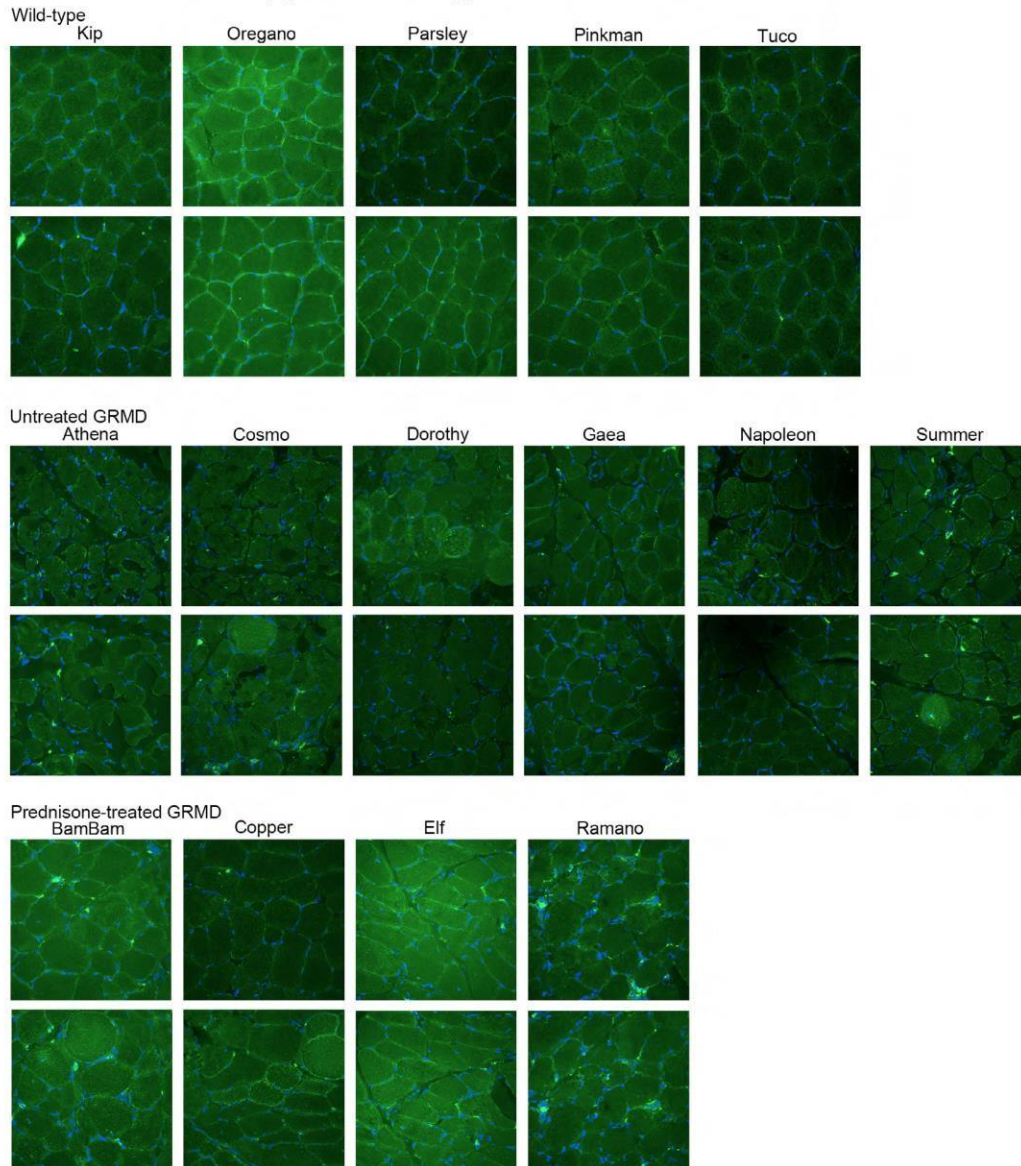
Figure S2. Immunofluorescence images from individual dogs which were used for fluorescent quantification. Images are displayed under the individual dogs name and have been grouped into wild-type, untreated GRMD, and prednisone-treated GRMD in order to better observe similarities and differences between individuals and groups. (Scale bar=50 μm).

Reprinted from Disease Models and Mechanisms:

Levels of α7 integrin and laminin-α2 are increased following prednisone treatment in the *mdx* mouse and GRMD dog models of Duchenne muscular dystrophy;

Ryan D. Wuebbles, Apurva Sarathy, Joe Kornegay and Dean J. Burkin.

Disease Models and Mechanisms 6(5): 1175–1184 Published by The Company of Biologists 2013 doi: 10.1242/dmm.012211

Chapter 3

A NOVEL α7 INTEGRIN ENHANCING SMALL MOLECULE AMELIORATES PATHOLOGY IN THE *MDX* MOUSE MODEL OF DUCHENNE MUSCULAR DYSTROPHY

ABSTRACT

Duchenne muscular dystrophy (DMD) is a catastrophic neuromuscular disease caused by mutations in the dystrophin gene. Loss of dystrophin disrupts the link between the extracellular matrix and the actin cytoskeleton leading to weakened sarcolemmal integrity. The α7 integrin encoded by the ITGA7 gene is a laminin binding protein at the sarcolemma that is elevated in the skeletal muscle of DMD patients and the *mdx* mouse model. Previous transgenic mouse studies have proven α7 integrin to be a major modifier of disease progression in mouse models of muscular dystrophy. Therefore, we hypothesized that drugs that promote α7 integrin expression in muscle would be therapeutic in the treatment of DMD. Utilizing high-throughput drug discovery technology, we identified a kinase inhibitor SU9516, as an enhancer of ITGA7 expression in our assay. We found that SU9516 increased α7B integrin protein levels in telomerized murine C2C12 and immortalized human DMD myotubes. Preclinical studies with oral delivery of 5mg/kg/day SU9516 treatments in the *mdx* mouse model ameliorated the dystrophic pathology and improved muscle force and function in the diaphragms of dystrophic mice at 10 weeks of age. Additionally, SU9516 treated *mdx* mice had elevated α7B and β1D integrin levels in both diaphragm and gastrocnemius skeletal muscle. Together, our results describe a first in-class integrin enhancing therapeutic agent SU9516 for the treatment of DMD.

INTRODUCTION

Duchenne muscular dystrophy (DMD) is one of the most common forms of muscular dystrophy affecting 1 in every 3,500 males [217,218,231]. DMD patients suffer from progressive muscle weakness, impaired mobility and premature death [2]. DMD is caused by reading frame mutations/deletions in the *Dmd* gene which prevent the normal expression of the dystrophin protein [3,4,232]. In healthy muscle, dystrophin is an integral part of the sarcolemmal stabilizing dystrophin glycoprotein complex (DGC) which links laminin in the extracellular matrix (ECM) to the myofiber actin cytoskeleton [119,233]. The DGC thus provides structural continuity between muscle fibers during contraction. The absence of dystrophin in DMD skeletal muscle leads to sarcolemmal damage during muscle contraction as the force is not appropriately distributed to the muscle fiber cytoskeleton [234]. Progressive damage results in multiple rounds of degeneration and regeneration leading to elevated levels of inflammation, necrosis, fibrosis and muscle fiber loss.

There are currently no definitive therapies available for DMD patients and the corticosteroids, prednisone and deflazacort are the only treatments available with limited positive effect [210,211,213,214,219]. Several therapeutic approaches have been developed with the aim of restoring dystrophin expression and shown efficacy in animal models of DMD. These include virally mediated gene delivery, myoblast cell transfer, exon-skipping and stop-codon read-through [91,235–243]. Many of these approaches have significant technical obstacles including delivery and immune response. Other strategies include sarcolemmal stabilization through ECM alterations (Laminin-111, Biglycan, and Galectin-1), enhanced membrane repair (MG53), anti-fibrotics (Tranilast, Imatinib,

Sildenafil), and antiinflammatories (VBP15, deflazacort, prednisone, Resveratrol, pyrrolidine dithiocarbamate (PDTC), ursodeoxycholic acid UDCA) [56,141,155,244–250]. Another alternative therapeutic approach currently being investigated is enhancement of proteins with similar functions to dystrophin or other members of the DGC/UGC (utrophin, α, β-dystroglycan, α7β1 integrin, nNOS, α,γ-SG). Transgenic overexpression of many of these proteins partially ameliorates dystrophic disease progression in mouse models of DMD [128,149,196,251–254]. Both α7β1 integrin and utrophin, function similarly to dystrophin by linking the muscle fiber actin cytoskeleton to the ECM thereby stabilizing the sarcolemma.

The α7β1 integrin protein is the predominant laminin binding integrin in skeletal, cardiac and vascular smooth muscle [165]. It is normally distributed along the sarcolemma at costameres and is elevated at neuromuscular and myotendinous junctions in skeletal muscle [166,167]. The α7β1 integrin protein has structural and signaling functions that contribute to muscle development and physiology and was originally identified as a marker for muscle differentiation [177]. Loss of the α7 integrin in dystrophin deficient *mdx* mice leads to a very severe dystrophic phenotype where mice do not survive past 4 weeks of age [198,226]. Conversely, transgenically enhanced expression of the α7β1 integrin ameliorates the development of muscular dystrophy and extends longevity in α7BX2-*mdx/utr*$^{-/-}$ transgenic mice more than three-fold [195]. Multiple mechanisms appear to contribute to α7 integrin mediated rescue of dystrophin deficient muscle including maintenance of myotendinous and neuromuscular junctions, enhanced muscle hypertrophy and regeneration, and decreased apoptosis and cardiomyopathy [175,196,230,255].

Enhanced α7 integrin also protects muscles against exercise-induced damage [197]. Interestingly, recent evidence suggests that prednisone may maintain function in the GRMD dog model by stabilizing the α7 integrin protein levels [201]. Together, these observations support the idea that the α7β1 integrin is a major disease modifier in DMD.

Recently, it was shown that systemic Laminin-111 or Galectin-1 protein treatments in the *mdx* mouse lead to elevated expression of both utrophin and α7β1 integrin [56,141]. However, the costs and delivery methods associated with protein therapeutics may be problematic for DMD patients. Therefore, a small molecule capable of enhancing α7 Integrin would be ideal. Here we report the discovery and preclinical assessment of a first in class integrin enhancing drug SU9516 for the treatment of DMD.

MATERIALS AND METHODS

Experimental design

To assess the benefits of SU9516 as a therapeutic for DMD, we conducted *in vitro* experiments to compare α7 integrin levels in murine C2C12 and human myogenic cell lines. These experiments were followed by a preclinical assessment of the drug in *mdx* mice which were treated with a dose of 5mg/kg/day SU9516 for 7 weeks. To assess the effect of SU9516 on overall muscle strength, an experimenter blinded to the experimental mice groups measured body weights and conducted weekly forelimb grip strength measurements. Additionally, *ex vivo* muscle contractility experiments were performed to quantify functional differences in the diaphragm muscles across all experimental mice. Hydroxyproline content of the diaphragm muscle was performed to

quantify fibrosis in all experimental mice. Disease markers such as centrally nucleated fiber counts and Feret's diameter of myofibers in diaphragm muscle of *mdx* mice were measured in a blinded fashion.

Cell Culture

C2C12 myoblasts were originally purchased from ATCC and grown and maintained in growth media comprising DMEM (Sigma) containing 20% FBS (Atlanta Biologicals), 1% Penicillin/Streptomycin (P/S) (GIBCO) + 1% L-Glutamine (GIBCO). Myoblasts were maintained below 70% confluence until use in assay. Myoblasts were differentiated into myotubes in DMEM, 2% horse-serum (Atlanta Biologicals), and 1% P/S + L-Glutamine. All cells were incubated at 37ºC with 5% CO_2. Assays were performed on myoblasts and myotubes between passages 8 and 14. Human DMD myoblasts were a generous gift from Dr. Kathryn North (The Royal Children's Hospital, Victoria, Australia) and used under an approved IRB from the University of Nevada, Reno. DMD myogenic cells were grown in F10 media (GIBCO, Grand Island, NY) supplemented with 20% FBS, 1% CEE, 0.5 mM $CaCl_2$, 1% L-glutamine and 1% PS. Human DMD myoblasts were differentiated to myotubes in F10 media supplemented with 2% horse serum, 1% Lglutamine and 1% PS. Statistical analysis was performed using Graphpad Prism software and unpaired t-test comparison against the DMSO control treatment group for the SU9516 treated C2C12 and human DMD myotubes.

Myoblast α7$^{+/LacZ}$ integrin FDG assay

α7$^{+/LacZ}$ myoblasts were originally isolated and maintained as described [56]. A total of 5000 α7$^{+/LacZ}$ myoblasts were dispensed in 100μL growth media using a 12-well multipipette (Rainin) onto Nunc black sided TC coated 96-well plate. After 24 hours up to 1μl of compound in DMSO was added to the myoblast plates from pre-made working drug plates using a 1μl 96-well pin tool or using an 8-well automatic multichannel pipette. Each working drug plate contained a column of a positive control (sodium butyrate (Fluka) and at least one column containing DMSO alone. After incubating for 48 hours the media was aspirated, and cells were lysed with 50μL of Mammalian Protein Extraction Reagent (MPER) (Thermo) per well followed by incubation at room temperature for 10 minutes. β-galactosidase (β-gal) activity in each well was quantified by adding 50μL of FDG assay solution (20% 0.1M sodium phosphate buffer pH 7.0 (Sigma), 0.2% 1M MgCl$_2$ (Sigma), 0.2% 20mM fluorescein di-galactoside (FDG) (Marker Gene Technologies)) and incubating the plates in the dark for 20 minutes at room temperature. Stop solution (2x TE) was then added (100μl/well) and plates were read for fluorescence on the Victor V (PerkinElmer) with an excitation filter at 485 nm, an emission filter at 535 nm, and a 0.1s/well count time.

Myotube α7 integrin FDG assay

A total of 25,000 α7$^{+/LacZ}$ myoblasts were dispensed in 100μL growth media. After 24 hours, growth media was aspirated, wells were washed with 200μL PBS, and 100μL/well of differentiation media was added. Differentiation media was changed

daily between 72 and 120 hours, and up to 1μL compounds in DMSO were added as previously described once wells contained differentiated myotubes. The FDG fluorescence assay was performed as described in the myoblast screen with the one notable exception being the incubation after FDG solution addition being shortened from 20 minute to 5 minutes at RT due to the higher levels of β-gal in myotubes.

Immunoblotting

Protein was extracted from cell pellets or tissue powdered in liquid nitrogen. RIPA was used as the lysis buffer with a 1:100 dilution of 0.5M NaF and 1M Na_3VO_4 and a 1:500 dilution of protease inhibitor cocktail. Protein was quantified using a Bradford assay and equal quantities were separated using SDS polyacrylamide gel electrophoresis. The α7B and β1D integrin were detected as was previously described [177]. Signals were detected using WesternSure[TM] PREMIUM Chemiluminescent Substrate (LI-COR). Protein loading was normalized to either α-tubulin (1:1000 mouse-monoclonal, abcam) or GapDH (1:1000, rabbit-monoclonal, Cell Signaling). Quantitation was performed using Image J software.

Quantitative RT-PCR

Total RNA from powdered mouse diaphragm muscle was isolated using Trizol (Invitrogen, Grand Island, NY) followed by a R01 DNase treatment (Promega, Madison, WI), and cDNA was made with random hexamers (IDTDNA) and Superscript III (Invitrogen, Grand Island, NY) using standard procedures. Quantitative Real-time was performed using Quanta Perfecta SYBR-Green with ROX Master Mix and were run and

analyzed as previously described [227]. Mouse primers for *mItga7* and *mGapdh* were used as previously described [227]. Mouse primers for *mLama2* were: F-ctgggagtcagcagtcagaagat and R-ctttatgccactgtccattgcaca.   Mouse primers for *mPax7* were: F-atcaagccaggagacagcttgc and R-tgtgtggacaggctcacgtttt.   Mouse primers for *mItgB1d* were: F-gaaaatgaatgccaagtggga and R-gagaccagctttacgtccata.   Mouse primers for *mMrf4* were: F-ttcttgagggtgcggatttcct and R- gcatccacgtttgctcctcctt.

Immunofluorescence

For *in vivo* immunofluorescence analysis, 10-μm sections of diaphragm and gastrocnemius muscles from mice were removed using a Leica Cryostat and immunofluorescence was performed using antibodies against α7B integrin and β1D as previously described[177], followed by FITC-donkey-anti-rabbit (1:1000, Jackson ImmunoResearch, Baltimore, MD) and mounted using Vectashield containing DAPI (H1500, Vector Laboratories, CA).   Images were taken using an Olympus Fluoview FV1000 Laser Confocal Microscope using consistent settings for all images, and intensity evaluation was performed using FV10-ASW3.1 software histogram function. Counts were averaged across all images for each group and graphed using GraphPad Prism software.

Statistical analysis and Curve-fitting

Statistical analysis was performed using Graphpad Prism software and unpaired ttest comparison against the DMSO control treatment group for the SU9516 treated

C2C12 and human DMD myotubes. Graphpad prism software was also used to fit curves using nonlinear regression analysis with log (agonist) vs. response with a variable slope. A constraint equal to 1 was placed on the bottom of the curve and either 2 or 2.5 at the top (when needed) in order to produce appropriate EC_{50} values. Averaged data are reported as the mean ± the standard error of the mean (s.e.m.). Comparison for two groups was performed using a Student's *t*-test and between multiple groups using Kruskal-Wallis one way ANOVA on ranks for nonparametric data. *P*<0.05 was considered statistically significant.

Animals

Three-week-old female *mdx* mice were treated with a daily dose of 5mg/kg SU9516 until 10 weeks of age. Forelimb grip strength data was collected every week from 5 weeks of age to 10 weeks of age as described previously. Body weight was also monitored every week. All animals were treated according to rules and regulations specified in the IACUC. At the end of the study, the diaphragm of the mice were appropriately harvested for either contractile measurements or phrenic nerve stimulation and recording studies.

Pharmacokinetic and Toxicity studies with SU9516

The robust effects of SU9516 on α7 Integrin protein levels *in vitro* led us to perform preliminary studies on the toxicity and pharmakinetics (PK) in CD1 mice. Initially, it was determined that SU9516 was soluble in 10% hydroxypropyl-β-cyclo-

dextrin (HPBCD) and 90% saline (vehicle) and could be delivered by oral gavage. Next, a PK experiment was conducted using a single 10mg/kg SU9516 dose in CD1 mice and examining serum, intestine, and muscle concentrations by mass spectrometry over the course of 24 hours.

Hydroxyproline Assay

The hydroxyproline assay was performed as described in Van Ry et al., 2015[141]. Briefly, diaphragm samples were homogenized in 500ul of 0.5 M acetic acid. Samples are centrifuged in a speed vacuum to completely dry. Samples are then hydrolyzed samples in 6 N HCL followed by heat blocking at a 110 degrees Celsius overnight. The samples were then re- suspended in citrate-acetate buffer (500 µl/10 mg tissue). 10 µl of resuspended sample were transferred into a new Eppendorf tube and 400 ul of freshly prepared Chloramine T reagent was added and mixed gently. Samples were then incubated at room temperature for 20 min. 500 ul of freshly prepared Ehrlich's reagent was then added and samples incubated at 65°C for 15 min. 200 ul of each sample was transferred to a clear 96well plate. Samples were run in triplicate and absorbance was measured at 550 nm.

Forelimb grip strength measurement

Forelimb grip strength was measured with a computerized grip strength meter (Columbus Instruments, Columbus, OH). The grip strength meter has a bar attached to a

force transducer and a digital display. The mice were first acclimated to the apparatus for approximately 5 min. Mice were then allowed to grab the pulling bar by holding it from the tip of the tail. The mouse was gently pulled away from the grip bar. When the mouse could no longer grasp the bar, the reading was recorded. Protocol was repeated six times with at least 30 sec rest between trials. Normalized grip strength was obtained by dividing the absolute grip strength with the body weight. All grip strength data collected was done so in a blinded fashion.

Isometric Contractile function

Dissection: Prior to this procedure the mice were euthanized by cervical dislocation under anesthesia. The dissection was performed as per guidelines described in mMoorwood et al., 2013. In brief, an incision was made in the skin to expose the abdominal and chest cavity. Using bone scissors, and starting above the diaphragm insertion, a cut was made around the entire rib cage following the line of the rib and through the spine. The intact diaphragm was removed from the mouse, and placed in a dissecting dish filled with oxygenated Ringers, following which a 2-4 mm strip of the diaphragm was cut from the central tendon to the ribs along the orientation of the fibers in the central portion of the lateral hemi diaphragms. Using bone scissors, the rib on either side of the strip was cut, leaving approximately 1-2 mm overhang of rib on either side of the diaphragm strip. Sutures were tied to the central tendon as well as to each of the laterally protruding rib ends, and then those were tied together to make a large loop. The uncut hemi diaphragm was embedded in a mixture of 2:3 (v/v) *OCT* and 30% sucrose.

Isometric Contraction Protocol: The optimal stimulation conditions as well as the optimal length (L_o) for the diaphragm was determined as described by Moorwood et al., 2013. At L_o the maximum isometric twitch tension as well as the maximum isometric tetanic tension (achieved at 100Hz for the diaphragm) was recorded. A force-frequency relationship study was carried out over a wide range of frequencies (10Hz-150Hz). Fatigue of the diaphragm muscle was carried out after a rest period of 10 minutes. The muscle was fatigued for a 5 minute period with a 100Hz tetanic stimulus applied after every 30 seconds. At the end of the fatigue period, the muscle was allowed to recover in the oxygenated Ringers buffer for 5 minutes after which the maximum tetanic tension was measured again at 100Hz stimulus to gauge recovery in force generated by the muscle.

After the isometric contraction experiments, the muscle was carefully removed from the transducer and returned to the dish with Ringers solution. The sutures were carefully removed from the muscle and the muscle was carefully dissected away from the bony insertion as well as the central tendon. The muscle was blotted gently and weighed. The cross sectional area was then calculated as follows: CSA (mm^2) =mass (mg)/ [(L_o mm)*(L/L_o)*(1.06 mg/mm^3)]. The ratio L/L_o is 1 for the diaphragm muscle. Diaphragm strips were then soaked in 0.1% procion orange to determine the extent of dissection damage.

Intracellular microelectrode recording post phrenic nerve stimulation

The diaphragm was dissected and pinned flat in a Sylguard lined 6 cm petri dish continuously perfused with a modified Krebs-Ringer solution maintained at 23℃. Great care was taken in order maintain a viable phrenic nerve that was then aspirated by a suction electrode where supra threshold stimulation could be applied. Following successful attachment to the suction electrode, the tissue was then incubated for 15 minutes with μconotoxin (1 μM). μ-conotoxin selectively blocks voltage-dependent Na^+ channels and possesses a much higher sensitivity for muscle versus neuronal Na+ channels. The application of this drug to the muscle essentially "paralyzes" the muscle fibers and isolated neuronal readings can be obtained free of any muscle interference. Microelectrodes filled with 3 mol/L KCl solution, had tip resistances of approximately 30-60 MΩ and were advanced into skeletal muscle fibers within 2mm of the nerve terminal. End plate potentials were amplified using an Axoclamp 900A amplifier (Axon Instruments, Foster City, CA) and digitized using Digidata 1550 (Axon Instruments) to a PC running Axoscope software (version 14.1; Axon Instruments). Following impalement of the muscle cell with μ-conotoxin, a baseline was established for 5 minutes before stimulation was applied.

Video image acquisition

Functional imaging was performed on a Nikon Eclipse FN1 upright fluorescence microscope using Nikon Plan Fluor 4x lens (Nikon, USA). Image sequences were captured using an Andor Neo (Andor Technology, Belfast, UK) sCMOS camera and captured on a Windows-based PC using Nikon NIS Elements 4.1 (Nikon, USA). Image

sequences were recorded at 25 frames per second processed as 8-bit intensity units and analyzed using in house custom written software (Volumetry G7; G.W.H.).

Drugs and solutions

Modified Krebs-Ringer solution contained (mM): NaCl, 121.0; KCl, 5.0; NaHCO$_3$, 24.0; NaH$_2$PO$_4$, 0.4; MgCl$_2$, 0.5; CaCl$_2$, 1.8; glucose, 5.5 (continuously gassed with 5% CO2–95% O$_2$, pH 7.3–7.4). μ-conotoxin was purchased from Sigma-Aldrich (St. Louis, MO, USA).

RESULTS

Identification of SU9516 as an integrin enhancing drug utilizing a high throughput drug screen

Using a mouse muscle cell-based reporter assay previously described [56] we screened the LOPAC library and identified a small molecule SU9516 that increased expression at the α7 integrin promoter. The LOPAC library consists of ~1200 drug-like molecules with known activities. SU9516 dose-response curves for myoblasts (Figure 1A) and myotubes (Figure 1B) were generated for treatments ranging from 0.5-40μM. The drug is toxic at higher concentrations. The magnitude of increased expression and concentration of maximal effect varied between myoblasts (~5μM) and myotubes (~12μM). α7 integrin protein enhancing effects of SU9516 treatments were verified by Western Blot analysis in C2C12 mouse myogenic cell lines (DMSO vs 12 μM SU9516,

*P<0.05) (Figure 1C) and in human DMD patient myotubes (20nM-10µM, *P<0.05, **P<0.01, ***P<0.001) (Figure 1D). These data demonstrate that SU9516 targets an increase in α7 integrin in mouse and patient DMD myogenic cell lines suggesting a conserved mechanism of action.

Pharmacokinetic assessment of SU9516 in CD1 mice shows low absorption.

The metabolism of SU9516 was investigated in order to select an optimal dose for initiating a preclinical study in *mdx* mice. For toxicity and pharmacokinetic (PK) studies, CD1 mice were treated via oral gavage with a dose of 10 mg/kg/day. Blood serum draws were performed post treatment over a period of 24 hours. The serum half-life- $t_{1/2}$ was 1.03 hours (supplementary Figure S1A) after a single dose of drug. This concentration appeared to be above/at the toxic limit as the CD1 mice used in the study showed torpidity 24 hours post-treatment and the entire first batch of mice died. The results also showed high levels in the intestine (low absorption) and low muscle availability with a single dose. Preliminary toxicity and western blot analyses using a dose curve treatment were carried out in WT mice to determine the dose of the drug that elucidates that maximum increase in α7 integrin. Daily treatments of vehicle, 2.5 mg/kg, 5 mg/kg and 10 mg/kg doses of SU9516 were administered via oral gavage for 4 days. A dose of 5mg/kg/day was determined to be a safe dose at which the mice are active and also show the maximum increase in α7A integrin protein levels in skeletal muscle (supplementary Figure S1B).

SU9516 promotes an increase in α7B and β1D integrin in *mdx* skeletal muscle.

In order to determine if SU9516 exhibited on target *in vivo* activity, female *mdx* mice were treated from 3 weeks to 10 weeks of age with either 5 mg/kg/day of SU9516 or vehicle alone. At 10 weeks of age, mice were sacrificed and the diaphragm and gastrocnemius tissues were examined for α7B and β1D. A 2-fold and a 2.9 fold increase was seen in α7B and β1D levels respectively in the diaphragm of *mdx* mice (P<0.05) (Figure 2 A, B and C). Protein analysis in the gastrocnemius showed a 2-fold increase in α7B (P<0.001) and a 1.7-fold increase in β1D levels (P<0.05) with SU9516 treatments compared to vehicle treated mice (Figure 2, D, E and F). Immunofluorescence analysis confirmed normal sarcolemmal localization of α7B and β1D integrin in the diaphragm and the gastrocnemius muscles (Figure 2, G and H). Together, these data show that daily oral delivery of SU9516 over a course of 7 weeks, directly leads to elevated levels of the α7β1 integrin protein in *mdx* mice.

We also performed qRT-PCR analysis on the diaphragms of the mice to determine the transcript levels of *Itga7*, Itgb1d, *Pax7*, *Lama2* and *Mrf4*. No changes were observed in the levels of Itga7, *Itgb1D* and *Pax7* transcripts (P>0.05) (supplementary Figure S2A, S2B and S2C) between vehicle treated and SU9516 treated groups. The levels of *Mrf4* in the SU9516 treated mice showed a trend towards 1.2 fold lower expression than the vehicle treated *mdx* mice (supplementary Figure S2D). Interestingly, a 1.7 fold decrease was observed for *Lama2* transcript levels (P<0.05) (supplementary Figure S2E) in SU9516 treated *mdx* mice compared to vehicle treated controls. This data suggests that SU9516 stabilizes the levels of *Lama2* and *Mrf4*

transcript toward WT levels in the diaphragm muscle of *mdx* mice potentially through a negative feedback mechanism, owing to the increase in α7 integrin protein in SU9516 treated myofibers.

SU9516 treatments improved *in vivo* outcome measures and muscle function in *mdx* mice

Over the course of preclinical treatments, the SU9516 treated *mdx* mice showed decreased body mass gain compared to vehicle treated controls at 9 and 10 weeks of age ($P<0.05$) (Figure 3A), following a trend towards WT body masses. In order to determine whether SU9516 treatment increased muscle strength we performed the forelimb grip test each week of treatment. Normalized forelimb grip strength of the sixth trial/pull showed that WT mice exhibited the greatest resistance to fatigue while SU9516 treated mice fatigued less compared to their vehicle treated counterparts in weeks 7, 8 and 9 ($P<0.05$) (Figure 3B). The average of all trials for forelimb grip strength also indicated that SU9516 treated *mdx* mice had progressive improvements in muscle function with continued treatment, compared to vehicle treated animals ($P<0.05$) (supplementary Figure S3A).

Similar to the muscles of DMD patients, the diaphragm muscles of *mdx* mice are unable to produce a normal level of developed force [256,257]. Measurements of active force developed by diaphragm muscles from WT mice, *mdx* mice treated with either vehicle or SU9516 were therefore performed in independent experiments. Results revealed that diaphragm muscles from SU9516 treated mice had higher developed tetanic

force (118.1 $\pm$ 7.914 mN/mm^2) compared with vehicle treated mice (87.5 $\pm$ 6.106 mN/mm^2) (*P<0.01) (Figure 3C).

The diaphragm muscle of SU9516 treated *mdx* mice produced higher specific force amplitudes (~26-29% increase) compared with vehicle treated counterparts at peak tension (150 Hz) as well as all other stimulation frequencies from 65Hz to 150 Hz (P<0.05 SU9516 vs Vehicle, # P<0.05, ## P<0.01 Vehicle vs WT, + P<0.05, ++ P<0.01 SU9516 vs WT) (Figure 3D). *Mdx* diaphragm muscles were also examined for fatigue as revealed by the percent decline in amplitude relative to the initial amplitude, throughout serial stimulations; no improvements in resistance to fatigue were evident in SU9516 treated *mdx* relative to vehicle treated controls (Figure 3E). WT mice showed a negligible percent of fatigue compared to all the *mdx* mice in both treatment groups which fatigued to ~80% of the initial amplitude. However, after ten minutes of recovery post the fatigue protocol, the SU9516 treated *mdx* diaphragms recovered to a greater extent (~8%) compared to the vehicle treated diaphragms (P<0.05) (Figure 3F).

In addition to *ex vivo* studies utilizing the diaphragm, *in vivo* muscle function tests with direct electrical stimulation of the plantar flexors was performed to assess improvements in muscle function in other muscle groups. There was a strong trend towards increased muscle isometric tetanic tension in the SU9516 treated *mdx* compared to the vehicle treated counterparts (P=0.06) (supplementary Figure S3B). Taken together, these results indicate that the small molecule compound SU9516 and its ability to target the α7β1 integrin signaling pathway in skeletal muscle could be of tremendous clinical significance for DMD.

SU9516 improved neuromuscular kinetics of the *mdx* hemidiaphragm

Next, we sought to determine whether improvements in active force developed in SU9516 treated diaphragms could be attributed to underlying changes in neuromuscular transmission. Diaphragm muscle contractions were evoked through phrenic nerve stimulation at 10, 20 and 40 Hz frequencies, and several parameters related to neuromuscular transmission were measured. Contractions were video recorded and post process analyzed using in house designed custom algorithms (Volumetry G7, G.W.H.). Representative traces of the contractile response of the diaphragms are depicted in Figure 4A. **WT:** At 10Hz stimulation, a small amplitude sustained (<100 μm) contraction with superimposed phasic contractions was observed. At 20Hz stimulation a much larger contraction occurred, peaking 10-20s after the onset of stimulation then decaying until the end of the stimulation. All preparations showed some degree of hysteresis at ~20 Hz stimulation as the repeat stimulation at the same frequency resulted in significantly less distortion being produced. 40Hz stimulation consistently produced smaller contractile responses compared to 20Hz, however the decay rate of contraction was similar. **Vehicle *mdx*:** The trace for a vehicle treated *mdx* mice showed response similar to WT at 10Hz stimulation, but with noticeable hysteresis/inhibition between stimulations. At 20Hz, there was a reduced peak and rapid decay of contraction, with apparent loss of structural integrity or resting tone (see negative displacement values during stimulation). 40Hz stimulation did not evoke any contractile response. **SU9516-*mdx*:** SU9516-treated mice showed a robust contractile response to 10Hz stimulation, albeit with some hysteresis/inhibition observed in the repeat stimulation. The contractile response to 20

and 40 Hz were similar consisting of a smaller peak contraction and slow decay, but contraction was maintained during the course of the stimulation.

At 10Hz and 20Hz frequencies no differences in peak amplitudes were observed between vehicle and SU9516 treated animals, however at 40 Hz frequency, the average peak amplitude attained by the SU9516 treated diaphragms was higher than the vehicle group by ~2.6-fold (P<0.05) (Figure 4B). Analysis of the integrated area under the curve (AUC) from the contractile responses showed trends towards increased AUC composites for SU9516 treated diaphragms compared to vehicle treated controls (P=0.07 for SU9516 vs Vehicle at 40Hz) (Figure 4C).

End plate potentials (EPPs) were recorded by an intracellular recording electrode at 10, 20 and 40Hz frequencies; time to 50% EPP amplitude from peak EPP amplitude during 10 Hz stimulation did not vary between WT, vehicle and SU9516 treated animals; and did not reach 50% of peak amplitude within the first 60 seconds of stimulation (Figure 4E). However at 20 Hz stimulation frequencies the vehicle treated *mdx* EPP reached 50% of peak amplitude significantly faster (20Hz: WT 88.77 ± 3.84 s, vehicle 44.11 ± 2.06 s, SU9516 57.11 ± 2.71 s, n=3, P<0.01; 40Hz: WT 46.33 ± 2.96 s, vehicle 22.0 ± 2.25 s, SU9516 30.29 ± 4.55 s) (Figure 4D and E).

The resting membrane potential (RMP) in dystrophic fibers is approximately 3 to 8 mV less negative than in age-matched non dystrophic fibers [258–260]. Intracellular recordings of the muscle fibers in diaphragms of all experimental animals showed that while the RMP was higher in WT compared to the *mdx* mice, SU9516 treated *mdx* showed a recovery in RMP compared to vehicle treated dystrophic fibers (P<0.05)

(supplementary Figure S4A). Another parameter that was measured was the miniature end plate potential (MEPP) which is the response generated by a single acetylcholine containing vesicle. While some electrophysiological studies have shown large reductions in MEPPS in adult *mdx* mice, compared with controls [260], one previous investigation reported only a statistically insignificant trend toward reduced MEPP in *mdx* muscles [261]. Our results corroborate a decreased trend in *mdx* myofibers compared to WT; SU9516 restores the MEPP in *mdx* myofibers towards WT levels (supplementary Figure S4B). The experiments results from the phrenic nerve stimulation of the mice diaphragms are summarized in Table1. Taken together, these results show that treatment with SU9516 aids in restoration of RMP in dystrophic fibers and alleviates the deficit in neuromuscular transmission observed in DMD.

SU9516 improves regeneration and ameliorates pathology in the *mdx* diaphragm

Histopathological analysis of the diaphragm showed a 5.5% increase in the percentage of centrally nucleated myofibers of SU9516 treated *mdx* diaphragm compared to vehicle treated diaphragms (*P<0.05) (Figure 5A). Additionally, immunofluorescence analysis indicated a 3.3% increase in the percentage of embryonic myosin heavy chain (eMHC) positive fibers in the SU9516 treated group compared to the vehicle treated controls (*P<0.05) (Figure 5B and C). Minimum Feret's diameter of fibers through the length of the diaphragm, showed a trend of larger fibers in the SU9516 treated *mdx* muscles compared to the vehicle treated group and this distribution more closely followed the fiber size distribution in the diaphragm of WT mice (Figure 5D). Hydroxyproline assay and Sirius Red staining for collagen was performed on the

diaphragms of the *mdx* mice. The hydroxyproline assay showed a trend towards decreased hydroxyproline content in the SU9516 treated tissues however this change was not significant (P>0.05); Sirius red staining showed a decreased area of collagen as quantified by Image J (Figure 5E and supplementary Figure S5). Together these results indicate SU9516 improved muscle regeneration and reduced pathology in dystrophin deficient muscle.

DISCUSSION

This study is the first of its kind to present evidence of the benefits of using an integrin enhancing therapeutic in the *mdx* mouse model of DMD. SU9516 is an indolinone compound, which has been shown to be a potent inhibitor of CDK2 along with a host of other kinases [262]. *In vitro* experiments in this study showed that SU9516 increased the protein levels of α7B integrin in human DMD patient and C2C12 myogenic cells, thereby demonstrating that the drug has a conserved mechanism of action in murine and human species. Additionally, a seven week treatment of 5mg/kg/day SU9516 increased the protein levels of α7B and β1D integrin in the skeletal muscle of dystrophin-deficient *mdx* mice, thereby demonstrating *in vivo* on-target activity. In DMD patients, the skeletal muscles progressively weaken, pathology is severe and patients lose their ability to walk by 8 years of age. In *mdx* mice, however, the dystrophic pathology in most skeletal muscles is comparatively mild and plateaus post 3 months of age. In contrast, the *mdx* diaphragm is more severely and progressively affected in *mdx* mice and thus is more representative of the muscle pathology in DMD

patients [14]. Hence, in our study, the diaphragm muscle of mdx mice was selected for the evaluation of therapeutic benefit of SU9516.

Functional tests performed on the experimental mice included the forelimb grip strength measurement tests. Our results showed that while all the experimental *mdx* mice started off with no significant differences between groups during the early period of treatment. However, continued SU9516 treatment showed significant improvements in the forelimb strength exerted by the *mdx* mice compared to the vehicle treated *mdx* group, in the later phase of the treatment regime. The *ex vivo* muscle contraction experiments performed in the diaphragms of *mdx* mice showed that SU9516 increased the specific force developed by the *mdx* diaphragm. A fatigue protocol applied to the diaphragm muscle across all experimental groups showed that although all *mdx* mice fatigued to 80% of their initial force, the SU9516 treated diaphragms were able to recover from fatigue by an 8% margin over the vehicle treated group. Additionally, phrenic nerve stimulation and intracellular recordings of the myofibers in the diaphragm that the SU9516 treated *mdx* muscles showed greater success in peak amplitude attained and had improved resting membrane potential (RMP).

Dystrophin in addition to maintaining sarcolemmal integrity is also thought to maintain intracellular homeostasis. Dystrophic membranes have depolarized resting membrane potentials [259,263–265] that could be attributed to higher resting intracellular free Ca^{2+} concentrations, in skeletal muscle cells from *mdx* mice and DMD patients compared with normal cells [266–270]. It is possible that elevation of the α7β1 integrin complex with SU9516 treatment restores intracellular Ca^{2+} levels in *mdx* myofibers and improvements

in parameters like peak amplitude, time to 50% EPP and RMP, could be attributed to restored Ca^{2+} signaling with SU9516 treatment. In addition to functional improvements, SU9516 also showed improvements in myofiber regeneration and a decrease in fibrosis with treatment. Together, these improvements in histopathology and function could be attributed to the increased expression of α7β1 integrin at the sarcolemma of muscle which helps restore the sarcolemmal integrity in the *mdx* muscle.

This study demonstrates for the first time a small molecule integrin enhancing compound prevents the progression of muscle disease in the *mdx* mouse model of DMD. This therapeutic may have implications for the treatment of DMD and other muscular dystrophies. Two small molecules which have a similar backbone structure to SU9516 have entered clinical trials for colorectal cancer (SU5416/semaxinib) or have been given FDA approval multi-targeted receptor-tyrosine kinase inhibitors for the treatment of renal cell carcinoma and gastrointestinal stromal tumor (SU11248/Sunitinib). Given that these related compounds are undergoing or have completed clinical trials for other indications, SU9516 or an analog may be a candidate to fast track for the treatment of DMD.
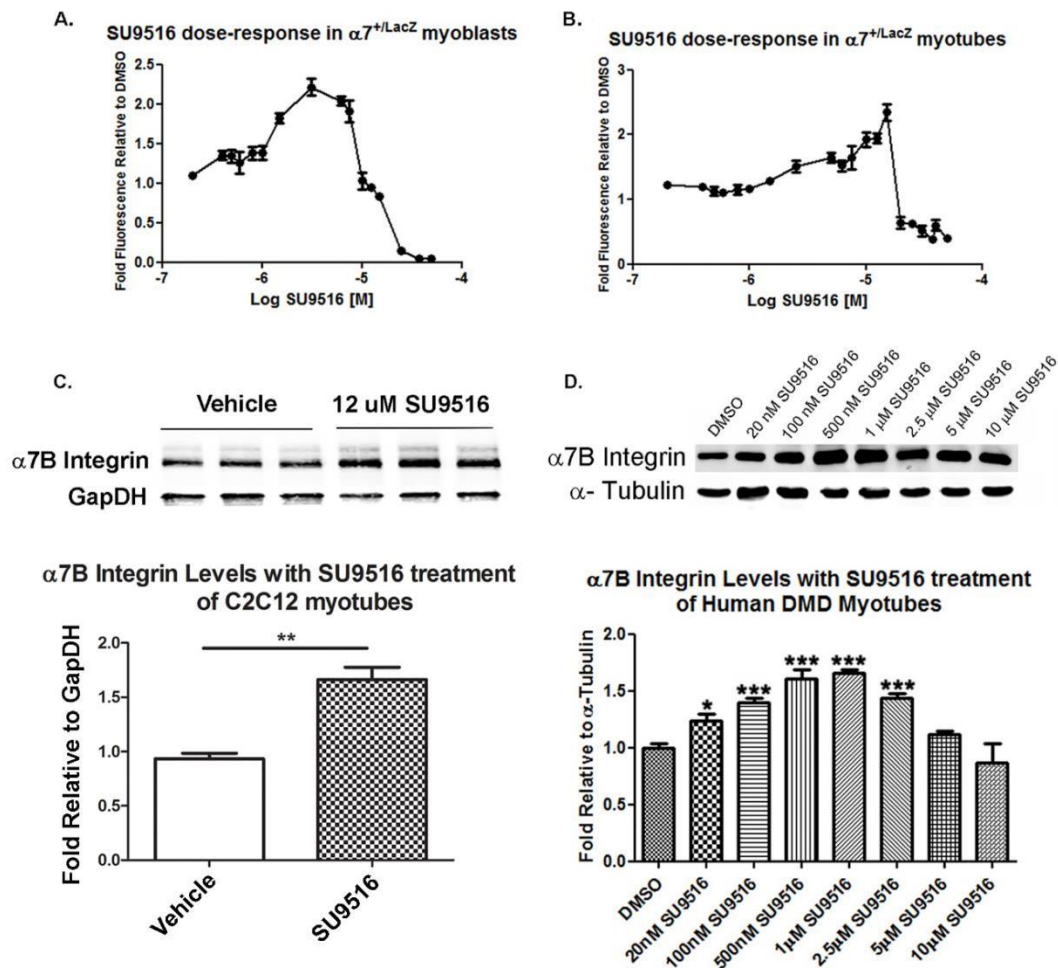
Figure 1: Identification of a novel α7 integrin drug utilizing myogenic cell lines. SU9516 shows an increase in β-Galactosidase activity in (**A**) α7 [+/lacZ] myoblasts and (**B**) α7 [+/lacZ] myotubes over a wide range of concentrations. Western blot analysis confirmed that treatment with 12 μM SU9516 increased the levels of α7B integrin post 48 hrs in (**C**) C2C12 myotubes (n=3). SU9516 increased the levels of α7B integrin in telomerized human DMD patient myotubes over a wide range of concentrations (n=3/conc.). ***P<0.001, **P<0.01, *P<0.05
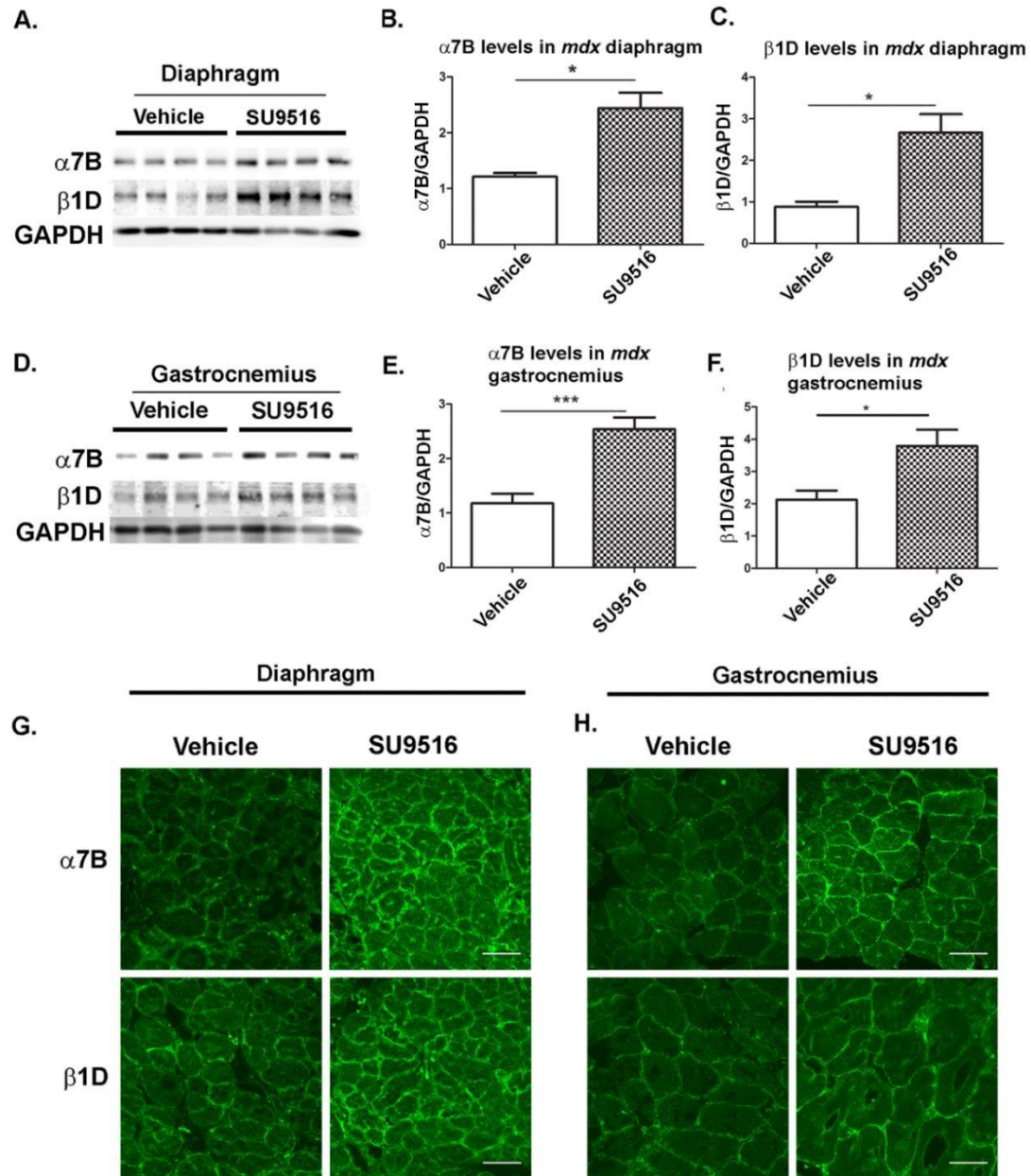
Figure 2: SU9516 increases α7β1 integrin levels in the skeletal muscle of *mdx* mice.

Western blot analysis performed in the diaphragm and the gastrocnemius muscle of

10week old *mdx* mice showed (**A**) an increase in levels of α7B and β1D integrin in the

diaphragm of the SU9516 treated *mdx* mice. This increase is quantified in (**B**) where an

~2-fold increase in α7B and an (**C**) ~3.4 fold increase in β1D was observed in the diaphragm of SU9516 treated *mdx* mice. (**D**) Western blot analysis in the gastrocnemius showed an increase in levels of α7B and β1D integrin in SU9516 treated *mdx* mice. These increases were quantified in (**E**) where an ~2 fold increase in α7B and an (**F**) ~1.7 fold increase was observed in SU9516 treated *mdx* mice. Immunofluoresence performed on 10 μm cryosections for α7B and β1D integrin in (**G**) the diaphragm and (**H**) the gastrocnemius muscle of *mdx* mice showed sarcolemmal localization. (N=4 diaphragms/group, N=4-6 gastrocnemius/group, *P<0.05, ***P<0.001)
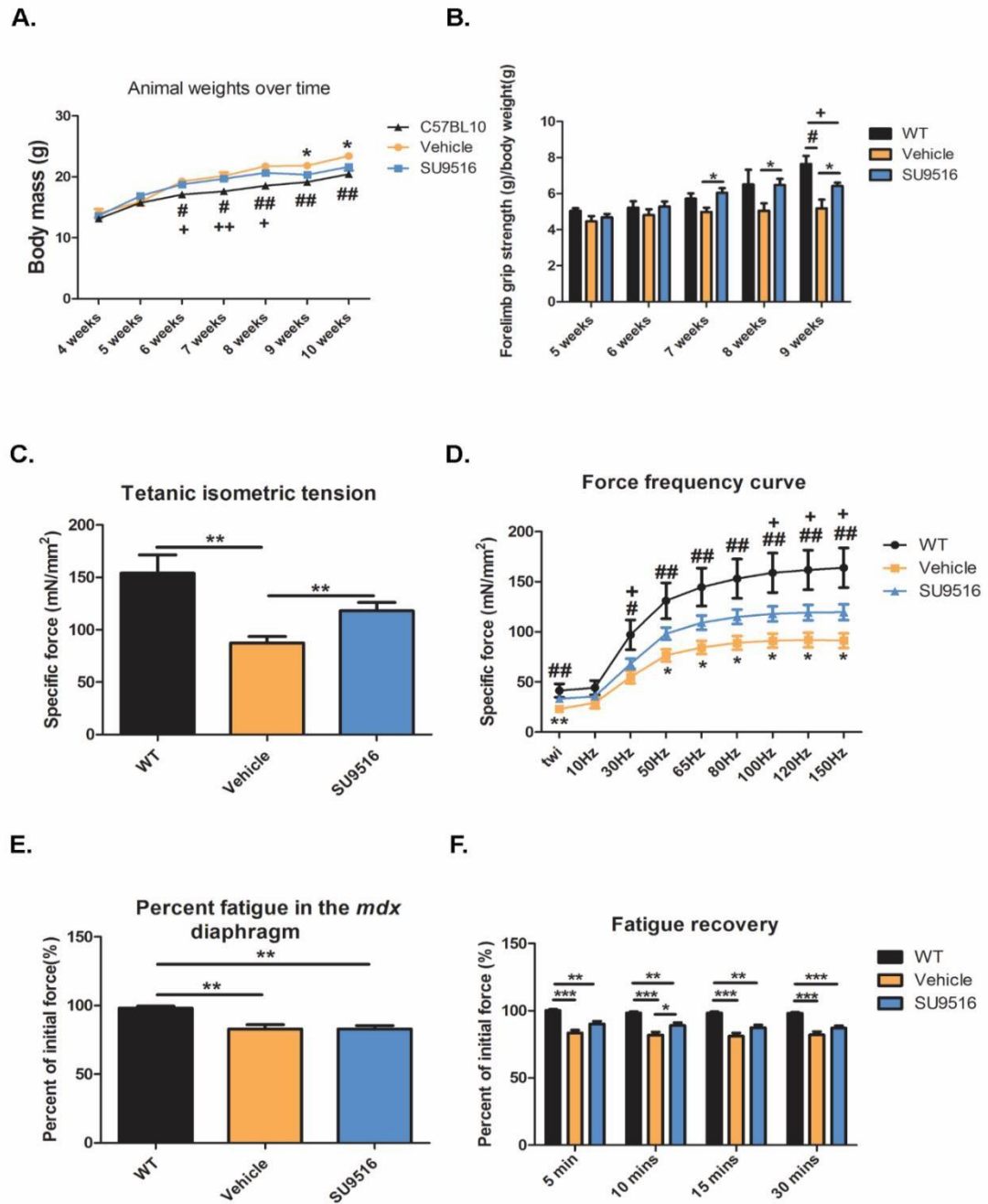
Figure 3: SU9516 improves *in vivo* outcome measures and diaphragm muscle function in the *mdx* mice. A) SU9516 treated mice showed a smaller gain in body mass

compared to vehicle treated controls in weeks 9 and 10. WT animals showed the least increase in body weight over time. Forelimb grip strength performed weekly by an experimenter blinded to the experimental groups showed that **B)** SU9516 treated *mdx* mice showed greater resistance to fatigue compared to vehicle treated *mdx* mice as represented by the force in the sixth trial/pull of forelimb grip force. **C)** At 10 weeks of age, mouse diaphragm muscle function was assessed in an *ex vivo* contraction protocol. At a 100Hz tetanic stimulus, SU9516 treated *mdx* mice showed significantly greater isometric tetanic tension compared to vehicle treated controls. **D)** A force-frequency protocol to measure tetanic tension generated by the diaphragm over a wide range of frequencies showed that SU9516 treated diaphragms produced significantly higher tension compared to vehicle treated diaphragms during twitch and 50-150Hz frequencies. **E)** *Mdx* diaphragms in both SU9516 and vehicle treated groups fatigued to ~80% of the initial force. **F)** SU9516 diaphragms recovered by ~8% compared to vehicle, 10 minutes post recovery from fatigue.*P<0.05,

P<0.01, ***P<0.001. In **(A) Body weights and **(D)** Specific force: #P<0.05, ##P<0.01 Vehicle vs wt, +P<0.05 SU9516 vs WT, ++P<0.01
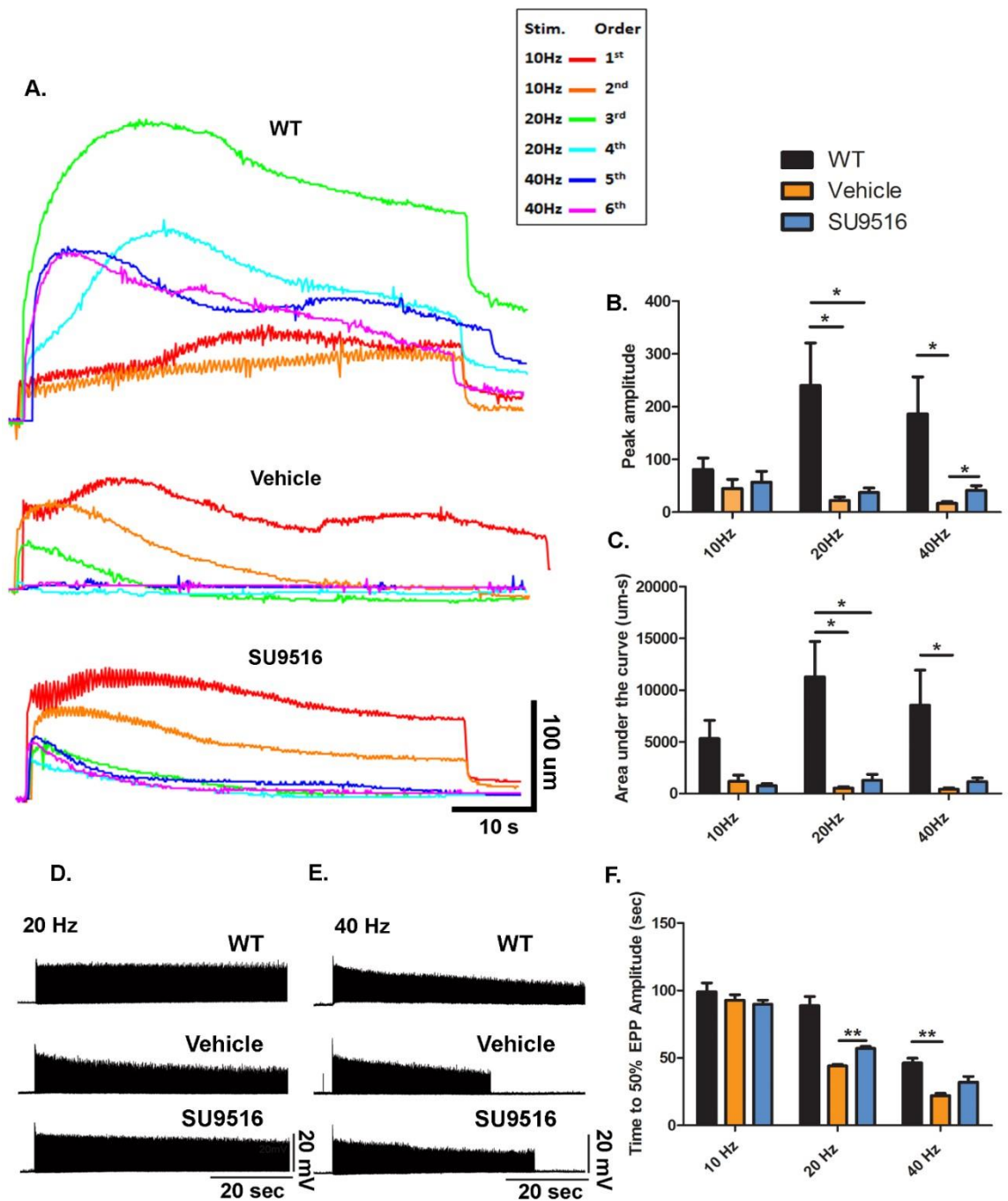
Figure 4: Contraction of diaphragm to phrenic nerve stimulation in wild type, vehicle and SU9516-treated mice. **A)** Traces of the contractile response of diaphragms

from a WT, vehicle and SU9516 treated *mdx* mouse to repeated stimulations at 10, 20 & 40Hz for ~40s. **B)** WT mice showed greater peak amplitude compared to *mdx* mice in both treatment groups. SU9516 treated *mdx* mice showed a higher peak amplitude at 40Hz stimulation compared to vehicle treated *mdx* mice (N=5, *P<0.01). **C)** The composite integration of the area under the curve showed trends towards increases in the SU9516 treatment group compared to the vehicle treated group at 20 and 40 Hz stimulations (N=4,P>0.05). Action potential trains for all experimental groups are depicted in **D)** 20 Hz and **E)** 40 Hz. **F)** Time to failure or time to 50% of the first end plate potential (EPP) in the stimulation train indicated that the SU9516 treated *mdx* mice showed an increase in time to failure compared to the vehicle treated counterparts. (N=3/group, *P<0.01).

	WT	*MDX* + Vehicle	*MDX* + SU9516
Resting Membrane Potential (mV)	73.9 ± 0.96	63.7 ± 1.04	69.18 ± 0.85 p<0.001
Peak EPP Amplitude (mV)	28.24 ± 0.88	27.66 ± 0.86	26.69 ± 0.34 p=ns
EPP Duration (ms)	23.95 ± 0.39	24.52 ± 0.32	24.36 ± 0.26 p=ns
Peak MEPP Amplitude (mV)	1.71 ± 0.04	1.33 ± 0.06	1.63 ± 0.08 p<0.005
MEPP Duration (ms)	10.84 ± 0.55	7.76 ± 0.57	8.41 ± 0.52 p=ns
Time to 50% amplitude 10Hz (s)	99.11 ± 3.68	92.88 ± 4.05	89.78 ± 2.81 p=ns
Time to 50% amplitude 20Hz (s)	88.78 ± 3.84	44.11 ± 2.06	57.11 ± 2.71 p<0.005
Time to 50% amplitude 40Hz (s)	46.33 ± 2.96	22.0 ± 2.25	30.29 ± 4.55 p=ns

Table 1- Neuromuscular parameters measured post phrenic nerve stimulation of diaphragm.   This table summarizes the parameters measured in the neuromuscular kinetic experiments performed via phrenic nerve stimulation of the diaphragm of experimental mice. p values indicate level of significance between the SU9516 vs Vehicle treated *mdx* mice.
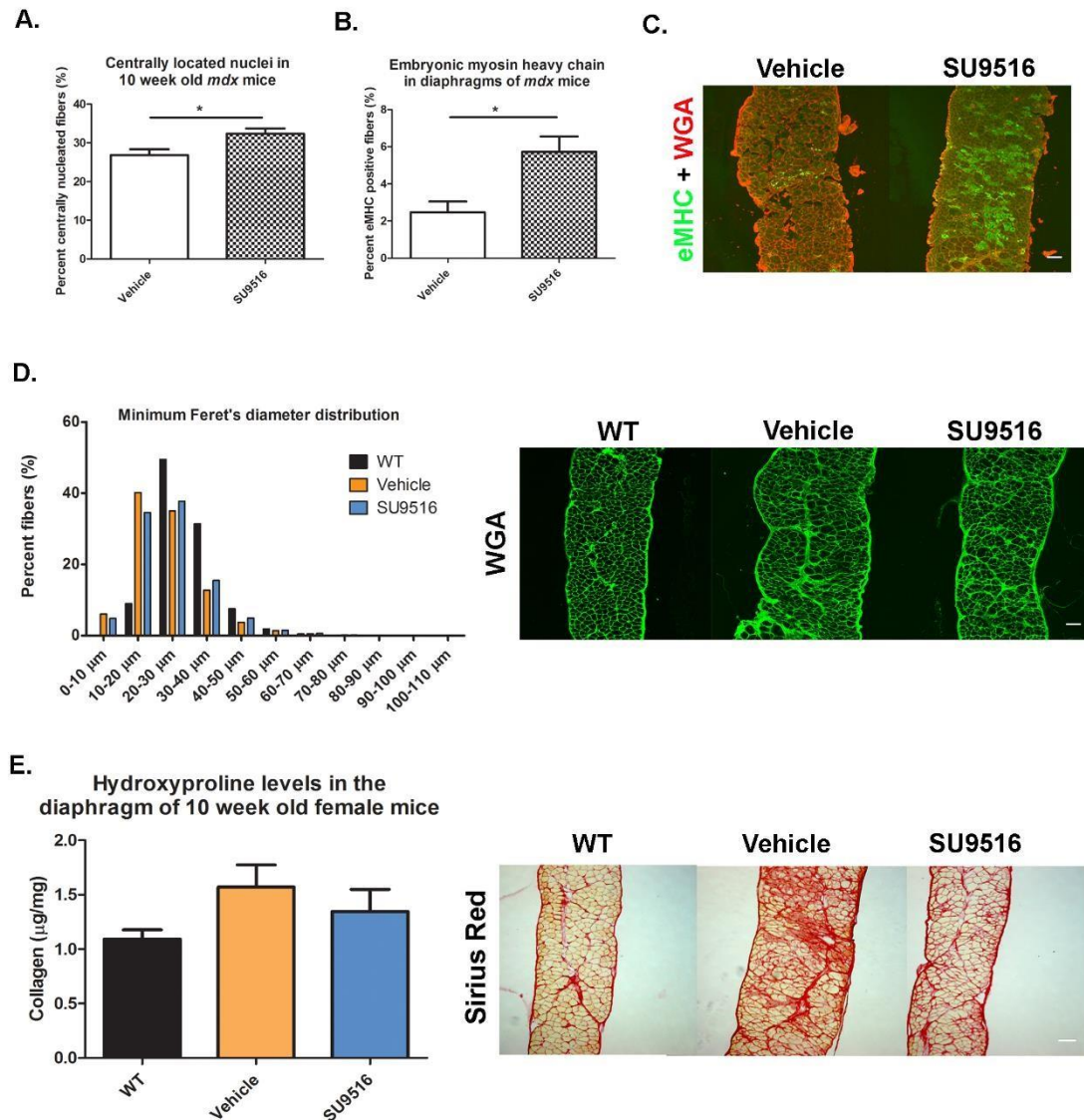
Figure 5: SU9516 treatment ameliorates disease pathology in *mdx* mice. A) SU9516 treated *mdx* diaphragms showed a 5.5% increase in the percent of centrally nucleated fibers over vehicle treated diaphragms. **B)** The percentage of embryonic myosin heavy chain (eMHC) positive fibers in the diaphragm of SU9516 treated *mdx* was higher than the vehicle treated *mdx* by 3.3%. **C)** eMHC staining in immunoflorescence images of

diaphragms from vehicle and SU9516 treated *mdx* mice. SU9516 treated diaphragms show an increase in eMHC positive fibers. **D)** Fiber size distribution in the diaphragm of WT, vehicle and SU9516 treated mice was assessed utilizing 10 µm cryosections stained with wheat germ agglutinin followed by minimum Feret's diameter measurements. The distribution of fiber size in SU9516 treated diaphragms shifted towards larger myofibers following the trend towards WT fiber size distribution. **E)** Hydroxyproline content was non-significantly reduced in SU9516 treated *mdx* diaphragms compared to vehicle treated controls (P=0.46). Sirius Red staining showed a decrease in collagen positive areas within the SU9516 treated *mdx* diaphragm cross-sections. Magnification 10X Scale Bar =100 µm (N=3-4 WT, N=5-7/*mdx* treatment group. *P<0.05). Scale bar =100 µm.

A.

Serum PK of 10 mg/kg SU9516 in CD1 mice

B.

| | 1 | 2 | 3 | 4 |

α7A

α-Tubulin

1 = Vehicle
3 = 5mg/kg/day SU9516

2 = 2.5mg/kg/day SU9516
4 = 10 mg/kg/day SU9516
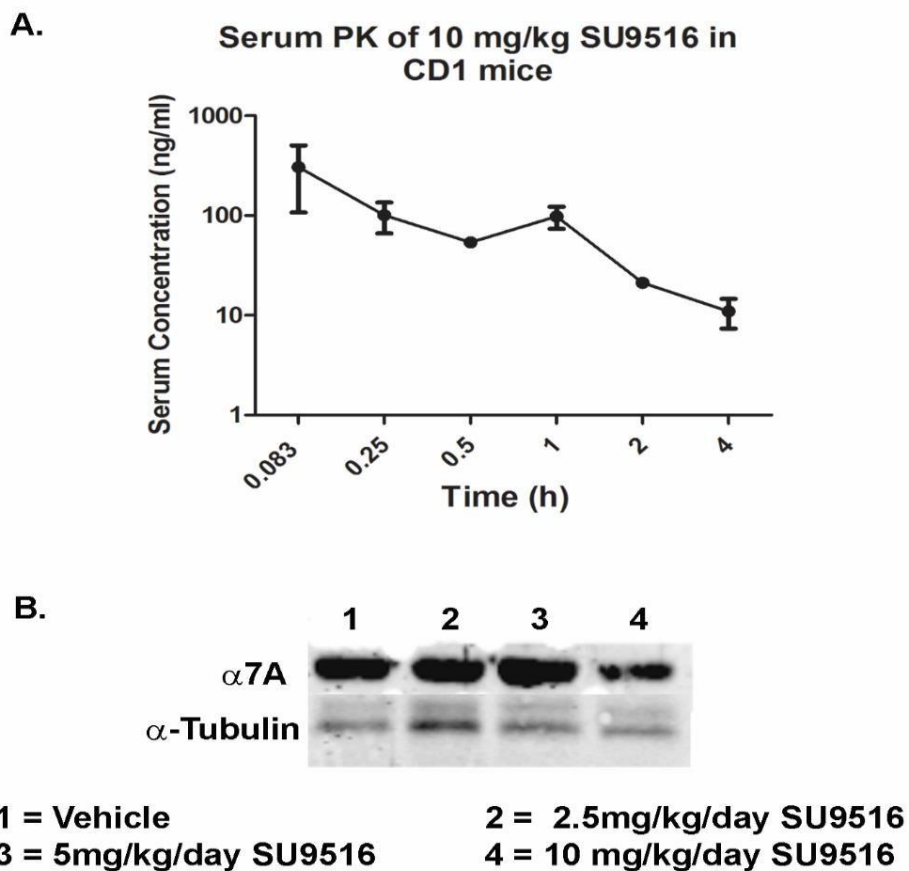
Fig. S1. Serum Pharmacokinetics and optimal drug dose for SU9516. **(A)** The serum concentrations of SU9516 over the course of 4 hours after the administration of a single 10 mg/kg dose via oral gavage. **(B)** WT mice were administered four doses of drug for a period of one week and the 5 mg/kg/day SU9516 treatment resulted in the maximum increase in integrin α7A in the gastrocnemius muscle.
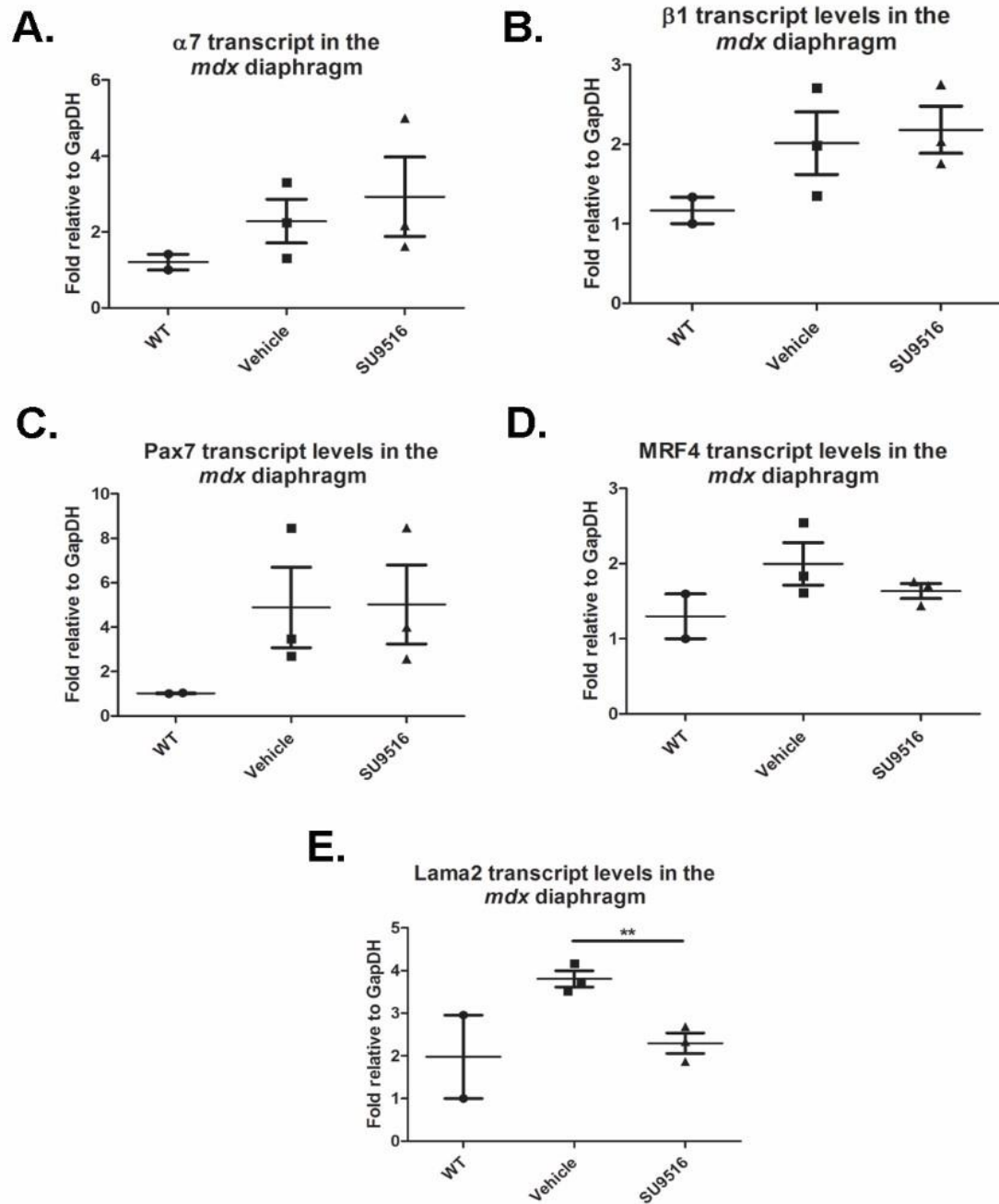
Fig. S2- SU9516 decreases the level of Lama2 transcript in *mdx* diaphragms. qPCR

analysis was performed on the diaphragms of mice across all experimental groups**.**

SU9516 showed no significant changes in the transcript levels of **A)** α7 **B)** β1 **C)** Pax7.

D) A strong trend towards a decrease in myogenic regulatory factor 4 (MRF4) was observed in the diaphragm of SU9516 treated mice. **E)** A significant decrease in transcript levels of LAMA2 was observed in the SU9516 treated mdx diaphragms compared to the vehicle treated controls, n=2 WT, n=3/treatment group, **P<0.01.

A.

B.
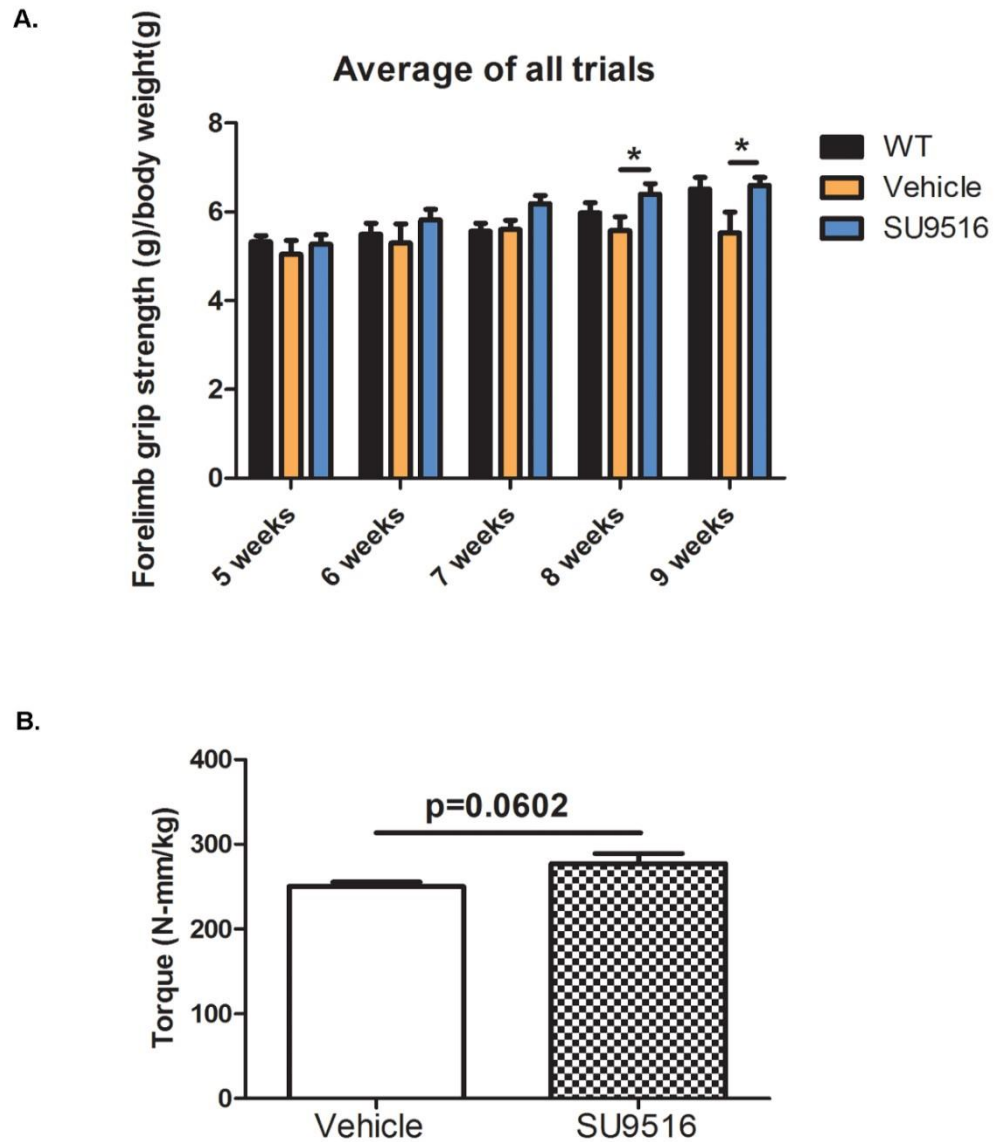
Figure S3- SU9516 treatment improves muscle function in *mdx* mice. **(A)**The average of all forelimb grip strength trials showed a significant increase in the SU9516 treated mice compared to vehicle treated controls, WT n=6, n=14 *mdx*/treatment

*P<0.05. **(B)** An *In vivo* isometric contraction experiment that stimulates the plantar flexor group of muscles and measures force output showed that SU9516 treated mice showed a strong trend towards improved torque compared to their vehicle treated counterparts n=4/*mdx* treatment group, P=0.06.

A.
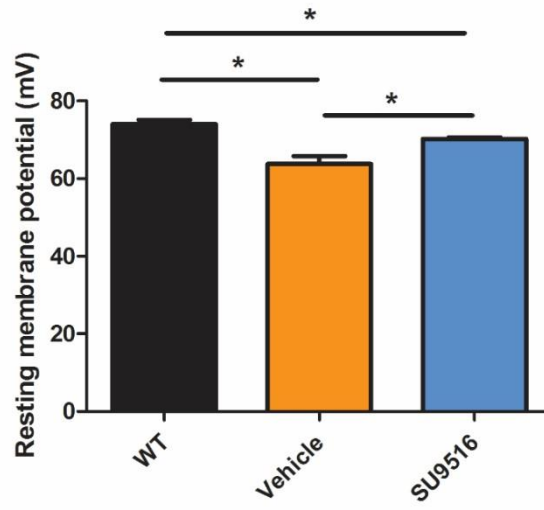
B.
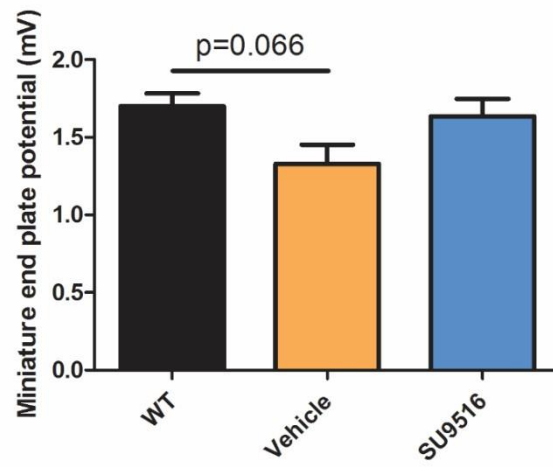
Figure S4- SU9516 improves the resting membrane potential in *mdx* muscle fibers.

(A) SU9516 treatment increases the resting membrane potential of mdx myofibers towards WT levels, n=3**,** *P<0.05 **(B)** SU9516 treatment increases miniature end plate potentials in *mdx* myofibers towards WT levels.
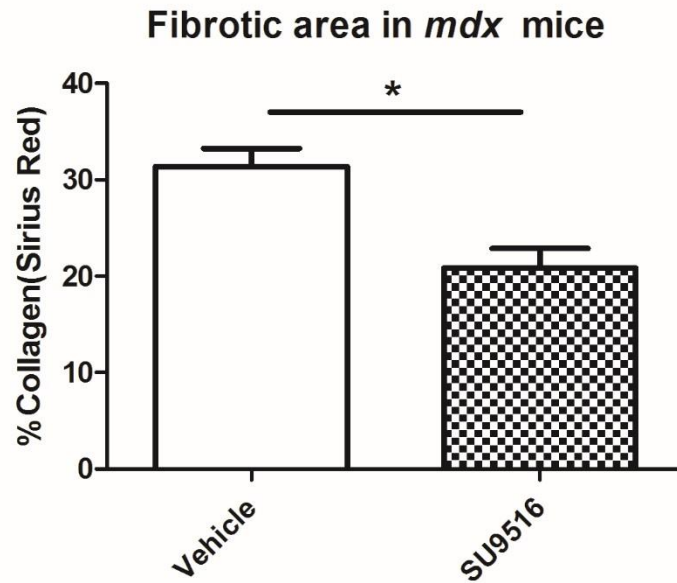
Figure S5- SU9516 treatment decreases Sirius Red positive area in *mdx* diaphragms. Image J was used to quantify the fibrotic area in the diaphragms of *mdx* mice. SU9516 treated diaphragms showed a smaller percentage of fibrotic area compared to the vehicle treated group, n=5, *P<0.05

Chapter 4

THE MOLECULAR TARGETS OF SU9516 IN SKELETAL MUSCLE

ABSTRACT

The α7β1 integrin is a heterodimeric receptor in skeletal muscle that also links laminin to the actin cytoskeleton. Studies have shown that transgenic overexpression of the α7 integrin alleviates disease progression and improves survival of mouse models of DMD, while loss of the α7 integrin in dystrophin-deficient *mdx* mice exacerbates muscle disease. Together, these results support the hypothesis that the α7β1 integrin is a major modifier of disease progression in DMD and a target for drug-based therapies. Utilizing a high throughput chemical screen developed in our lab, we identified a potent integrin enhancing drug called SU9516 that increased the levels of α7B in both murine and human DMD patient cells. Previously, preclinical studies showed there was a significant improvement in diaphragm muscle contractility and forelimb grip strength of *mdx* mice treated with a 5 mg/kg/day dose of SU9516 from 3 weeks to 10 weeks of age. Additionally, analysis of muscle tissue via western blot showed an enhanced expression of α7B and β1D integrin protein in the skeletal muscle of SU9516 treated mice. The current study shows that *in vitro* treatment of SU9516 in C2C12 myoblasts downregulated the expression of MAP4k4 which led to enhanced fusion of myoblasts during differentiation. Additionally, the kinase targets of SU9516 in human DMD patient cells were determined using KiNativ technology. The mechanism by which the drug enhances α7B integrin in muscle was investigated in this chapter and our results demonstrate that the therapeutic benefits of SU9516 are likely brought about by its kinase inhibitor activity including the inhibition of the p65-NF-κB pathway. Hence, the small molecule integrin enhancing compound SU9516 could serve as a novel pharmacological therapeutic in the treatment of DMD.

INTRODUCTION

Duchenne muscular dystrophy (DMD) is one of the most common forms of muscular dystrophy affecting 1 in every 3,500 males [218,231]. DMD patients suffer from progressive muscle weakness, impaired mobility and premature death [2]. DMD is caused by reading frame mutations/deletions in the *DMD* gene which prevent the translation of the dystrophin protein [3,4,232]. In healthy muscle, dystrophin forms a scaffold upon which the dystrophin glycoprotein complex (DGC) forms and links laminin in the extracellular matrix (ECM) to the actin cytoskeleton [271], thereby providing structural integrity to skeletal and cardiac muscle. The absence of dystrophin in DMD leads to loss of the DGC that causes sarcolemmal fragility and muscle damage during muscle contraction. Progressive damage results in inflammation, necrosis, fibrosis and muscle weakness. There is currently no effective treatment or cure for DMD.

Several therapeutic approaches have been developed with the aim of restoring dystrophin expression and shown efficacy in animal models of DMD. These include virally mediated delivery and expression of dystrophin, myoblast cell transfer and engraftment, exon-skipping and stop-codon read-through [91, 228–236,247]. Currently, none of these methods have been approved as therapies for DMD patients. An alternative approach is to target and enhance levels of proteins which modify disease progression and act to partially compensate for the absence of dystrophin [272]. These disease modifiers include utrophin, IGF-1, α7β1 integrin, GalNac, nNOS and Adam12[87,128,134,195,252,253,273,274].

The α7β1 integrin is the predominant laminin binding integrin in skeletal, cardiac and vascular smooth muscle [165]. It is distributed along the sarcolemma at costameres and is localized at neuromuscular and myotendinous junctions in skeletal muscle [166,167]. The α7β1 integrin has structural and signaling functions that contribute to muscle development and physiology and was originally identified as a marker for muscle differentiation [163,177]. Loss of the α7 integrin in dystrophin deficient *mdx* mice leads to a more severe dystrophic phenotype and reduced viability with mice dying prematurely by 4 weeks of age [198,226]. Conversely, it was reported that enhanced expression of the α7β1 integrin ameliorates the development of muscular dystrophy and extends longevity in α7BX2- *mdx/utr*^{-/-} transgenic mice more than three-fold [195]. Multiple mechanisms appear to contribute to α7 integrin mediated rescue of dystrophin deficient muscle including maintenance of myotendinous and neuromuscular junctions, enhanced muscle hypertrophy and regeneration, and decreased apoptosis and cardiomyopathy [196]. Enhanced α7 integrin also protects muscles against exercise-induced damage [197]. Together, these observations support the idea that the α7β1 integrin is a major disease modifier in DMD.

To translate transgenic mouse studies into potential therapies for DMD, we initiated a drug discovery program to identify chemical probes that increase α7 integrin in skeletal muscle. We have previously reported on the generation and characterization of an α7 integrin knockout line of mice [204] in which the LacZ gene is inserted into intron 1, downstream of the endogenous α7 integrin promoter. Thus, β-galactosidase functions as a reporter for α7 integrin expression in these animals. Primary myogenic cells were

isolated from a heterozygous mouse ($\alpha7\beta gal^{+/-}$) so that the cells express $\alpha7$ integrin and also report for transcription of the integrin. The myogenic reporter cells were designated $\alpha7\beta gal^{+/-}$ and were used to identify two molecules, valproic acid and laminin-111, in preliminary screens and have been successfully tested in mouse models of DMD [56,205]. A drug called SU9516 was one of the top compounds identified through this drug screen and our *in vivo*-studies with the drug in *mdx* mice (described in Chapter 3) are proof-of-principle for the use of *in vitro* screening methods in allowing identification of pharmacological agents for integrin upregulation.

SU9516 (3-[1-(3H-imidazol-4-yl)-meth-(Z)-ylidene]-5-methoxy-1, 3-dihydroindol-2-one) is a 3-substitued-indolinone compound that binds to cdk2 and selectively inhibits its catalytic kinase activity [207]. X-ray crystallography studies showed that the small molecule compound inhibited cdk2/cyclin A through competitive inhibition of ATP [262]. In human leukemic cells, SU9516 caused the pronounced down-regulation of the antiapoptotic protein Mcl-1 through transcriptional repression, increased proteasomal degradation, inhibition of RNA Pol II CTD phosphorylation and oxidative damage [208]. SU9516 has also been reported to inhibit glycogen synthase kinase 3β (GSK-3β), which is involved in normal cell death [207]. Levels of inactive p-S9–GSK3β are reduced and total GSK3β are elevated in the muscles of patients with myotonic dystrophy type 1 (DM1) [275]. Inhibition of GSK3β in both DM1 cell culture and mouse models reduced muscle weakness and myotonia in DM1 mice [275]. Hence, compounds normalizing GSK3β activity might be beneficial for improving muscle

function in patients with DM1. Thus, SU9516 has demonstrated its potential as a viable pharmacological drug for the development of antineoplastic therapeutics.

A previous study described in Chapter 3 of this dissertation, identified SU9516 as an α7β1 integrin enhancing drug (Sarathy et al., unpublished). Functional and histopathological improvements with drug treatment in the *mdx* mouse model suggest potential therapeutic efficiency for the drug in the treatment of Duchenne muscular dystrophy. It was verified that SU9516 enhances α7B integrin expression in C2C12 murine myogenic cell lines and human patient DMD cells over a wide range of concentrations. Additionally, SU9516 also showed *in vivo* on target activity for α7B and β1D in the skeletal muscle of treated *mdx* mice. However, the molecular mechanism by which SU9516 enhances integrin is unknown. It remains to be determined whether inhibition of one or more known kinase targets of SU9516 may be involved in the elevation of the α7 integrin levels in myogenic cell lines.

MATERIALS AND METHODS

Tissue Culture

C2C12 cells used in this study were purchased from ATCC and myoblasts were grown and maintained in DMEM without phenol red (Sigma) containing 20% FBS (Atlanta Biologicals), 1% Penicillin/Streptomycin (P/S) (GIBCO) + 1% L-Glutamine (GIBCO). Myoblasts were maintained below 70% confluence until use in assay. Myoblasts were differentiated into myotubes in DMEM without phenol red, 1% horse-

serum (Atlanta Biologicals), and 1% P/S + L-Glutamine. All cells were incubated at 37ºC with 5% CO_2. Assays were performed on myoblasts and myotubes between passages 8 and 14. To determine whether SU9516 affects protein levels of MAP4k4, we harvested C2C12 cells at 24, 48, 72 and 96 hours after switching the cells to differentiation media with either SU9516 or DMSO.

Myotube α7 integrin FDG assay

α7$^{+/LacZ}$ myoblasts were originally isolated and maintained as described [56]. A total of 25,000 α7$^{+/LacZ}$ myoblasts were dispensed in 100μL growth media. After 24 hours, growth media was aspirated, wells were washed with 200μL PBS, and 100μL/well of differentiation media was added. Differentiation media was changed daily between 72 and 120 hours, and up to 1μL compounds in DMSO were added as previously described once wells contained differentiated myotubes. The FDG fluorescence assay was performed as described in the myoblast screen with the one notable exception being the incubation after FDG solution addition being shortened from 20 minute to 5 minutes at RT due to the higher levels of β-gal in myotubes.

Immunobloting

Protein was extracted from cell pellets or tissue powdered in liquid nitrogen. RIPA was used as the lysis buffer with a 1:100 dilution of 0.5M NaF and 1M Na_3VO_4 and a 1:500 dilution of protease inhibitor cocktail. Protein was quantified using a Bradford assay and equal quantities were separated using SDS polyacrylamide gel

electrophoresis. The α7B and β1D integrin were detected as was previously described [177]. Signals were detected using WesternSure™ PREMIUM Chemiluminescent Substrate (LI-COR). Protein loading was normalized to either α-tubulin (1:1000 mouse-monoclonal, abcam) or GapDH (1:1000, rabbit-monoclonal, Cell Signaling). Quantitation was performed using Image J software.

Immunofluorescence

For *in vitro* immunofluorescence analysis in C2C12 cells, anti-myosin heavy chain antibody was used at a dilution of 1:1000. Cells grown in chamber slides, fixed with 4% paraformaldehyde and blocked in PBS containing 2% bovine serum albumin (Sigma), 0.1% Tween 20, and 0.05% Triton X-100 (American Bioanalytical) for 1 h at room temperature. The cells were then incubated with the MF20 monoclonal antibody (MAb) against MHC (1:40; DSHB) for 2.5 h and subsequently with an Alexa Fluor 488conjugated secondary antibody (1:200; Invitrogen) for 1 h at room temperature. Cells were mounted with Vectashield reagent with DAPI (4′,6-diamidino-2-phenylindole; Invitrogen). *In vivo* immunofluorescence analysis: p-p65 and p65-NF-κB antibodies were used at a dilution of 1:1000, rabbit polyclonal followed by Rb anti-HRP 1:2000 (Cell Signaling). Signals were detected using WesternSure™ PREMIUM Chemiluminescent Substrate (LI-COR). Protein loading was normalized to either α-tubulin (1:1000 mouse-monoclonal, abcam) or GapDH (1:1000, rabbit-monoclonal, Cell Signaling). Quantitation was performed using Image J software.

KiNativ Assay

A probe based chemoproteomics (KiNativ) assay was used to identify muscle specific kinase(s) regulated by SU9516 [276]. DMD myotubes were cultured as previously described [201] and treated with the 0.1, 0.5 and 1μM SU9516 for 48 hours. Proteins from control and treated DMD myoblasts and myotubes were harvested and incubated with the KiNativ probe (biotinylated acyl phosphates of ATP and ADP) following the manufacturer's protocol (ActivX Biosciences, Inc., Torrey Pines, CA). Proteins were sent to ActiveX Biosciences and subjected to LC-MS/MS to identify the molecular signature of biotin labeled proteins in the samples and control vs treated proteins compared and kinases in which activation was inhibited by SU9516 were identified.

Statistical analysis and Curve-fitting

Statistical analysis was performed using Graphpad Prism software and unpaired t-test comparison against the DMSO control treatment group for the SU9516 treated C2C12 and human DMD myotubes. Graphpad prism software was also used to fit curves using nonlinear regression analysis with log (agonist) vs. response with a variable slope. Averaged data are reported as the mean ± the standard error of the mean (s.e.m.). Comparison for two groups was performed using a Student's *t*-test and between multiple groups using Kruskal-Wallis one way ANOVA on ranks for nonparametric data. *P*<0.05 was considered statistically significant.

RESULTS

SU9516 promotes fusion of C2C12 myoblasts

SU9516 treatment of myoblasts produced significant morphological changes and appeared to promote the differentiation of myogenic cells even in growth media. In order to determine if SU9516 treatment led to faster fusion/differentiation rates we began to differentiate C2C12 cells in the presence of 12 μM SU9516 or DMSO alone. 72 hours post differentiation, SU9516 treated myotubes appeared larger with more nuclei than the DMSO treated controls. This was quantified by measuring average myofiber widths which was increased 3-fold for SU9516 treated cells over DMSO (***$P<0.001$) (Figure 1 A and B). The fusion index was increased 3-fold in SU9516 treated myobalsts (***$P<0.001$) (Figure 1C) and there was a shift toward myotubes containing more nuclei/myotube with SU9516 treatment (*$P<0.05$, ***$P<0.001$) (Figure 1D). These results supported the idea that SU9516 promoted myogenic fusion and differentiation.

A recent study showed that siRNA mediated MAP4k4 silencing and reduction of MAP4k4 protein promotes a similar morphology and enhanced myotube formation as seen in SU9516 treated C2C12 myoblasts [277]. Additionally, SU9516 was also identified as an inhibitor of MAP4k4 activity [278]. To determine whether SU9516 affects protein levels of MAP4k4, we harvested C2C12 cells every 24 hours after switching the cells to differentiation media with either SU9516 or DMSO. Total levels of MAP4k4 were evaluated at each time point. 24 hours post differentiation with SU9516 treatment, the levels of total MAP4k4 were reduced 2-fold relative to DMSO treated controls (*$P<0.05$) (Figure 1E). These reduced levels were also observed at 48 hours of differentiation

relative to controls (P>0.05) (Figure 1F), however, the levels of MAP4k4 protein also dropped in the DMSO treated cells at 72 and 96 hours of differentiation (P>0.05) (Figure 1G and H).

SU9516 treatment reduces the levels of the tetraspanin CD82 in C2C12 myoblasts during differentiation

The tetraspanins are multi-span membrane proteins that mediate intercellular interactions and are found in close association with membrane proteins like integrins, other tetraspanins and chemokines. CD82 (also known as KAI1) is a member of the tetraspanin family of proteins. It has previously been shown that CD82 regulates the molecular packing of α4 integrin within clusters, thereby regulating the local molecular density of α4. CD82 can form tetraspanin enriched microdomains (TEMs), through its association with several membrane proteins such as cell adhesion molecules, growth factor receptors and signaling molecules, including integrins [279,280]. Thus far, there is no literature that describes an interaction between α7β1 integrin and CD82 in skeletal muscle. Our previous experiments with SU9516 treatment in C2C12 myoblasts showed that SU9516 promoted differentiation and enhanced fusion. We differentiated C2C12 cells in the presence of 12 μM SU9516 or DMSO alone and hypothesized that SU9516 treatment enhances the levels of α7B integrin early during differentiation. Our results confirmed our hypothesis. The treatment with SU9516 enhanced levels of α7B integrin 48 hours post differentiation compared to DMSO treated C2C12 cells. Levels of α7B integrin were elevated and maintained at 48, 72 and 96 hours post differentiation in the

SU9516 treated cells (Figure 2A and C). Additionally, in our study we showed that the levels of CD82 were dramatically reduced post 24 hours in differentiation media in SU9516 treated cells (Figure 2B and C). The levels of CD82 remain downregulated in the SU9516 treatment group 48 and 96 hrs post differentiation. This data demonstrates that CD82 downregulation precedes the upregulation of α7B integrin with SU9516 treatment in differentiating C2C12 cells.

Pharmacological inhibition of MAP4k4 does not elevate β-Galactosidase activity in α7$^{+/lacZ}$ myotubes

SU9516 is a known inhibitor of MAP4k4 activity [278]. Based on our previous findings that SU9516 downregulates the levels of total MAP4k4 protein and enhances myoblast fusion, we hypothesized that inhibition of MAP4k4 may be responsible for the enhanced expression of α7 integrin in myogenic cell lines. To test our hypothesis we tested seven known inhibitors of MAP4k4 activity in α7$^{+/lacZ}$ myoblasts and myotubes, over a wide range of concentrations (0.625 μM to 50 μM). Of these, four inhibitors showed a >1 ratio of fold fluorescence relative to DMSO in myoblasts (Figure 3A). However, only one inhibitor showed a >1 ratio of fold fluorescence relative to DMSO in myotubes (Figure 3B). These data suggest that the increase in α7 integrin in myoblasts can be attributed at least partially to MAP4k4 inhibition, possibly due to enhanced myoblast fusion. However, the inhibition of MAP4k4 is likely by itself not responsible for the increase in α7 integrin in myotubes.

SU9516 inhibits SPAK in human DMD myotubes

SU9516 is a known ATP mimetic and a CDK2 inhibitor [262]. Therefore, we sought to identify the kinase targets of SU9516 in human DMD patient myotubes as determined by the KiNativ assay. Human DMD patient myotubes were treated with 0.01, 0.1, 0.5 and 1μM concentrations of SU9516 after which, lysates were run through a KiNativ *in situ* kinase profiling screen to identify drug targets. In order to minimize off-target kinase inhibition which occurred at lower concentrations than the effective α7 Integrin enhancing range, the 10nM SU9516 treated lysate was used as the negative control. The percent inhibition of the kinases obtained in this 10nM treatment were therefore subtracted from the other treatments percentages. The kinases inhibited with maximum potency were the PFTAIRE1 kinase, the STE20/SPS1-related proline-alanine-rich protein kinase (STK39/STLK3/SPAK) and the SPAK homolog oxidative stress response -1 (OSR1) kinases. The activity of the SPAK/OSR1 kinases was inhibited ~80% at the lowest concentration of 0.1 μM SU9516 (Table 1). These results helped us consider potential mechanisms of action through which SU9516 treatment enhances α7 integrin expression.

Pharmacological inhibition of PFTAIRE1 does not elevate β-Galactosidase activity in α7$^{+/lacZ}$ myotubes

Previous studies (Results shown in Chapter 3) have shown that SU9516 increased levels of α7B in human DMD myotubes in a dose dependent manner (Figure 1, Chapter 3, Sarathy et al., unpublished). Based on the findings from the KiNativ screen (Table1),

we observed that SU9516 inhibited PFTAIRE1 with high potency and in a dose dependent manner. Hence, we sought to determine whether the pharmacological inhibition of PFTAIRE1 is responsible for the elevation in α7B levels in myotubes. To test our hypothesis we tested the activity of two known inhibitors of PFTAIRE1 in α7$^{+/lacZ}$ myoblasts and myotubes, over a wide range of concentrations (0.625 μM to 50 μM). These inhibitors were a generous gift from our collaborators at the NCGC, NIH. Both inhibitors showed a >1 ratio of fold fluorescence relative to DMSO in myoblasts (Figure 4A). However, none of the inhibitors showed a >1 ratio of fold fluorescence relative to DMSO in myotubes (Figure 4B). These data suggest that the increase in α7B integrin in myoblasts can be attributed at least partially to PFTAIRE1 inhibition. However, the inhibition of PFTAIRE1 is likely by itself not responsible for the increase in α7 integrin in differentiated myotubes.

Pharmacological inhibition of SPAK/OSR1 elevates β-Galactosidase activity in α7$^{+/lacZ}$ myotubes.

Previous studies (Results shown in Chapter 3) have shown that SU9516 increased levels of α7B in human DMD myotubes in a dose dependent manner (Figure 1, Chapter 3, Sarathy et al., unpublished). Based on the findings from the KiNativ screen, we observed that SU9516 inhibited the SPAK/OSR1 kinases with high potency and in a dose dependent manner. Hence, we sought to determine whether the pharmacological inhibition of SPAK/OSR1 activity may be responsible for the elevation in α7B levels in myotubes. To test our hypothesis we tested the activity of an inhibitor of SPAK/OSR1

kinase activity namely, a chemical STOCK1S-50699 in $\alpha7^{+/lacZ}$ myotubes, over a wide range of concentrations (3.9 nM to 1 μM). STOCK1S-50699 (Asinex BAS 00116897) has been shown to interact with the CCT domain of SPAK and OSR1 kinases and consequently prevents their activation by upstream WNK (with no lysine) kinases [281]. This inhibitor has been shown to potently suppress SPAK/OSR1 activity and NCC/NKCC1 phosphorylation. The inhibitor attained a 1.5- fold fluorescence relative to DMSO in myotubes (Figure 5).   This inhibitor attained levels of relative fold fluorescence that were almost as high as SU9516 in $\alpha7^{+/lacZ}$ myotubes. Additionally, the SPAK/OSR1 inhibitor exhibited a higher potency than SU9516, albeit with toxicity at higher concentrations. This preliminary chemical screen suggests that the inhibition of SPAK/OSR1 activity is the molecular mechanism by which SU9516 elevates the levels of α7 integrin in myogenic cell lines and skeletal muscle.

SU9516 inhibits the activation of p65-NF-κB in the *mdx* diaphragm

In order to gain further insight into the mechanism of action by which SU9516 treatment attenuated dystrophic pathology and enhanced myofiber regeneration, we investigated the p65-NF-kB pathway. It has been shown that pharmacological inhibition of p65-NF-κB pathway in 3 week old *mdx* mice increased the number of e-MyHC fibers by 47% [282]. In our studies, histopathological analysis of diaphragm muscle sections showed an ~8.8% increase in e-MyHC fibers with SU9516 treatment accompanied by an increase in centrally nucleated fibers, compared to vehicle treated *mdx* mice. Hence, we hypothesized that SU9516 inhibits the p65-NF-kB pathway, thereby promoting myofiber regeneration in dystrophic muscle. We treated human DMD patient myotubes with a

1µM concentration of SU9516 and observed an ~2.6-fold downregulation of p-p65-NF-κB compared to the vehicle treated myotubes (Figure 6A). Additionally. western blot analysis of protein lysates from the diaphragms of 10 week old WT, vehicle and SU9516 treated *mdx* mice showed a decreased level of p-p65 NF-κB in SU9516 treated mice diaphragms compared to vehicle treated controls (P<0.05) (Figure 6B).

To determine whether the inhibition of the p65-NF-kB pathway is involved in the enhanced expression of α7 integrin, we looked at the effect of an IKKβ inhibitor called IKK-2 inhibitor IV (IKKi) (Calbiochem), using the α7$^{lacZ/+}$ cell-based screening assay. While IKKi showed lower potency compared to SU9516, it attained a relative fold fluorescence of ~1.3 fold over DMSO for lacZ activity at a concentration of 0.625µM (supplementary Figure S1A). Additionally, we also looked at a molecular target upstream of IKKβ, namely the TNF receptor associated factor 6 (TRAF6)-CD40 interaction. The TRAF6-CD40 and the downstream p65-NF-kB pathway are depicted as a schematic in Figure 7. We asked the question of whether inhibition of the CD40-TRAF6 (purchased at Calbiochem) interaction upstream of the p65-NF-kB pathway could lead to an increase in α7β1 integrin. Similar to the IKKi, we observed that while CD40-TRAF6 showed lower potency compared to SU9516, it attained a relative fold fluorescence of ~1.3 fold over DMSO for lacZ activity at a concentration of 0.625µM (supplementary Figure S1). Our data suggests that the inhibition of the p65-NF-kB pathway by SU9516 in skeletal muscle and myogenic cell lines may be partially responsible for the increase in α7β1 integrin. A novel proposed mechanism of action by which SU9516 increases α7 integrin expression via inhibition of p65-NF-kB and the SPAK/OSR1 kinases is depicted in Figure 8. These results shed light on a novel

pathway that can be further investigated for the development integrin enhancing therapeutics for DMD.

DISCUSSION

DMD is a devastating muscle disease for which there is currently no cure or effective treatment option. We have recently identified SU9516 as an α7 integrin enhancing small molecule in a chemical screen, however the mechanism of action by which this drug increases α7 in skeletal muscle remains unknown. This study sheds light on several pathways that are potential therapeutic targets for drug development in DMD. Results from this study demonstrate that SU9516 enhances fusion and promotes differentiation in mouse myogenic cell lines (Figure 1). One of the drug targets identified as significantly downregulated with SU9516 treatment was MAP4k4 (Figure 1). Recently, it was shown that MAP4k4 was a suppressor of myogenic differentiation and the expression of a Map4k4 -inactive mutant promoted myotube formation, therefore implicating the kinase activity of Map4k4 for the inhibition of muscle differentiation[277]. MAP4k4 was identified as a kinase target of SU9516 in a study that investigated the kinase targets of commercially available kinase inhibitors [278]. Our study confirms that SU9516 downregulates MAP4k4 protein levels during differentiation. This result has significant implications for the use of SU9516 as a drug that could potentially override the impaired differentiation and regeneration program seen in DMD. Additionally, SU9516 can also be considered a viable co-adjuvant for myoblast transplantation studies, owing to its ability to enhance myoblast fusion. Pharmacological treatment of α7$^{+/lacZ}$

myotubes with known inhibitors of MAP4k4 did not show an increase in the β-galatcosidase activity as depicted in Figure 3. However, the inhibitors showed an increase in β-galatcosidase activity in $\alpha7^{+/lacZ}$ myoblasts. Hence, this experiment suggests that the MAP4k4 inhibition is responsible for the increase in α7B protein levels in myoblasts, potentially through enhanced fusion and differentiation. However this pathway is not responsible for the integrin increase seen in myotubes, which are a more suited model for clinical investigation of DMD drugs.

A molecular target we investigated was the tetraspanin CD82. Tetraspanins are involved in the regulation of several critical cellular processes namely cell adhesion, migration, fusion and proliferation [283]. Additionally it is known that CD82 inhibits integrins, epidermal growth factor receptor (EGFR), hepatocyte growth factor or c-Met and urokinase receptor (u-PAR) or CD87 [284]. Recently it was shown utilizing flow cytometry, that in CD82-null endothelial cells (CD82-null ECs), integrin α6 and αV were upregulated in the ECs. However, the increase in surface level of integrins was not accompanied by an increase in integrin α6 mRNA [285]. It can therefore be suggested that the increase in integrin with elimination of CD82 could be a result of changes in protein turnover rather than increased transcription of integrin genes. The results from this study as well as results reported in Chapter 3 of this dissertation demonstrate the increases in α7β1 integrin protein levels with SU9516 treatment in both murine and human myogenic cell lines as well as *in vivo* in the *mdx* mouse model of DMD (Sarathy et al., unpublished). However, our studies also showed that there was no corresponding increase in the transcript levels of integrin α7 and β1 in skeletal muscle of *mdx* mice. Hence, we looked at levels of CD82 to see whether SU9516 targets the tetraspanin

thereby elevating the levels of α7B integrin in skeletal muscle via a protein turnover mechanism. Our results demonstrated that SU9516 downregulated the levels of CD82, 24 hours post differentiation and this decrease preceded the increase in α7B integrin which was only seen 48 hours post treatment in C2C12 myogenic cell lines (Figure 2). Further experiments to show effects of CD82 downregulation need to be performed to investigate the interactions between CD82 and α7β1 integrin in skeletal muscle.

Our study also identified SU9516 as an inhibitor of p65-NF-κB signaling activation in human DMD myotubes as well as in *mdx* skeletal muscle. Increased NF-κB activity in *mdx* mice is associated with both immune cells and regenerative muscle fibers and inhibiting NF-κB signaling either genetically or by pharmacological means promoted formation of new myofibers in response to degeneration[282]. NF-κB has been implicated as a negative regulator of myogenesis[282]. Hence, we conclude that the increase in centrally nucleated myofibers and eMHC-positive myofibers seen in the diaphragm of SU9516 treated *mdx* mice could be attributed to SU9516 inhibition of p65 activation. In DMD, inflammatory response to myofiber damage is a secondary effect of the disease that further exacerbates the pathogenesis. A therapeutic target for developing anti-inflammatory therapies for DMD is NF-κB, a pro-inflammatory transcription factor that is active in the dystrophin deficient muscle of both DMD patients and the *mdx* mouse [286,287]. The NF-κB pathway plays a role in inducing the ubiquitin-proteasome pathway in muscle [288] causing increased protein degradation [289,290]. In the cytoplasm of mammalian cells, under non-stress conditions, NFκB remains in an inactive state; bound to the inhibitor protein IκB. When induced by a variety of specific cell stimuli like TNF-α, the activated IκB kinase (IKK) complex phosphorylates the IκB inhibitory protein (IκB).

Once phosphorylated, IκB is targeted for polyubiquitination and subsequent degradation by the 26S proteasome. This event leads to the nuclear translocation of NF-κB, where it regulates transcription of genes encoding a wide array of factors involved in inflammation, immunity, cell proliferation, differentiation, and survival[291,292]. In mammals, the NF-κB family consists of five subunits, p65 (RelA), c-Rel, RelB, p50, and p52 [293]. Knockout of p65, but not other subunits of NF-κB, enhances myogenic activity in MyoD-expressing mouse embryonic fibroblasts[294]. *In vivo* studies showed that haploinsufficency of p65 enhances muscle regeneration in the skeletal muscle of both *mdx* and wild-type (wt) mice[282]. Additionally, AAV-mediated delivery of p65-shRNA alleviated muscle pathologies in *mdx* mice by selectively reducing NF-κB/p65 activity[295]. Previously, treatment of *mdx* mice *in vivo* with therapies targeted to inhibit NF-κB activation have been shown to ameliorate the dystrophic pathology, including infliximab [296], N-acetylcysteine (NAC) [297], pyrrolidine dithiocarbamate (PDTC) [298] and VBP15 [247]. These genetic and pharmacological studies show that the p65 NF-κB subunit plays a crucial role in muscle health and points to a potential target for DMD therapy. Our study showed that pharmacological inhibition of the p65-NF-κB signaling pathway, utilizing IKKi, a known inhibitor of IKKβ and p65-NF-κB in myogenic cell lines[282], increased the β-galactosidase activity in $α7^{lacZ/+}$ myotubes. Hence, we suggest that the increase in protein levels of α7B and β1D with SU9516 treatment can be attributed at least partially to the inhibition of p65 activation in myofibers.

The TNF receptor-associated factor 6 (TRAF6) is an adaptor protein which acts as a signaling intermediate for several receptor-mediated signaling events and subsequently leads to the stimulus-dependent activation of several signaling pathways

[299,300]. It is known that TRAF6 is a signal transducer for the activation of IκB kinase (IKK) and the subsequent activation of NF-κB in response to proinflammatory cytokines, bacterial products, Toll/IL1 family and from receptors such as receptor activator of NF-κB (RANK) and CD40 [300,301]. A previous study showed that targeted deletion of TRAF6 improved muscle strength and reduced the dystrophic pathology and the activation of proinflammatory transcription factor nuclear factor-kappa B (NF-κB) in 7-week-old *mdx* mice[302]. Our study showed that pharmacological inhibition of the CD40-TRAF6 interaction increased the lacZ activity in α7$^{lacZ/+}$ myotubes and this suggests that the increase in protein levels of α7B with SU9516 treatment, can be attributed at least partially to the inhibition of p65 activation in myofibers, thereby corroborating our observations with the IKKi dose response treatment of α7$^{lacZ/+}$ myotubes. Future investigation into this pathway would involve assessing the levels of α7 integrin in an *mdx*; p65$^{+/-}$ haploinsufficieny model to confirm whether inhibition of p65NF-κB is responsible for the elevation of α7B integrin.

The KiNativ assay indicated that SU9516 potently inhibited 3 kinases in human DMD myotubes- PFTAIRE1, SPAK and OSR1. Currently, there is no significant literature describing the roles of these kinases in skeletal muscle or muscle disease models. Identified in the murine nervous system, the PFTAIRE1 kinase belongs to the Cdc2-related serine/threonine family of protein kinases and is known to be a critical regulator of cyclins and the cell cycle [303,304]. Our results showed that while known inhibitors of the PFTAIRE1 pathway increased β-galactosidase activity in α7lacZ$^{+/-}$ myoblasts, the inhibitors did not increase β-galactosidase activity in myotubes. This suggests that PFTAIRE1 inhibition by SU9516 may be responsible for the increase in

α7B seen in myoblasts, however an unlikely mechanism by which α7B is elevated in myotubes with SU9516 treatment.

The SPAK-OSR1 kinases are phosphorylated by the (with no lysine) upstream kinases WNK1 and WNK4 [305]. When activated, the SPAK-OSR1 kinases phosphorylate and activate the Na^+ Cl^- cotransporter (NCC) and the Na^+ K^+ $2Cl^-$ cotransporters (NKCC2) that control salt reabsorption in the kidney [306,307]. There is no current literature that describes the role of the SPAK/OSR1 kinases in maintaining skeletal muscle homeostasis. Our study showed that pharmacological inhibition of the SPAK/OSR1 signaling pathway, increased the β-galactosidase activity in α7$^{lacZ/+}$ myotubes, 1.5-fold over DMSO treated myotubes with a greater potency than SU9516. This result suggests that the increase in muscle protein levels of α7B and β1D with SU9516 treatment *in vivo*, can be attributed to the inhibition of the SPAK/OSR1 activation in myofibers. The mechanism by which the inhibition of SPAK/OSR1 elevates α7 integrin expression is unknown and future studies will include an investigation of the WNK-SPAK/OSR1 mediated regulation of ubiquitination and endocytosis of α7 integrin.

It was shown in an inflammatory intestinal bowel disease model that the knockdown of pro-inflammatory NF-κB (p65) by siRNA decreased SPAK expression significantly and NF-κB-binding site on the SPAK gene was essential for stimulated SPAK promoter activity by TNF-α [308]. It is known that p65-NF-κB, is abnormally active in the dystrophin deficient muscle of both DMD patients and the *mdx* mouse [286,287,309]. This could potentially lead to the abnormal activation of the SPAK-NCC phosphorylation in dystrophic muscle. Patients with DMD have an elevated muscular

sodium concentration[310] and the abnormal activation of the NCC channels in DMD may be responsible for the increased intracellular sodium load. This may suggest that through the inhibition of p65- NF-κB activation, SU9516 inhibits the abnormal activation of the SPAK kinase-NCCNKCC cascade, thereby restoring the ion homeostasis in myofibers of dystrophic mice. The proposed signaling mechanism of how the TRAF6- p65-NF-kB-SPAK/OSR1 pathway regulates Na$^+$ ion balance is depicted in Figure 7. While the inhibitors used in this study targeted at the MAP4k4, PFTAIRE1, SPAK/OSR1 and the p65-NF-κB pathway elicited interesting preliminary results that shed light on the potential mechanisms of action by which SU9516 increases α7β1 integrin expression in muscle, it must be noted that the inhibitors are not specific to the kinases described in this study. Future studies would include using molecular biology approaches to eliminate the expression of the aforementioned kinases and assess levels of α7β1 integrin. Together, this study identifies some of the molecular targets of the small molecule integrin enhancing drug SU9516. The identification of these pathways is important for the further development of SU9516 as a candidate for DMD treatment. This therapeutic may have implications for the treatment of DMD and other forms of muscle disease.
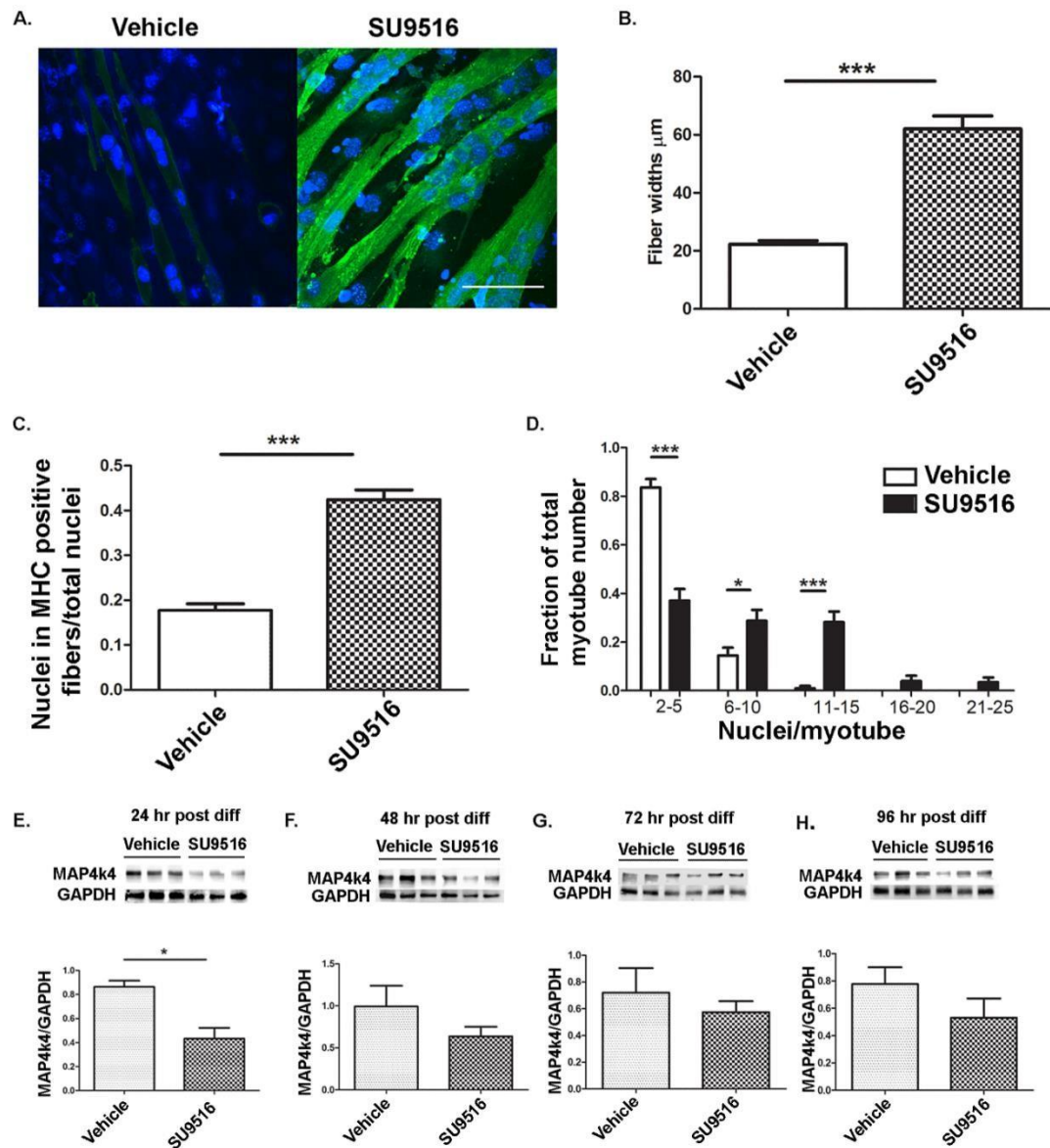
Figure 1:- SU9516 promotes fusion in C2C12 myoblasts through MAP4k4 downregulation. C2C12 myoblasts were differentiated with 12 μM SU9516 or DMSO. Post 24, 48, 72 and 96 hrs cells (n=3/group) were fixed and immunostained for MHC. (**A**) Myofibers stained at 72 hrs (green-MHC; blue-DAPI) Magnification 40X, Scale bar=100μm. (**B**) At 72 hrs, myotube diameters were increased with SU9516 treatment

versus DMSO (**C**) The fusion index at 72 hrs calculated from the ratio of the number of nuclei in MHC-positive myotubes to the total number of nuclei in one field for five random microscopic fields. SU9516 treatment promoted myoblast fusion (**D**) SU9516 treatment increased fraction of total myotubes with higher numbers of nuclei. Results represent means and SEM for three independent experiments. *P<0.05 *** $P < 0.001$. (**E**) SU9516 downregulates total MAP4k4 protein levels at 24 hours post differentiation *P<0.05, however (**F**) (**G**) and (**H**) the levels of MAP4k4 were significantly different from the DMSO treated cells with consecutive days of differentiation.

A.
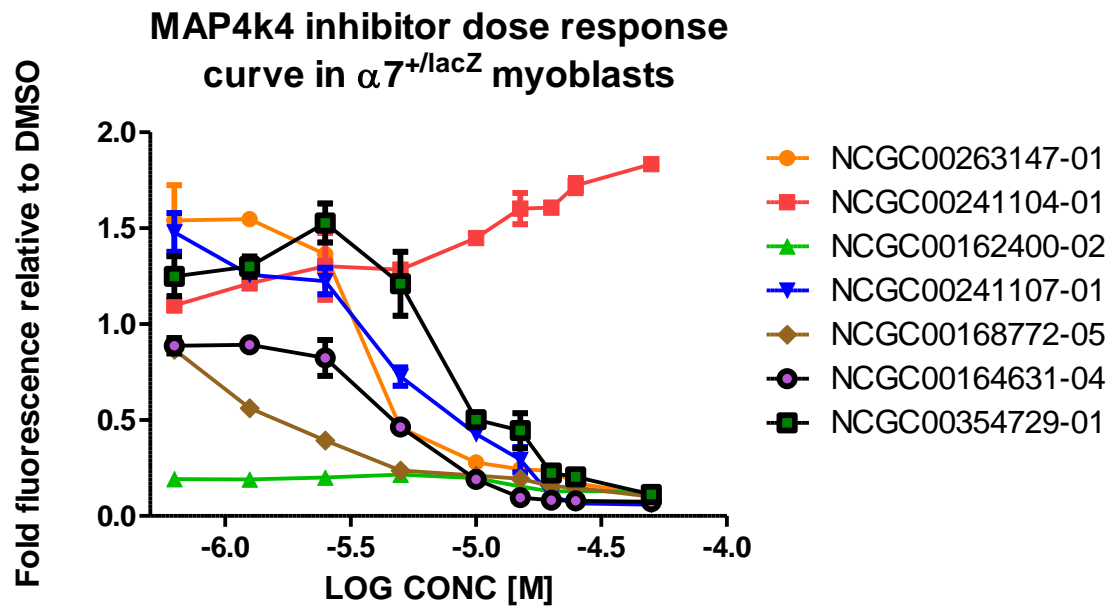
B.
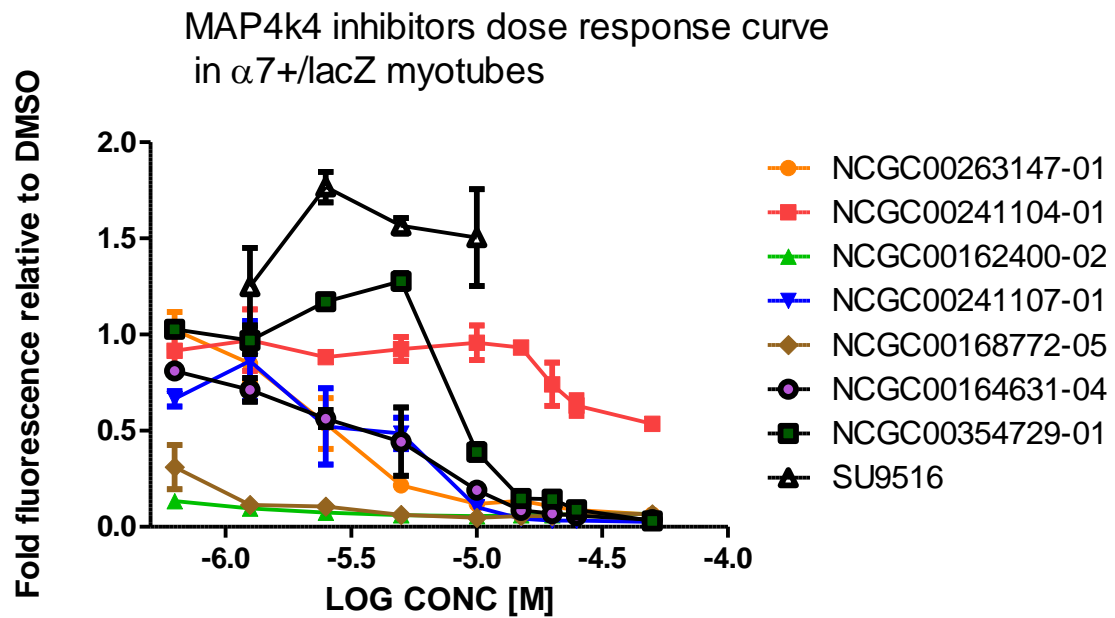
Figure 2:- MAP4k4 inhibition increases β-Galactosidase activity in α7$^{+/lacZ}$ myoblasts but not myotubes. A) A dose curve with different concentrations of 7 MAP4k4 inhibitors was generated by treating α7$^{+/lacZ}$ myoblasts. 4 of the 7 inhibitors showed a >1 fold fluorescence over DMSO. **B)** A dose curve with different concentration of 7 different MAP4k4 inhibitors was generated by treated α7$^{+/lacZ}$ myotubes. None of the inhibitors showed a >1fold fluorescence over DMSO.
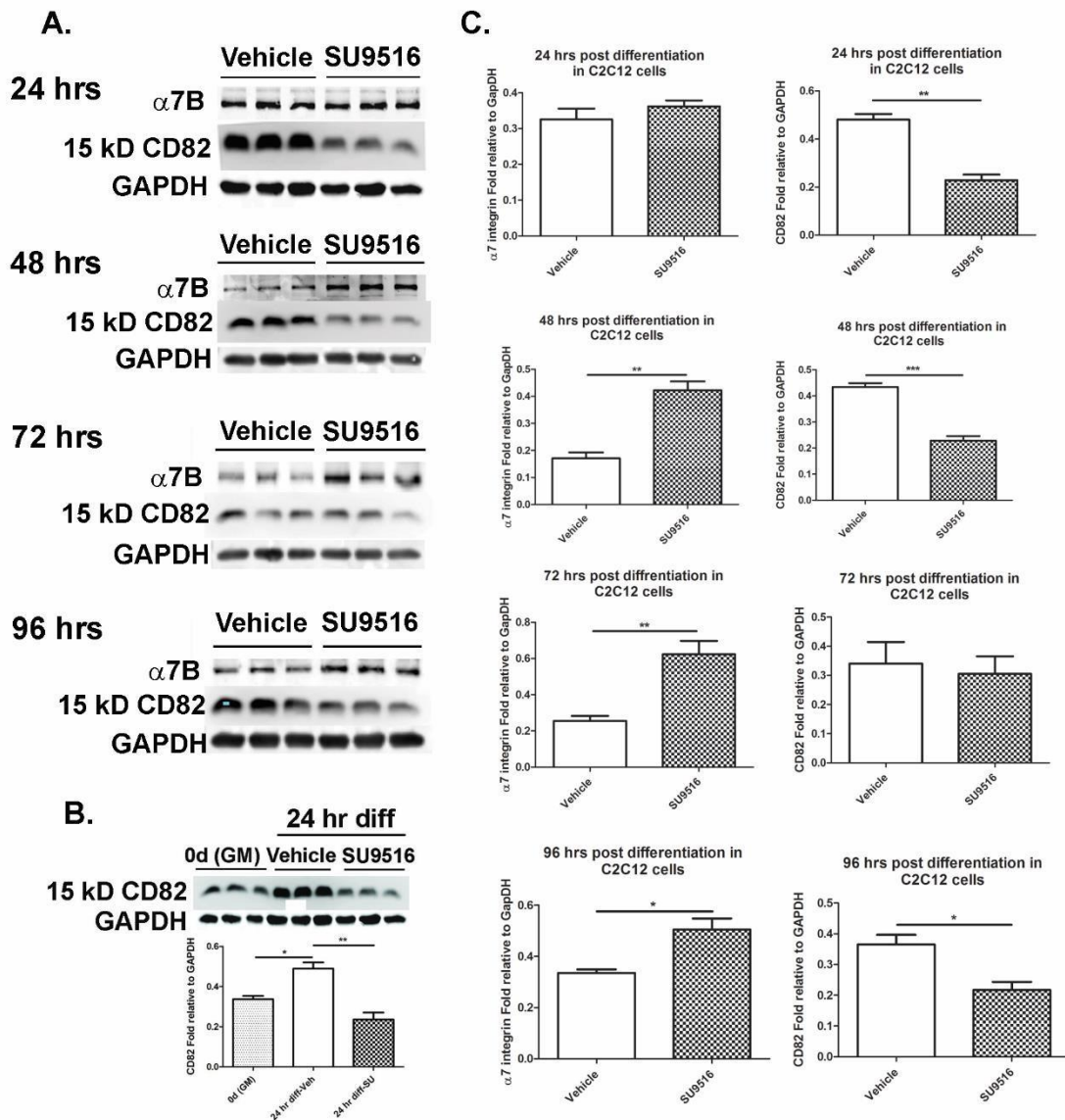
Figure 3- CD82 downregulation with SU9516 treatment precedes α7 integrin level increases during differentiation. C2C12 myoblasts were differentiated with 12 μM SU9516 or DMSO. Post 24, 48, 72 and 96 hrs cells (n=3/group) were harvested and analyzed for the levels of CD82 (KAI1) and α7B integrin. **A)** Western blot images depicting the levels of CD82 and α7B integrin over the course of 96 hours of differentiation. CD82 levels are downregulated at 24 hours, while integrin α7B levels

are upregulated and maintained 48 hours post treatment with SU9516. **B)** Western blot images and analysis show that levels of CD82 are significantly upregulated post 24 hours differentiation and significantly downregulated with SU9516 treatment in differentiating C2C12 myoblasts. **C)** Quantification of the levels of α7B and CD82 in differentiating C2C12 myoblasts show that CD82 levels decrease at 24 hours of SU9516 treatment and α7B integrin levels are upregulated at 48 hours of treatment. While CD82 levels are not significantly downregulated at 72 hrs, the levels of α7B are maintained and elevated 48 hours post differentiation.   Results represent means and SEM for three independent experiments. *P<0.05, **P<0.01, *** $P < 0.001$.   GM-Growth media

Kinase	Reference	Sequence	Labeling Site	SU9516 1 µM	SU9516 0.5 µM	SU9516 0.1 µM	IC50 (µM)
ABL, ARG	UniRef100_P005	LMTGDTYTAHAGAKFPIK	Activation Loop	-4.4	33.1	32.0	>1
ABL, ARG	UniRef100_P005	YSLTVAVKTLKEDTMEVEEFLK	Lys1	-92.4	-33.6	15.8	>1
AKT1	UniRef100_P317	GTFGKVILVK	ATP Loop Anchor G2	-10.8	-22.6	-9.0	>1
AKT2, AKT3	UniRef100_Q9Y2	GTFGKVILVR	ATP Loop Anchor G2	-19.3	-33.7	-15.0	>1
AMPKa1, AMPKa2	UniRef100_P546	DLKPENVLLDAHMNAK	Lys2	-50.9	-1.5	-3.8	>1
ANPb	UniRef100_P205	GMAFLHNSIISSHGSLKSSNCV	Lys2	4.8	-73.2	-48.8	>1
ARAF	UniRef100_P103	DLKSNNIFLHEGLTVK	Lys2	-11.9	-13.6	-2.8	>1
AurA	UniRef100_O149	DIKPENLLLGSAGELK	Lys2	30.8	14.4	18.9	>1
AurA	UniRef100_O149	FILALKVLFK	Lys1	18.2	31.6	29.9	>1
BRAF	UniRef100_P150	DLKSNNIFLHEDLTVK	Lys2	11.6	18.0	13.6	>1
CaMK1a	UniRef100_Q140	LVAIKCIAK	Lys1	-21.5	-17.7	-14.0	>1
CaMK1d	UniRef100_Q8IU	LFAVKCIPK	Lys1	-16.4	-17.0	-14.3	>1
CaMK2b	UniRef100_Q53H	LCTGHEYAAKIINTK	Lys1	20.0	22.5	18.3	>1
CaMK2d	UniRef100_Q135	IPTGQEYAAKIINTKK	Lys1	21.0	27.6	7.6	>1
CaMK2g	UniRef100_Q135	TSTQEYAAKIINTK	Lys1	27.2	21.4	12.3	>1
CaMKK2	UniRef100_Q96R	DIKPSNLLVGEDGHIK	Lys2	-34.8	12.2	26.4	>1
CASK	UniRef100_O149	ETGQQFAVKIVDVAK	Lys1	10.3	16.0	-1.4	>1
CCRK	UniRef100_Q8IZ	DLKPANLLISASGQLK	Lys2	-2.9	-25.3	-19.2	>1
CDC2	UniRef100_Q5H9	DLKPQNLLIDDKGTIK	Lys2	9.8	13.5	32.4	>1
CDK2	UniRef100_P249	DLKPQNLLINTEGAIK	Lys2	60.3	61.8	45.0	<0.1
CDK4	UniRef100_P118	DLKPENILVTSGGTVK	Lys2	64.0	45.1	26.9	0.59
CDK5	UniRef100_Q005	DLKPQNLLINR	Lys2	76.9	70.3	31.4	0.26
CDK7	UniRef100_P506	DLKPNNLLLDENGVLK	Lys2	-20.8	-87.4	-92.6	>1
CHK2	UniRef100_O960	DLKPENVLLSSQEEDCLIK	Lys2	10.6	-0.4	1.9	>1
CSK	UniRef100_P412	VSDFGLTKEASSTQDTGKLPVI	DFG Motif	4.8	-1.1	-2.1	>1
DCAMKL1	UniRef100_O150	DIKPENLLVYEHQDGSK	Lys2	17.3	20.9	26.2	>1
DGKA	UniRef100_P237	IDPVPNTHPLLVFVNPKSGGK	ATP	-49.5	-58.4	-37.6	>1
DGKQ	UniRef100_P528	GRLLTALVLPDLLHAKLPPDSC	ATP	-26.5	-85.8	-27.6	>1
DNAPK	UniRef100_P785	KGGSWIQEINVAEK	ATP	-42.2	-15.3	-39.1	>1
eEF2K	UniRef100_O004	YIKYNSNSGFVR	ATP	-1.1	-36.8	-24.8	>1
EGFR	UniRef100_P005	LLGAEEKEYHAEGGKVPIK	Activation Loop	17.8	-18.1	-48.5	>1
EGFR	UniRef100_P005	IPVAIKELR	Lys1	-14.4	-24.3	-43.8	>1
Erk1	UniRef100_P273	DLKPSNLLINTTCDLK	Lys2	22.1	13.1	23.6	>1
Erk2	UniRef100_P284	DLKPSNLLLNTTCDLK	Lys2	21.0	8.9	16.5	>1
FER	UniRef100_P165	TSVAVKTCKEDLPQELK	Lys1	-4.2	8.1	-1.4	>1
FES	UniRef100_P073	LRADNTLVAVKSCR	Lys1	10.6	-0.4	12.4	>1
FRAP	UniRef100_P423	IQSIAPSLQVITSKQRPR	ATP	-16.9	-8.8	-1.2	>1
FYN, SRC, YES	UniRef100_P129	QGAKFPIKWTAPEAALYGR	Activation Loop	12.0	26.1	33.5	>1
GCK	UniRef100_Q128	DIKGANLLLTLQGDVK	Lys2	48.1	34.6	31.8	>1
GCN2	UniRef100_Q9P2	DLKPVNIFLDSDDHVK	Lys2	8.5	-31.4	-7.1	>1
GSK3A	UniRef100_P498	DIKPQNLLVDPDTAVLK	Lys2	37.0	13.4	2.3	>1
GSK3B	UniRef100_P498	DIKPQNLLLDPDTAVLK	Lys2	14.9	13.6	20.4	>1
HER2/ErbB2	UniRef100_P046	GIWIPDGENVKIPVAIKVLR	Lys1	-1.6	-3.0	-29.8	>1
HPK1	UniRef100_Q929	DIKGANILINDAGEVR	Lys2	29.8	0.0	-22.1	>1
IKKa	UniRef100_O151	DLKPENIVLQDVGGK	Lys2	9.5	12.8	27.1	>1
IKKb	UniRef100_O149	DLKPENIVLQQGEQR	Lys2	20.7	-19.4	-1.7	>1
ILK	UniRef100_Q134	WQGNDIVVKVLK	Lys1	-19.6	-1.9	8.4	>1
ILK	UniRef100_Q134	ISMADVKFSFQCPGR	Protein Kinase Domain	-53.8	5.8	26.9	>1
IRAK1	UniRef100_P516	AIQFLHQDSPSLIHGDIKSSNV	Lys2	-13.4	0.6	-7.9	>1
IRAK4	UniRef100_Q9N	DIKSANILLDEAFTAK	Lys2	19.7	3.4	-0.3	>1
JAK1 domain2	UniRef100_P234	IGDFGLTKAIETDKEYYTVK	DFG Motif	-47.7	-49.9	-44.7	>1
JNK1, JNK2, JNK3	UniRef100_P459	DLKPSNIVVK	Lys2	-13.2	-4.4	-19.0	>1
KHS1	UniRef100_Q9Y4	NVHTGELAAVKIIK	Lys1	9.5	-1.6	-8.6	>1
KHS2	UniRef100_Q8IV	NVNTGELAAIKVIK	Lys1	-34.5	4.1	-1.5	>1
LATS2	UniRef100_Q9NI	DIKPDNILIDLDGHIK	Lys2	-17.2	-24.1	-7.4	>1
LKB1	UniRef100_Q158	DIKPGNLLLTTGGTLK	Lys2	26.2	17.6	12.0	>1
LOK	UniRef100_O948	DLKAGNVLMTLEGDIR	Lys2	-56.1	2.0	23.8	>1

MAP2K1, MAP2K2	UniRef100_P365	DVKPSNILVNSR	Lys2	15.3	15.9	2.7	>1
MAP2K1, MAP2K2	UniRef100_P365	KLIHLEIKPAIR	Lys1	8.5	30.6	-2.1	>1
MAP2K3	UniRef100_P467	DVKPSNVLINK	Lys2	14.0	-2.0	-8.5	>1
MAP2K4	UniRef100_P459	DIKPSNILLDR	Lys2	21.7	13.5	17.0	>1
MAP2K6	UniRef100_P525	DVKPSNVLINALGQVK	Lys2	7.8	6.9	8.5	>1
MAP2K7	UniRef100_O147	DVKPSNILLDER	Lys2	6.2	-34.3	-59.9	>1
MAP3K2	UniRef100_Q9Y2	ELAVKQVQFDPDSPETSKEVN	Lys1	1.2	-19.4	-0.6	>1
MAP3K2, MAP3K3	UniRef100_Q9Y2	DIKGANILR	Lys2	34.1	6.3	-2.5	>1
MAP3K4	UniRef100_Q9Y6	DIKGANIFLTSSGLIK	Lys2	5.7	-59.5	-75.4	>1
MAP3K5	UniRef100_Q996	DIKGDNVLINTYSGVLK	Lys2	-12.0	-3.7	-30.7	>1
MARK1	UniRef100_Q9P0	DLKAENLLLDGDMNIK	Lys2	11.9	9.3	-5.3	>1
MARK2, MARK3	UniRef100_P274	DLKAENLLLDADMNIK	Lys2	-3.3	26.3	12.4	>1
MARK3	UniRef100_P274	EVAIKIIDKTQLNPTSLQK	Lys1	18.1	30.5	26.3	>1
MARK3, MARK4	UniRef100_Q96L	EVAIKIIDK	Lys1	-14.6	-16.8	2.0	>1
MAST1, MAST2	UniRef100_Q6P0	DLKPDNLLITSMGHIK	Lys2	-93.1	-19.8	-2.5	>1
MAST3	UniRef100_O603	DLKPDNLLITSLGHIK	Lys2	27.8	2.7	-6.9	>1
MAST4	UniRef100_O150	DLKPDNLLVTSMGHIK	Lys2	-9.6	18.9	27.9	>1
MER, TYRO3	UniRef100_Q064	KIYSGDYYR	Activation Loop	-29.4	8.4	1.2	>1
MET	UniRef100_P085	DMYDKEYYSVHNK	Activation Loop	-46.9	-5.8	-19.2	>1
MLKL	UniRef100_Q8NI	APVAIKVFK	Lys1	-2.0	18.5	10.3	>1
MSK1 domain1	UniRef100_O755	DIKLENILLDSNGHVVLTDFGL!	Lys2	29.5	27.4	1.8	>1
MSK2 domain1	UniRef100_O756	DLKLENVLLDSEGHIVLTDFGL!	Lys2	27.2	19.4	-18.1	>1
MST1	UniRef100_Q130	ETGQIVAIKQVPVESDLQEIIK	Lys1	25.5	21.7	6.4	>1
MST2	UniRef100_Q131	ESGQVVAIKQVPVESDLQEIIK	Lys1	33.5	15.6	-9.0	>1
MST3	UniRef100_Q9Y6	DIKAANVLLSEHGEVK	Lys2	22.5	13.6	-6.0	>1
MST4, YSK1	UniRef100_O005	DIKAANVLLSEQGDVK	Lys2	45.4	35.0	7.7	>1
NDR1	UniRef100_Q152	DIKPDNLLLDSK	Lys2	6.5	-16.1	-2.0	>1
NEK1	UniRef100_Q96P	DIKSQNIFLTK	Lys2	-0.1	-5.2	-8.3	>1
NEK3	UniRef100_P519	SKNIFLTQNGK	Activation Loop	8.3	-30.3	2.1	>1
NEK4	UniRef100_P519	DLKTQNVFLTR	Lys2	-5.1	-32.7	-9.6	>1
NEK6, NEK7	UniRef100_Q8TI	DIKPANVFITATGVVK	Lys2	9.4	-2.0	-9.0	>1
NEK7	UniRef100_Q8TI	AACLLDGVPVALKK	Lys1	-8.0	-19.5	2.7	>1
NEK8	UniRef100_Q86S	DLKTQNILLDK	Lys2	-6.5	-9.5	-15.4	>1
NEK9	UniRef100_Q8TI	DIKTLNIFLTK	Lys2	12.8	-12.8	-5.5	>1
NuaK1	UniRef100_O602	VVAIKSIR	Lys1	1.4	23.7	-9.9	>1
OSR1	UniRef100_C9JI0	DVKAGNILLGEDGSVQIADFG	Lys2	85.1	82.8	81.4	<0.1
p38a	UniRef100_Q165	QELNKTIWEVPER	Protein Kinase Domain	28.0	28.2	47.3	>1
PCTAIRE2, PCTAIRE3	UniRef100_Q005	SKLTENLVALKEIR	Lys1	21.3	14.3	-7.5	>1
PDK1	UniRef100_O155	EYAIKILEK	Lys1	28.8	3.9	34.0	>1
PFTAIRE1	UniRef100_O949	LVALKVIR	Lys1	78.6	67.4	36.0	0.20
PHKg2	UniRef100_P157	ATGHEFAVKIMEVTAER	Lys1	-31.1	2.6	23.6	>1
PIK3C3	UniRef100_Q8NI	TEDGGKYPVIFKHGDDLR	ATP	-42.1	-18.2	-52.1	>1
PIK3CD	UniRef100_O003	VNWLAHNVSKDNRQ	ATP	7.4	0.2	-21.6	>1
PIP4K2A	UniRef100_P484	AKELPTLKDNDFINEGQK	ATP	-0.8	21.7	15.5	>1
PIP4K2B	UniRef100_P783	AKDLPTFKDNDFLNEGQK	ATP	-15.6	0.1	-10.4	>1
PIP4K2C	UniRef100_Q8TB	TLVIKEVSSEDIADMHSNLSNY	ATP	-46.7	1.2	14.9	>1
PITSLRE	UniRef100_P211	DLKTSNLLLSHAGILK	Lys2	-41.0	-30.2	-41.6	>1
PKR	UniRef100_P195	DLKPSNIFLVDTK	Lys2	-0.5	-10.8	-2.1	>1
PLK1	UniRef100_P533	CFEISDADTKEVFAGKIVPK	Lys1	26.1	32.3	18.5	>1
PRPK	UniRef100_Q96S	FLSGLELVKQGAEAR	ATP Loop	-24.0	-35.8	-26.4	>1
RAF1	UniRef100_P040	DMKSNNIFLHEGLTVK	Lys2	-39.7	24.3	33.9	>1
RSK1 domain1, RSK2 doma	UniRef100_P518	DLKPENILLDEEGHIK	Lys2	32.7	30.2	38.5	>1
RSK2 domain1	UniRef100_P518	DLKPENILLDEEGHIKLTDFGLS	Lys2	25.3	29.9	32.8	>1
RSK2 domain2	UniRef100_P518	DLKPSNILYVDESGNPESIR	Lys2	21.8	1.5	12.4	>1
RSK3 domain1	UniRef100_Q153	DLKPENILLDEEGHIKITDFGLSI	Lys2	43.7	39.7	38.3	>1
RSKL1	UniRef100_Q96S	VLGVIDKVLLVMDTR	ATP	-25.4	-0.2	27.0	>1
SGK	UniRef100_O001	HKAEEVFYAVKVLQK	Lys1	-38.3	-39.6	-19.9	>1
SGK3	UniRef100_Q96B	FYAVKVLQK	Lys1	36.0	11.6	-2.2	>1
SIK	UniRef100_P570	TQVAIKIIDK	Lys1	51.4	13.5	25.1	0.95
SLK	UniRef100_Q9H2	DLKAGNILFTLDGDIK	Lys2	22.0	-21.2	-13.3	>1

were therefore subtracted from the other treatment percentages. The kinases inhibited with maximum potency were the PFTAIRE1, STE20/SPS1-related proline-alanine-rich protein kinase (STK39/STLK3/SPAK) and the SPAK homolog oxidative stress response -1 (OSR1) kinase.
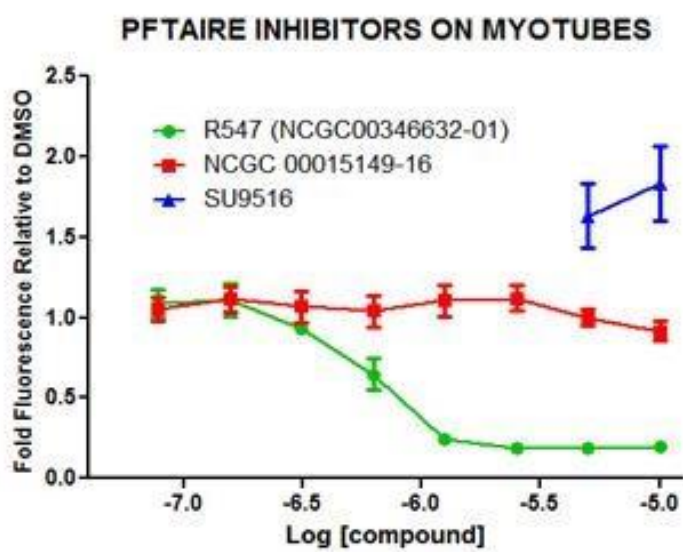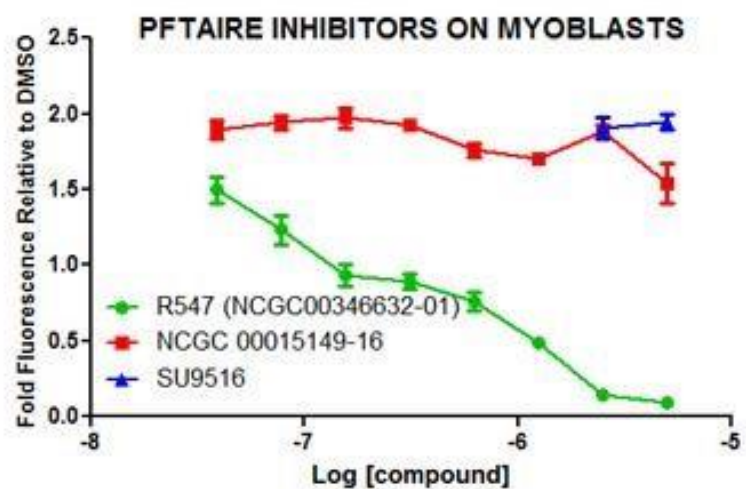
Figure 4- PFTAIRE1 inhibition increases β-Galactosidase activity in $\alpha7^{+/lacZ}$ myoblasts but not myotubes. A) A dose curve with different concentrations of 2 different PFTAIRE1 inhibitors was generated by treating $\alpha7^{+/lacZ}$ myoblasts. Both inhibitors showed a >1 fold fluorescence over DMSO. B) A dose curve with different concentration of 2 different PFTAIRE1 inhibitors was generated by treated $\alpha7^{+/lacZ}$ myotubes. None of the inhibitors showed a >1-fold fluorescence over DMSO. The X-axis represents the log of the concentration of the compound in mol/L or M units.
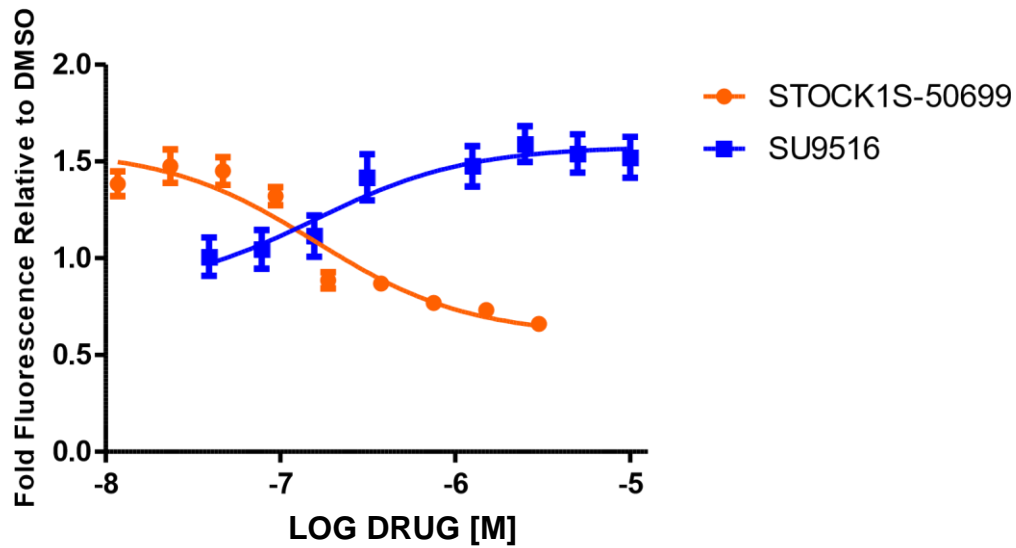
Figure 5- **Pharmacological inhibition of the SPAK/OSR1 activity in α7$^{+/lacZ}$ myotubes increases the β-galactosidase activity.** A dose curve with different concentrations of a chemical called STOCK1S-50699 an inhibitor of SPAK/OSR1 activity was generated by treating α7$^{+/lacZ}$ myotubes. At a concentration of 7.8 nM, this inhibitor showed a ~ 1.5 fold increase in lacZ activity relative to DMSO treatments. At concentrations >90 nM, the drug exhibits toxicity as is reflected in the drop in fold-fluorescence levels relative to DMSO.
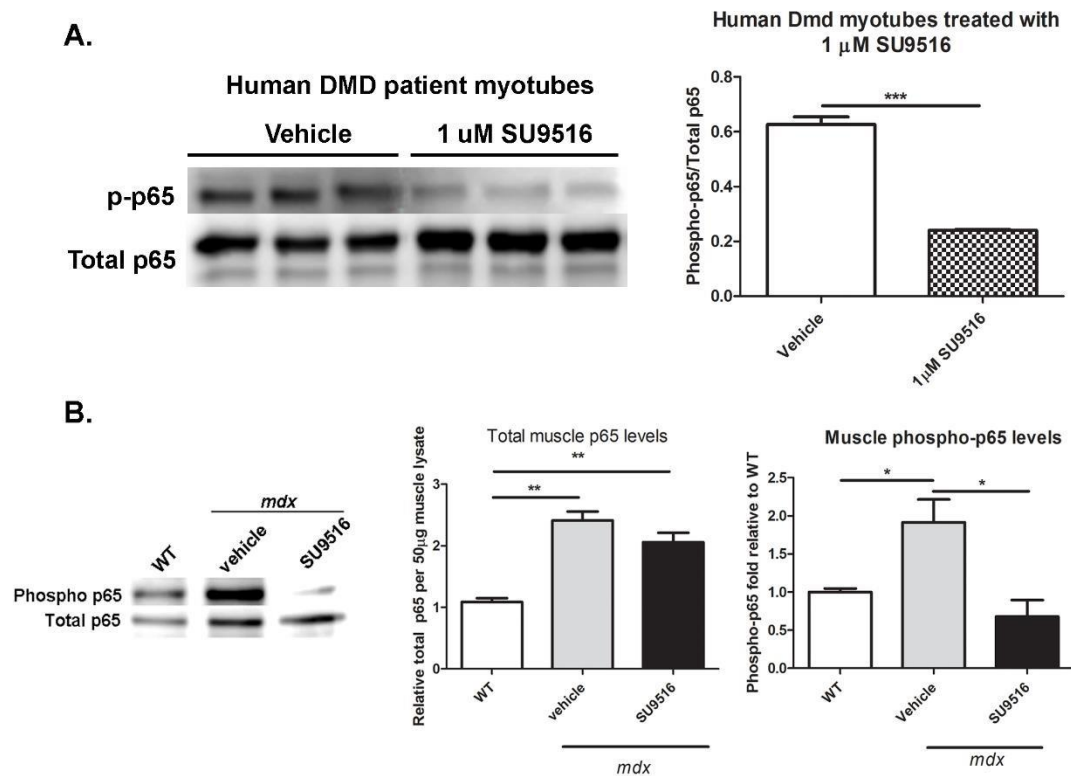
Figure 6 -SU9516 inhibits the activation of p65-NF-kB in human DMD myotubes and *mdx* skeletal muscle. A) Western blot analysis of phosphorylated p65-NF-kB showed that SU9516 treatment decreased the level of p-p65-NF-kB by ~2.6 fold in human DMD patient myotubes. **B)** Western blot analysis for total phosphorylated p65-NF-kB showed that SU9516 treatment decreases the level of p-p65-NF-kB by > 3-fold in the diaphragm of *mdx* mice, compared to the vehicle treated counterparts. (n=3 WT, n=4/*mdx* treatment group,*P<0.05, **P<0.01).
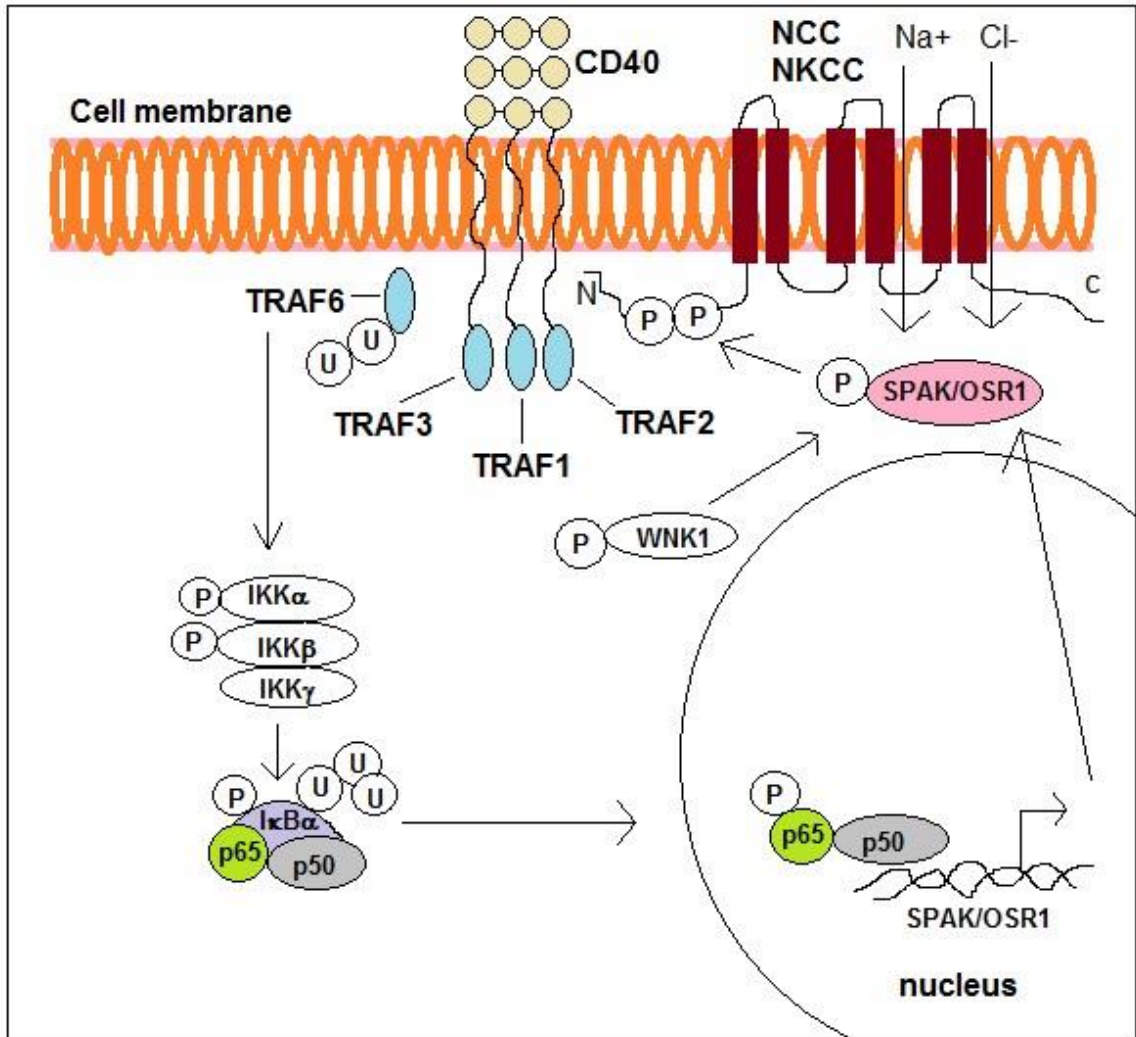
Figure 7- Schematic of a proposed mechanism by which TRAF6-p65-NF-κB pathway regulates SPAK/OSR1 kinase activity.
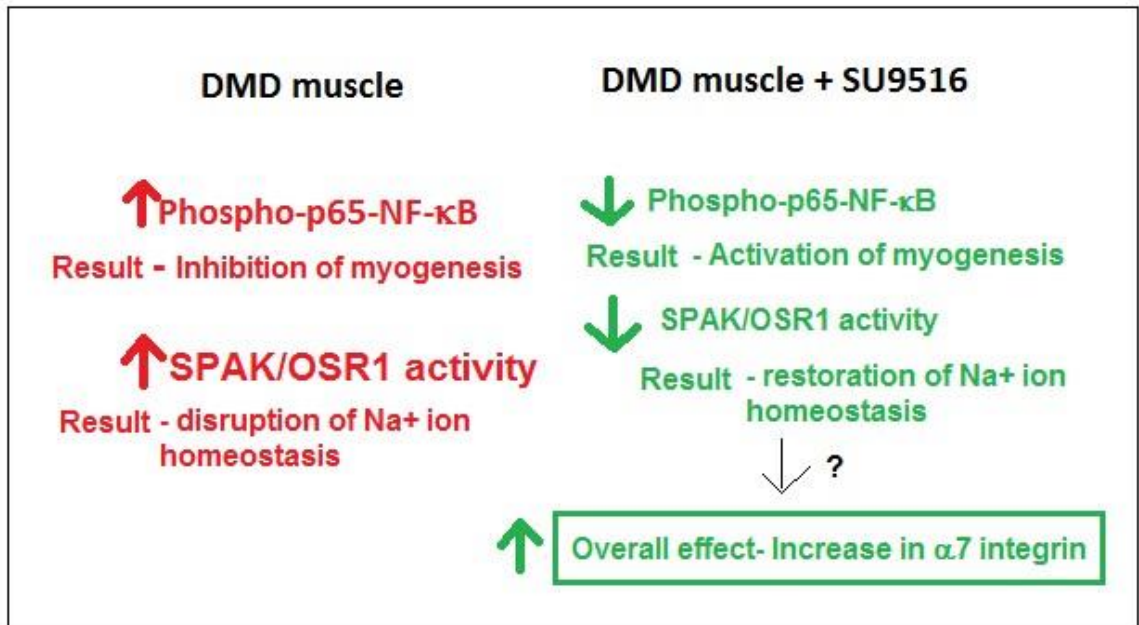
Figure 8- Proposed model for mechanism of action by which SU9516 elevates α7 integrin in dystrophic muscle fibers. In DMD muscle, we propose that the abnormal activation of the p65-NF-kB pathway results in an abnormal activation of the SPAK/OSR1 activity. SU9516 inhibits the activation of p65-NF-kB and therefore decreases the activity of SPAK/OSR1 kinases. This inhibitory effect of SU9516 results in an increase in the levels of α7 integrin through a mechanism that is currently unknown.
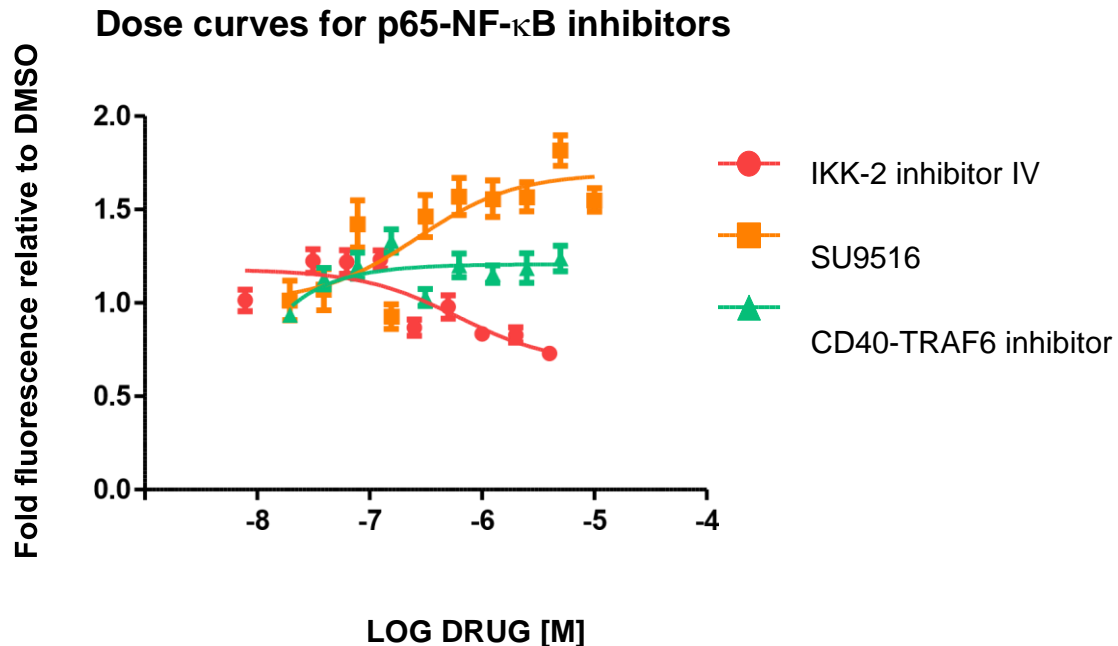
Figure S1- Dose response curves for inhibitors of the p65-NF-kB pathway in α7[+/lacZ]

myotubes. A dose curve with different concentrations of a IKK-2 IV inhibitor was

generated by treating α7[+/lacZ] myotubes. The inhibitor showed a >1 fold fluorescence

over DMSO between 31 nM-125 nM concentrations, but these levels were <1.5-fold

fluorescence over DMSO. A dose curve with different concentrations of CD40-TRAF6

inhibitor was generated by treating α7[+/lacZ] myotubes. The inhibitor showed a >1 fold

fluorescence over DMSO between 39 nM to 5µM concentrations, but these levels were

<1.5-fold fluorescence over DMSO. A dose-response curve for SU9516 was established

in α7[+/lacZ] myotubes and a >1.5 fold-fluorescence over DMSO was obtained between 625

nM to 10 µM concentrations.

Chapter 5

CONCLUSIONS AND FUTURE DIRECTIONS

It has been 30 years since the discovery of the dystrophin gene and the mutations in the gene that cause DMD, however there is still no cure for this fatal disease. The symptoms of the disease can be temporarily managed and lifespan can be slightly prolonged with appropriate medical attention including cardiac and respiratory care. However, DMD is a debilitating condition with patients suffering from progressive muscle weakness and eventual death in their 20s or 30s. Besides the emotional burden, DMD imposes a substantial financial burden on the patients and their families. A recent study showed that combining factors including income loss, finances from lost leisure time, and reduced quality of life (intangible costs), the mean annual household burden of DMD was between \$58,440 and \$71,900 [311]. The annual total societal burden as assessed across four countries- the United States, Germany, Italy and the United Kingdom, was between \$80,120 and \$120,910 per patient, and increased significantly as the disease progressed [311]. Hence, the need for clinical advancement of treatments for DMD has never been greater.

Genetic therapies for DMD that include AAV mediated delivery of mini-dystrophin genes, antisense oligonucleotides and stop-codon read through utilizing drugs such as gentamicin, are a straightforward approach to DMD treatments and aim at restoring dystrophin to the sarcolemma of the patient's myofibers. Cell-based transplantation therapies are also being explored. However, a serious problem associated with these aforementioned therapeutic modalities is the risk of developing a severe immune response to the virus and/or the dystrophin which is recognized as a neoantigen or non-self-gene. Cell based therapies also face similar problems in addition to scalability complications as well as ethical concerns. Protein therapeutics currently

being explored for DMD include Laminin-111, Galectin-1, MG53, Tat-Utrophin and Biglycan. However, a drawback of protein therapeutics could also be possibility of immunogenicity. While new methods directed towards protein therapeutic development seek to improve clinical efficacy, there is also the likelihood of potential immunogenic sequences in the modified proteins. The benefits of small molecule drugs include ease of manufacturing and delivery compared to protein therapies and patient preference for oral ingestion of a therapeutic (e.g., a tablet or capsule) over an injectable protein or antibody therapeutic. Therefore, it is our belief that small molecule drugs will continue to account for the majority of drugs in development and on the market in the future. Hence, our studies focus on the development of small molecule therapeutics for DMD.

Our lab is focused on α7β1 integrin as a therapeutic target for DMD. Recently, research has turned to the integrin family of adhesion molecules in an attempt to better understand the intracellular signal transduction pathway in normal and dystrophic skeletal muscle. Expression of the integrin family is developmentally regulated, the α7β1 integrin being the predominant laminin binding integrin in adult skeletal, cardiac and vascular smooth muscle. Integrins play major roles in muscle differentiation, and α7β1 integrin is a critical receptor for myoblast migration. In adult skeletal muscle, integrins are concentrated at the neuromuscular junction (NMJ) and the myotendinous junction providing an important link to the basement membrane in these specialized regions of muscle. Previous studies have indicated that the absence of the α7 integrin results in congenital myopathy in mice and humans whilst transgenic over-expression of the α7 integrin chain in the skeletal muscle of severely dystrophic mice has been shown to partially rescue the diseased phenotype [195,198]. These correlations suggested that

dystrophin and the α7β1 integrin may have complementary and overlapping functional and structural roles in maintaining skeletal muscle integrity.

As described in this dissertation, our initial studies focused on prednisone, the current front line therapeutic for DMD and the pathway by which the drug ameliorates dystrophic pathology. Prednisone is a corticosteroid that has been known to increase the life expectancy in DMD patients. Chapter 2 of this dissertation focuses on the pathway by which prednisone ameliorates some of the disease pathology and delays the progression of symptoms. It was demonstrated using muscle cells derived from both mice and human DMD patients, that prednisone increases the protein levels of α7 integrin in a dosedependent manner. We also report that prednisone treatment in the well-established *mdx* mouse model of DMD and the GRMD canine model increases protein levels of α7β1 integrin, as well as its ligand, laminin-α2, which is a critical component of the basement membrane. Additionally, we demonstrated that the GRMD dogs that were not treated with prednisone had reduced levels of laminin-α2 and α7 integrin proteins in their skeletal muscle. This translational study therefore provides evidence to show that prednisone, the current front line treatment for DMD, acts to increase laminin-211/221 (composed of α2, β1 and γ1 chains) in the muscle basal lamina which in turn stabilizes protein levels of α7β1 integrin in myogenic cells. These changes are potentially what contribute to improvements in muscle fiber integrity in dystrophin-deficient muscle and slow down disease progression. The results also suggest a shared mechanism for disease progression in GRMD dogs and humans, reinforcing the view that the canine model provides a useful tool for studies of the human disease. Despite the beneficial effects of prednisone, the improvement is temporary and, furthermore,

therapy is complicated by the wide range of associated negative side effects. Future studies to identify drugs that specifically target an increase in laminin-α2 and/or α7β1 integrin in muscle are likely to improve clinical outcomes and have fewer negative side effects for DMD patients. This study as well as several previous studies have implicated α7β1 integrin to be a major modifier of disease progression in DMD pathology.

Chapter 3 of this dissertation presents a novel first in-class integrin enhancing small molecule SU9516 for the treatment of Duchenne Muscular Dystrophy. SU9516 is an indolinone compound and a known potent inhibitor of CDK2 [262]. The drug is also an inhibitor of glyocgen synthase kinase 3 (GSK-3), which is involved in normal cell death [207]. In human leukemic cells, SU9516 caused the pronounced down-regulation of the antiapoptotic protein Mcl-1 through transcriptional repression, increased proteasomal degradation, inhibition of RNA Pol II CTD phosphorylation and oxidative damage [208]. Hence, the existing literature regarding SU9516 has well established its properties and potential as an anti-neoplastic therapeutic. Two small molecules which have a similar backbone structure to SU9516 have entered clinical trials for colorectal cancer (SU5416/semaxinib) or have been given FDA approval multi-targeted receptor-tyrosine kinase inhibitors for the treatment of renal cell carcinoma and gastrointestinal stromal tumor (SU11248/Sunitinib). Given that these related compounds are undergoing or have completed clinical trials for other indications, SU9516 or an analog may be a candidate to fast track for the treatment of DMD. SU9516 was first identified in a drug screen developed and described previously in our lab [56]. Briefly, undifferentiated α7$^{+/lacZ}$ myoblasts and differentiated myotubes were used to screen 433,000 compounds (48 hour treatment) and β-Galactosidase enzymatic activity was measured using the Fluorescein

diβ-D-galactopyranoside (FDG) assay. FDG is one of the most sensitive fluorogenic substrates available for detecting β-Galactosidase that cleaves FDG to produce fluorescein. The identification of a first in-class α7β1 integrin enhancing drug SU9516 provides further support for the utilization of this chemical screen to identify promising integrin enhancing compounds with the potential to make it to clinical trials for DMD. Results from *in vitro* experiments with SU9516 showed increases in the protein levels of α7B integrin in human DMD patient cells and C2C12 myogenic cells with drug treatment. In this study we show that a seven week treatment of 5mg/kg/day SU9516 increases the protein levels of α7B and β1D integrin in the skeletal muscle of dystrophin-deficient *mdx* mice, thereby demonstrating *in vivo* on-target activity. In DMD patients, the skeletal muscles progressively weaken, pathology is severe and patients lose their ability to walk by 8 years of age. In *mdx* mice, however, most of the skeletal muscle pathology is comparatively mild and appears to plateau after 3 months of age. In contrast, the diaphragm muscle is more severely and progressively affected in *mdx* mice and thus is more representative of the muscle pathology in DMD patients [14]. The *ex vivo* muscle contraction experiments performed on the diaphragm of the *mdx* mice showed that SU9516 increases the specific force produced by the *mdx* diaphragm. Additionally, we also showed via phrenic nerve stimulation and intracellular recordings of the myofibers in the diaphragm that the SU9516 treated *mdx* diaphragm muscles showed greater success in displacement, decay rate and action potential conduction compared to their vehicle treated counterparts. Hence, SU9516 not only shows *in vitro* and *in vivo* on-target activity for α7β1 integrin but also shows muscle contractility improvements

and improvements in neuromuscular kinetics of one of the most severely affected respiratory muscles affected in the mdx mouse; the diaphragm.

Chapter 4 discusses some of the numerous molecular pathways targeted by SU9516 that could be therapeutic for the treatment of DMD. It was determined that the inhibition of both MAP4k4 and the PFTAIRE1 kinases by pharmacological means, increased the β-galactosidase activity in $α7^{+/lacZ}$ myoblasts but not myotubes. Hence, the identification of a pathway or multiple pathways responsible for the increase in α7β1 integrin is yet to be elucidated. This study has identified a pathway, the inhibition of which may be partially responsible for the increase in α7β1 integrin in myofibers. This is the p65-NF-kB inflammatory pathway that is activated in dystrophic myofibers of DMD patients and the *mdx* mouse. Previous research has focused on the NF-κB pathway, which plays a role in exacerbating the pathophysiology in DMD patients and the *mdx* mouse [282,312]. Treatments that inhibit the activation of the NF-κB pathway have great potential for DMD, because prednisone, the current front line treatment for DMD inhibits this pathway [313]. Besides prednisone, several compounds have been shown to inhibit the NF-κB pathway and ameliorate pathology in the *mdx* mouse. As an example, inhibiting NF-κB signaling with Nemo Binding Domain (NBD) peptide alleviated some of the pathogenesis in dystrophic muscle and improved muscle function in mouse models of DMD [314,315]. Additionally, NBD treatment in GRMD dogs also exhibited an efficacious response, providing further support for its potential use as a DMD therapeutic [316].

Dystrophic membranes have depolarized resting membrane potentials [260,263–265]. Several studies indicate that resting intracellular free Ca^{2+} concentration is higher in skeletal muscle cells from the *mdx* mice and DMD patients compared with normal cells [258,266–270]. The exact mechanism by which the Ca^{2+} levels are elevated in the muscle is not known. Additional experiments to look at the effects of SU9516 on Ca^{2+} release at the neuromuscular junction, will determine whether SU9516 treatment restores the aberrant Ca^{2+} signaling in dystrophic muscle thereby alleviating the action potential failure as seen in SU9516 treated *mdx* mice. The level of $[Ca^{2+}]_{rest}$ modulates the transcription factor NFκB activity and iNOS expression in *mdx* myotubes [317]. Our study identified SU9516 as an inhibitor of p65-NF-κB signaling activation in skeletal muscle. Increased NF-kB activity in *mdx* mice is associated with both immune cells and regenerative muscle fibers and the inhibition of the p65-NF-κB pathway either genetically or by pharmacological means promoted formation of new myofibers in response to degeneration [282]. Our study confirms that the increase in centrally nucleated myofibers and embryonic myosin heavy chain positive myofibers seen in the diaphragm of SU9516 treated *mdx* mice can be attributed to SU9516 inhibition of p65 activation. Hence, this study presents not only an integrin enhancing drug with the ability to rescue the primary defect of sarcolemmal damage owing to a downregulation of the DGC components, but also an inhibitor of the NF-kB inflammatory pathway that is a major cause of secondary defects associated with this fatal disease. Furthermore, it is possible that SU9516 through the inhibition of p65-NF-kB activation is able to restore aberrant Ca^{2+} signaling with dystrophic muscle.

An important question asked in this study was whether the inhibition of the p65-NF-κB pathway caused an increase in α7 integrin. Our study showed that the pharmacological inhibition of the p65-NF-κB signaling pathway increased the βgalactosidase activity in α7$^{lacZ/+}$ myoblasts and myotubes. Through this finding we suggest that the increase in the protein levels of α7B and β1D in myofibers with SU9516 treatment, can be attributed at least partially to the inhibition of the p65-NF-κB pathway. It must be noted however, that the two p65-NF-kB pathway inhibitors used in our chemical screen, did not attain the levels of fold-fluorescence that SU9516 attained. However, additional experiments to verify this hypothesis will be performed in the future to confirm that p65-NF-κB is indeed the molecular pathway that regulates integrin levels in dystrophic myofbers. We seek to quantify the α7β1 integrin protein levels in the *mdx*;p65$^{+/-}$ mouse model to determine whether p65 haploinsufficency ameliorates some of the pathology in the *mdx* mouse through an α7β1 integrin mediated pathway.

One of the most critical and novel findings of this study was the identification of the SPAK/OSR1 kinases as being the molecular target that regulates levels of α7 integrin in skeletal muscle. A known inhibitor of the SPAK/OSR1 kinase activity showed robust increases (almost attaining comparable levels to SU9516) in β-galactosidase activity of α7$^{lacZ/+}$ myotubes. The oxidative stress-responsive kinase-1 (OSR1)/STE20/SPS1-related proline/alanine-rich kinases (SPAK) are involved in the regulation of NaCl cotransporter (NCC) through phosphorylation. In an inflammatory intestinal bowel disease model, it was shown that the knock-down of NF-κB (p65) by siRNA decreased SPAK expression significantly and NF-κB-binding site on the SPAK gene was essential for stimulated

SPAK promoter activity by TNF-α [308]. It is known that NF-κB is a pro-inflammatory transcription factor that is active in the dystrophin deficient muscle of both DMD patients and the *mdx* mouse [286,287]. This could potentially lead to the abnormal activation of the SPAK-NCC phosphorylation in dystrophic muscle. This suggests that through the inhibition of p65- NF-kB activation, SU9516 inhibits the abnormal activation of the SPAK kinase-NCC cascade, thereby restoring the Na^+ ion homeostasis in myofibers of dystrophic mice. Additionally, increased levels of α7β1 integrin with SU9516 treatment could bring about maintenance of intracellular Ca^{2+} levels in *mdx* myofibers. The improvement in parameters like maximum displacement of myofibers, decay rate, time to 50% EPP and resting membrane potential, could be attributed to the restored Ca^{2+} signaling with SU9516 treatment.

Finally, a novel molecular target of SU9516 identified in this study was CD82, a tetraspanin that is known to interact with integrins at the cell membrane. A previous study utilizing CD82 null endothelial cells (ECs) has shown that surface levels of cell adhesion molecules like CD44 and α6 integrin were upregulated as a result of possible protein turnover rather than gene transcription [318]. The CD44 antigen is a cell-surface glycoprotein involved in cell–cell interactions, cell adhesion and migration. Our results suggest that SU9516 mediated downregulation of CD82 could be responsible for the increase in α7 intgerin seen in myogenic cells lines and *in vivo*. CD82 is a known regulator of endocytosis and it is possible that the downregulation of CD82 with SU9516 inhibits the endocytosis of α7 integrin at the cell surface of a myogenic cell. Additionally, our results also showed that 24 hours post differentiation, the levels of CD82 were significantly elevated in the C2C12 myogenic cells compared to when they

were in proliferation/growth medium. This suggests that CD82 may have a role in early myogenic differentiation and further investigation into the role of this tetraspanin would help identify its role in myogenesis.

While the inhibitors used in this study targeted at the MAP4k4, PFTAIRE1 and the p65-NF-κB pathway elicited interesting preliminary results that shed light on the mechanism of action by which SU9516 increased α7β1 inetgrin expression in muscle, it must be noted that the aforementioned inhibitors are not specific to the kinases described in this study. Future studies would include using approaches to eliminate the expression of the aforementioned kinases and assess levels of α7β1 integrin. SPAK/OSR1/PFTAIRE1 knockout lines can be generated to determine whether the integrin is upregulated in these cell lines. Currently, we are employing Crispr/Cas9 technology to determine whether the knockout of these kinases or the combination of these kinases will ameliorate disease pathology. A summary of the molecular targets of SU9516 and the potential therapeutic benefits associated with the inhibition or downregulation of those targets is shown in Table 1.

Future studies with SU9516 would involve studying the effect of SU9516 over a longer duration of treatment. SU9516 may prove to be highly effective as a short term therapeutic for DMD, however its long term therapeutic benefits are questionable owing to the numerous off-target effects the drug generates. Currently, there are several drawbacks associated with SU9516 as a drug for the treatment of DMD. A serious issue with the drug is that it is fatal to the *mdx* mice at a dose of 10 mg/kg and it is critical that in order to move forward with the drug its toxicity be minimized. Additionally, it has

poor biodistribution and poor absorption in the serum and muscle. The half-life of the drug is extremely short at 30 minutes post oral ingestion. The chemical make-up or structure of a drug is the key determinant of its potency, specificity, dosing regimen and side effect profile and the chemical structure of SU9516 requires modifications to formulate a drug with improved pharmacokinetics. This is critical because even minor modifications in chemical and molecular structure can differentiate drugs and determine their success or failure in the marketplace. While targets are used for evaluating the drug characteristics of chemical compounds, sophisticated chemistry expertise is required to analyze the raw compound, understand its chemical composition, engineer it into a therapeutic candidate, and develop it into a drug. We expect the preference for drugs that are small molecules like SU9516 to continue to benefit companies with medicinal chemistry expertise. This dissertation presents a powerful new therapeutic strategy for the treatment of DMD; namely α7β1 integrin enhancing small molecule compounds.

Molecular Target	Effect of inhibition/downregulation	Clinical significance of SU9516 for DMD
MAP4k4 (HGK)	1. Promotes myogenic differentiation 2. Increases α7 integrin in myoblasts	1. Coadjuvant during myoblast transplantation. 2. DMD therapeutic
CD82 tetraspanin	Possible increase in surface α7 integrin in myoblasts	1. Coadjuvant during myoblast transplantation. 2. DMD therapeutic
PFTAIRE1	Increases α7 integrin in myoblasts	1. Coadjuvant during myoblast transplantation. 2. DMD therapeutic
SPAK/OSR1	1. Increases α7 integrin in myotubes 2. Restores Na^+ ion homeostasis in dystrophic myofibers	1. DMD therapeuticα7 integrin enhancing drug 2. Potential for improved neuromuscular kinetics in DMD patient muscle
p65-NF-κB	1. Increases α7 integrin in myotubes 2. Restores Ca^{2+} homeostasis in dystrophic myofibers 3. Ameliorates fibrosis 4. Activates the myogenic program in DMD.	1. DMD therapeutic- α7 integrin enhancing drug 2. Potential for improved neuromuscular kinetics in DMD patient muscle. 3. Anti-fibrotic therapeutic for DMD.

Table 1- Summary of critical targets of SU9516 and potential therapeutic implications of those molecular targets for DMD.

BIBLIOGRAPHY

1. Mendell, J. R. *et al.* Evidence-based path to newborn screening for Duchenne muscular dystrophy. *Ann. Neurol.* **71,** 304–13 (2012).

2. Pichavant, C. *et al.* Current status of pharmaceutical and genetic therapeutic approaches to treat DMD. *Mol. Ther.* **19,** 830–40 (2011).

3. Dunckley, M. G., Manoharan, M., Villiet, P., Eperon, I. C. & Dickson, G. Modification of splicing in the dystrophin gene in cultured Mdx muscle cells by antisense oligoribonucleotides. *Hum. Mol. Genet.* **7,** 1083–90 (1998).

4. Wilton, S. D., Honeyman, K., Fletcher, S. & Laing, N. G. Snapback SSCP analysis:
engineered conformation changes for the rapid typing of known mutations. *Hum. Mutat.* **11,** 252–8 (1998).

5. Dickson, G. *et al.* Co-localization and molecular association of dystrophin with laminin at the surface of mouse and human myotubes. *J. Cell Sci.* **103 (Pt 4,** 1223– 33 (1992).

6. Nallamilli, B. R. R., Ankala, A. & Hegde, M. Molecular diagnosis of duchenne muscular dystrophy. *Curr. Protoc. Hum. Genet.* **83,** 9.25.1–9.25.29 (2014).

7. Beggs, a H. *et al.* Exploring the molecular basis for variability among patients with Becker muscular dystrophy: dystrophin gene and protein studies. *Am. J. Hum. Genet.* **49,** 54–67 (1991).

8. Bushby, K. *et al.* Diagnosis and management of Duchenne muscular dystrophy, part 1: diagnosis, and pharmacological and psychosocial management. *Lancet Neurol.* **9,** 77–93 (2010).

9. Cyrulnik, S. E. *et al.* Cognitive and adaptive deficits in young children with Duchenne muscular dystrophy (DMD). *J. Int. Neuropsychol. Soc.* **14,** 853–61 (2008).

10. Bushby, K. *et al.* Diagnosis and management of Duchenne muscular dystrophy, part 2: implementation of multidisciplinary care. *Lancet. Neurol.* **9,** 177–89 (2010).

11. Eagle, M. *et al.* Managing Duchenne muscular dystrophy – The additive effect of spinal surgery and home nocturnal ventilation in improving survival. *Neuromuscul. Disord.* **17,** 470–475 (2007).

12. Sicinski, P. *et al.* The molecular basis of muscular dystrophy in the mdx mouse: a point mutation. *Science (80-.).* **244,** 1578–1580 (1989).

13. Bulfield, G., Siller, W. G., Wight, P. A. & Moore, K. J. X chromosome-linked muscular dystrophy (mdx) in the mouse. *Proc. Natl. Acad. Sci. U. S. A.* **81,** 1189–92 (1984).

14. Stedman, H. H. *et al.* The mdx mouse diaphragm reproduces the degenerative changes of Duchenne muscular dystrophy. *Nature* **352,** 536–9 (1991).

15. Chapman, V. M., Miller, D. R., Armstrong, D. & Caskey, C. T. Recovery of induced mutations for X chromosome-linked muscular dystrophy in mice. *Proc. Natl. Acad. Sci. U. S. A.* **86,** 1292–6 (1989).

16. Cox, G. A., Phelps, S. F., Chapman, V. M. & Chamberlain, J. S. New mdx mutation disrupts expression of muscle and nonmuscle isoforms of dystrophin. *Nat. Genet.* **4,** 87–93 (1993).

17. Im, W. B. *et al.* Differential expression of dystrophin isoforms in strains of mdx mice with different mutations. *Hum. Mol. Genet.* **5,** 1149–1153 (1996).

18. Danko, I., Chapman, V. & Wolff, J. A. The frequency of revertants in mdx mouse genetic models for Duchenne muscular dystrophy. *Pediatr. Res.* **32,** 128–31 (1992).

19. Haslett, J. N. *et al.* The influence of muscle type and dystrophin deficiency on murine expression profiles. *Mamm. Genome* **16,** 739–748 (2005).

20. Beastrom, N. *et al.* mdx(^{5}cv) mice manifest more severe muscle dysfunction and diaphragm force deficits than do mdx Mice. *Am. J. Pathol.* **179,** 2464–74 (2011).

21. Sharp, N. J. *et al.* An error in dystrophin mRNA processing in golden retriever muscular dystrophy, an animal homologue of Duchenne muscular dystrophy. *Genomics* **13,** 115–21 (1992).

22. Kornegay, J. N., Tuler, S. M., Miller, D. M. & Levesque, D. C. Muscular dystrophy in a litter of golden retriever dogs. *Muscle Nerve* **11,** 1056–64 (1988).

23. Valentine, B. A., Cooper, B. J., de Lahunta, A., O'Quinn, R. & Blue, J. T. Canine X-linked muscular dystrophy. *J. Neurol. Sci.* **88,** 69–81 (1988).

24. Kornegay, J. N. *et al.* Canine models of Duchenne muscular dystrophy and their use in therapeutic strategies. *Mamm. Genome* **23,** 85–108 (2012).

25. Childers, M. K. *et al.* Eccentric contraction injury in dystrophic canine muscle. *Arch. Phys. Med. Rehabil.* **83,** 1572–1578 (2002).

26. Childers, M. K. *et al.* Myofiber injury and regeneration in a canine homologue of Duchenne muscular dystrophy. *Am. J. Phys. Med. Rehabil.* **80,** 175–81 (2001).

27. Kornegay, J. N. *et al.* Contraction force generated by tarsal joint flexion and extension in dogs with golden retriever muscular dystrophy. *J. Neurol. Sci.* **166,** 115–121 (1999).

28. Kornegay, J. N., Cundiff, D. D., Bogan, D. J., Bogan, J. R. & Okamura, C. S. The cranial sartorius muscle undergoes true hypertrophy in dogs with golden retriever muscular dystrophy. *Neuromuscul. Disord.* **13,** 493–500 (2003).

29. Kornegay, J. N. *et al.* Contraction tension and kinetics of the peroneus longus muscle in golden retriever muscular dystrophy. *J. Neurol. Sci.* **123,** 100–7 (1994).

30. Kornegay, J. N., Sharp, N. J., Schueler, R. O. & Betts, C. W. Tarsal joint contracture in dogs with golden retriever muscular dystrophy. *Lab. Anim. Sci.* **44,** 331–3 (1994).

31. Valentine, B. A., Kornegay, J. N. & Cooper, B. J. Clinical electromyographic studies of canine X-linked muscular dystrophy. *Am. J. Vet. Res.* **50,** 2145–7 (1989).

32. McGreevy, J. W., Hakim, C. H., McIntosh, M. A. & Duan, D. Animal models of Duchenne muscular dystrophy: from basic mechanisms to gene therapy. *Dis. Model. Mech.* **8,** 195–213 (2015).

33. Chamberlain, J. S., Metzger, J., Reyes, M., Townsend, D. & Faulkner, J. A. Dystrophin-deficient mdx mice display a reduced life span and are susceptible to spontaneous rhabdomyosarcoma. *FASEB J.* **21,** 2195–204 (2007).

34. Li, D., Long, C., Yue, Y. & Duan, D. Sub-physiological sarcoglycan expression contributes to compensatory muscle protection in mdx mice. *Hum. Mol. Genet.* **18,** 1209–1220 (2009).

35. Mendell, J. R. *et al.* Randomized, double-blind six-month trial of prednisone in Duchenne's muscular dystrophy. *N. Engl. J. Med.* **320,** 1592–7 (1989).

36. Liu, J. M. K. *et al.* Effects of prednisone in canine muscular dystrophy. *Muscle Nerve* **30,** 767–73 (2004).

37. Bassett, D. I. *et al.* Dystrophin is required for the formation of stable muscle attachments in the zebrafish embryo. *Development* **130,** 5851–5860 (2003).

38. Bolanos-Jimenez, F. *et al.* Dystrophin and Dp71, two products of the DMD gene, show a different pattern of expression during embryonic development in zebrafish. *Mech Dev* **102,** 239–241 (2001).

39. Berger, J., Berger, S., Hall, T. E., Lieschke, G. J. & Currie, P. D. Dystrophindeficient zebrafish feature aspects of the Duchenne muscular dystrophy pathology. *Neuromuscul. Disord.* **20,** 826–832 (2010).

40. SCHAPIRA, G., DREYFUS, J. C. & JOLY, M. Changes in the flow birefringence of myosin as a result of muscular atrophy. *Nature* **170,** 494–5 (1952).

41. Li, M., Andersson-Lendahl, M., Sejersen, T. & Arner, A. Muscle dysfunction and structural defects of dystrophin-null sapje mutant zebrafish larvae are rescued by ataluren treatment. *FASEB J.* **28,** 1593–9 (2014).

42. Marinkovich, M. P. Tumour microenvironment: laminin 332 in squamous-cell carcinoma. *Nat. Rev. Cancer* **7,** 370–80 (2007).

43. Colognato, H. & Yurchenco, P. D. Form and function: The laminin family of heterotrimers. *Dev. Dyn.* **218,** 213–234 (2000).

44. Miner, J. H. & Yurchenco, P. D. Laminin functions in tissue morphogenesis. *Annu. Rev. Cell Dev. Biol.* **20,** 255–284 (2004).

45. Sasaki, T., Giltay, R., Talts, U., Timpl, R. & Talts, J. F. Expression and distribution of laminin alpha1 and alpha2 chains in embryonic and adult mouse tissues: an immunochemical approach. *Exp. Cell Res.* **275,** 185–199 (2002).

46. Ehrig, K., Leivo, I., Argraves, W. S., Ruoslahti, E. & Engvall, E. Merosin, a tissuespecific basement membrane protein, is a laminin-like protein. *Proc Natl Acad Sci U S A* **87,** 3264–3268 (1990).

47. Patton, B. L., Miner, J. H., Chiu, A. Y. & Sanes, J. R. Distribution and function of laminins in the neuromuscular system of developing, adult, and mutant mice. *J. Cell Biol.* **139,** 1507–1521 (1997).

48. Talts, J. F., Mann, K., Yamada, Y. & Timpl, R. Structural analysis and proteolytic processing of recombinant G domain of mouse laminin alpha2 chain. *FEBS Lett.* **426,** 71–6 (1998).

49. Suzuki, N., Yokoyama, F. & Nomizu, M. Functional sites in the laminin alpha chains. *Connect. Tissue Res.* **46,** 142–52 (2005).

50. Timpl, R. *et al.* Structure and function of laminin LG modules. *Matrix Biol.* **19,** 309– 317 (2000).

51. Ido, H. *et al.* The requirement of the glutamic acid residue at the third position from the carboxyl termini of the laminin ?? chains in integrin binding by laminins. *J. Biol. Chem.* **282,** 11144–11154 (2007).

52. Carafoli, F., Clout, N. J. & Hohenester, E. Crystal structure of the LG1-3 region of the laminin ??2 chain. *J. Biol. Chem.* **284,** 22786–27792 (2009).

53. Smirnov, S. P. *et al.* Contributions of the LG Modules and Furin Processing to Laminin-2 Functions. *J. Biol. Chem.* **277,** 18928–18937 (2002).

54. Carmignac, V. *et al.* Autophagy is increased in laminin α2 chain-deficient muscle and its inhibition improves muscle morphology in a mouse model of MDC1A. *Hum. Mol. Genet.* **20,** 4891–4902 (2011).

55. Silva-Barbosa, S. D. *et al.* Human myoblast engraftment is improved in lamininenriched microenvironment. *Transplantation* **85,** 566–575 (2008).

56. Rooney, J. E., Gurpur, P. B. & Burkin, D. J. Laminin-111 protein therapy prevents muscle disease in the mdx mouse model for Duchenne muscular dystrophy. *Proc. Natl. Acad. Sci. U. S. A.* **106,** 7991–6 (2009).

57. Goudenege, S. *et al.* Laminin-111: a potential therapeutic agent for Duchenne muscular dystrophy. *Mol. Ther.* **18,** 2155–63 (2010).

58. Koenig, M., Monaco, a P. & Kunkel, L. M. The complete sequence of dystrophin predicts a rod-shaped cytoskeletal protein. *Cell* **53,** 219–228 (1988).

59. Ervasti, J. M. Dystrophin, its interactions with other proteins, and implications for muscular dystrophy. *Biochim. Biophys. Acta* **1772,** 108–17 (2007).

60. Rybakova, I. N. Utrophin Binds Laterally along Actin Filaments and Can Couple Costameric Actin with Sarcolemma When Overexpressed in Dystrophin-deficient Muscle. *Mol. Biol. Cell* **13,** 1512–1521 (2002).

61. Ahn, A. H. Syntrophin binds to an alternatively spliced exon of dystrophin. *J. Cell Biol.* **128,** 363–371 (1995).

62. Suzuki, A. Mammalian alpha 1- and beta 1-syntrophin bind to the alternative splice- prone region of the dystrophin COOH terminus. *J. Cell Biol.* **128,** 373–381 (1995).

63. Chan, Y. M., Bönnemann, C. G., Lidov, H. G. & Kunkel, L. M. Molecular organization of sarcoglycan complex in mouse myotubes in culture. *J. Cell Biol.* **143,** 2033–44 (1998).

64. Brenman, J. E., Chao, D. S., Xia, H., Aldape, K. & Bredt, D. S. Nitric oxide synthase complexed with dystrophin and absent from skeletal muscle sarcolemma in Duchenne muscular dystrophy. *Cell* **82,** 743–752 (1995).

65. Sakamoto, A. *et al.* Both hypertrophic and dilated cardiomyopathies are caused by mutation of the same gene, delta-sarcoglycan, in hamster: an animal model of disrupted dystrophin-associated glycoprotein complex. *Proc. Natl. Acad. Sci. U. S. A.* **94,** 13873–8 (1997).

66. Yoshida, M. Biochemical evidence for association of dystrobrevin with the sarcoglycan-sarcospan complex as a basis for understanding sarcoglycanopathy. *Hum. Mol. Genet.* **9,** 1033–1040 (2000).

67. Crosbie, R. H., Heighway, J., Venzke, D. P., Lee, J. C. & Campbell, K. P. Sarcospan, the 25-kDa Transmembrane Component of the Dystrophin-Glycoprotein Complex. *J. Biol. Chem.* **272,** 31221–31224 (1997).

68. Rafii, M. S. *et al.* Biglycan binds to α- and γ-sarcoglycan and regulates their expression during development. *J. Cell. Physiol.* **209,** 439–447 (2006).

69. Chen, J. *et al.* Identification of functional domains in sarcoglycans essential for their interaction and plasma membrane targeting. *Exp. Cell Res.* **312,** 1610–1625 (2006).

70. Mercuri, E. & Muntoni, F. The ever-expanding spectrum of congenital muscular dystrophies. *Ann. Neurol.* **72,** 9–17 (2012).

71. Blake, D. J. Dystrobrevin dynamics in muscle-cell signalling: a possible target for therapeutic intervention in Duchenne muscular dystrophy? *Neuromuscul. Disord.* **12 Suppl 1,** S110–7 (2002).

72. Newey, S. E. *et al.* Syncoilin, a Novel Member of the Intermediate Filament Superfamily That Interacts with alpha -Dystrobrevin in Skeletal Muscle. *J. Biol. Chem.* **276,** 6645–6655 (2000).

73. Roberts, R. G. Dystrophins and dystrobrevins. *Genome Biol.* **2,** REVIEWS3006 (2001).

74. Kramarcy, N., Vidal, A., Froehner, S. & Sealock, R. Association of utrophin and multiple dystrophin short forms with the mammalian M(r) 58,000 dystrophinassociated protein (syntrophin). *J. Biol. Chem.* **269,** 2870–2876 (1994).

75. Peters, M. F., Kramarcy, N. R., Sealock, R. & Froehner, S. C. beta 2-Syntrophin: localization at the neuromuscular junction in skeletal muscle. *Neuroreport* **5,** 1577– 80 (1994).

76. Grady, R. M. *et al.* Role for alpha-dystrobrevin in the pathogenesis of dystrophindependent muscular dystrophies. *Nat. Cell Biol.* **1,** 215–20 (1999).

77. Percival, J. M., Anderson, K. N. E., Huang, P., Adams, M. E. & Froehner, S. C. Golgi and sarcolemmal neuronal NOS differentially regulate contraction-induced fatigue and vasoconstriction in exercising mouse skeletal muscle. *J. Clin. Invest.* **120,** 816–26 (2010).

78. Marshall, J. L. & Crosbie-Watson, R. H. Sarcospan: a small protein with large potential for Duchenne muscular dystrophy. *Skelet. Muscle* **3,** 1 (2013).

79. Miller, G., Wang, E. L., Nassar, K. L., Peter, A. K. & Crosbie, R. H. Structural and functional analysis of the sarcoglycan-sarcospan subcomplex. *Exp. Cell Res.* **313,** 639–51 (2007).

80. Davies, K. E. & Nowak, K. J. Molecular mechanisms of muscular dystrophies: old and new players. *Nat. Rev. Mol. Cell Biol.* **7,** 762–73 (2006).

81. Ervasti, J. M. Dystrophin, its interactions with other proteins, and implications for muscular dystrophy. *Biochim. Biophys. Acta* **1772,** 108–17 (2007).

82. Bladen, C. L. *et al.* The TREAT-NMD DMD Global Database: analysis of more than 7,000 Duchenne muscular dystrophy mutations. *Hum. Mutat.* **36,** 395–402 (2015).

83. Goemans, N. M. *et al.* Systemic administration of PRO051 in Duchenne's muscular dystrophy. *N. Engl. J. Med.* **364,** 1513–22 (2011).

84. Cirak, S. *et al.* Restoration of the dystrophin-associated glycoprotein complex after exon skipping therapy in Duchenne muscular dystrophy. *Mol. Ther.* **20,** 462–7 (2012).

85. Goyenvalle, A. *et al.* Functional correction in mouse models of muscular dystrophy using exon-skipping tricyclo-DNA oligomers. *Nat. Med.* **21,** 270–5 (2015).

86. Dent, K. M. *et al.* Improved molecular diagnosis of dystrophinopathies in an unselected clinical cohort. *Am. J. Med. Genet. A* **134,** 295–8 (2005).

87. Barton-Davis, E. R., Cordier, L., Shoturma, D. I., Leland, S. E. & Sweeney, H. L. Aminoglycoside antibiotics restore dystrophin function to skeletal muscles of mdx mice. *J. Clin. Invest.* **104,** 375–81 (1999).

88. Wagner, K. R. *et al.* Gentamicin treatment of Duchenne and Becker muscular dystrophy due to nonsense mutations. *Ann. Neurol.* **49,** 706–711 (2001).

89. Politano, L. *et al.* Gentamicin administration in Duchenne patients with premature stop codon. Preliminary results. *Acta Myol.* **22,** 15–21 (2003).

90. Malik, V. *et al.* Gentamicin-induced readthrough of stop codons in Duchenne muscular dystrophy. *Ann. Neurol.* **67,** 771–80 (2010).

91. Welch, E. M. *et al.* PTC124 targets genetic disorders caused by nonsense mutations. *Nature* **447,** 87–91 (2007).

92. Hoffman, E. P. & Connor, E. M. Orphan drug development in muscular dystrophy:
update on two large clinical trials of dystrophin rescue therapies. *Discov Med* **16,** 233–239 (2013).

93.   Finkel, R. S. *et al.* Phase 2a Study of Ataluren-Mediated Dystrophin Production in Patients with Nonsense Mutation Duchenne Muscular Dystrophy. *PLoS One* **8,** e81302 (2013).

94.   Bish, L. T. *et al.* Long-term restoration of cardiac dystrophin expression in golden retriever muscular dystrophy following rAAV6-mediated exon skipping. *Mol. Ther.* **20,** 580–9 (2012).

95.   Barbash, I. M. *et al.* MRI roadmap-guided transendocardial delivery of exonskipping recombinant adeno-associated virus restores dystrophin expression in a canine model of Duchenne muscular dystrophy. *Gene Ther.* **20,** 274–82 (2012).

96.   Wein, N. *et al.* Translation from a DMD exon 5 IRES results in a functional dystrophin isoform that attenuates dystrophinopathy in humans and mice. *Nat. Med.*
2014, 992–1000 (2014).

97.   Koo, T. & Wood, M. J. Clinical trials using antisense oligonucleotides in duchenne muscular dystrophy. *Hum. Gene Ther.* **24,** 479–88 (2013).

98.   Yokota, T. *et al.* Efficacy of systemic morpholino exon-skipping in duchenne dystrophy dogs. *Ann. Neurol.* **65,** 667–676 (2009).

99.   Le Guiner, C. *et al.* Forelimb treatment in a large cohort of dystrophic dogs supports delivery of a recombinant AAV for exon skipping in Duchenne patients. *Mol Ther* **22,** 1923–1935 (2014).

100.   Wang, B., Li, J. & Xiao, X. Adeno-associated virus vector carrying human minidystrophin genes effectively ameliorates muscular dystrophy in mdx mouse model. *Proc. Natl. Acad. Sci. U. S. A.* **97,** 13714–9 (2000).

101.   Yuasa, K. *et al.* Effective restoration of dystrophin-associated proteins in vivo by adenovirus-mediated transfer of truncated dystrophin cDNAs. *FEBS Lett.* **425,** 329– 36 (1998).

102. Kornegay, J. N. *et al.* Widespread muscle expression of an AAV9 human minidystrophin vector after intravenous injection in neonatal dystrophin-deficient dogs. *Mol. Ther.* **18,** 1501–8 (2010).

103. Wang, Z. *et al.* Sustained AAV-mediated dystrophin expression in a canine model of Duchenne muscular dystrophy with a brief course of immunosuppression. *Mol. Ther.* **15,** 1160–1166 (2007).

104. Yuasa, K. *et al.* Injection of a recombinant AAV serotype 2 into canine skeletal muscles evokes strong immune responses against transgene products. *Gene Ther.* **14,** 1249–1260 (2007).

105. Koo, T., Popplewell, L., Athanasopoulos, T. & Dickson, G. Triple trans-splicing adeno-associated virus vectors capable of transferring the coding sequence for fulllength dystrophin protein into dystrophic mice. *Hum. Gene Ther.* **25,** 98–108 (2014).

106. Hayashita-Kinoh, H. *et al.* Intra-Amniotic rAAV-Mediated Microdystrophin Gene Transfer Improves Canine X-Linked Muscular Dystrophy and May Induce Immune Tolerance. *Mol. Ther.* **23,** 627–637 (2015).

107. Peault, B. *et al.* Stem and progenitor cells in skeletal muscle development, maintenance, and therapy. *Mol Ther* **15,** 867–877 (2007).

108. Meregalli, M. *et al.* Perspectives of stem cell therapy in Duchenne muscular dystrophy. *FEBS J.* **280,** 4251–62 (2013).

109. Takahashi, K. & Yamanaka, S. Induction of Pluripotent Stem Cells from Mouse Embryonic and Adult Fibroblast Cultures by Defined Factors. *Cell* **126,** 663–676 (2006).

110. Charville, G. W. *et al.* Ex Vivo Expansion and In Vivo Self-Renewal of Human Muscle Stem Cells. *Stem cell reports* **5,** 621–32 (2015).

111. Love, D. R. *et al.* Tissue distribution of the dystrophin-related gene product and expression in the mdx and dy mouse. *Proc. Natl. Acad. Sci. U. S. A.* **88,** 3243–7 (1991).

112. Schofield, J., Houzelstein, D., Davies, K., Buckingham, M. & Edwards, Y. H. Expression of the dystrophin-related protein (utrophin) gene during mouse embryogenesis. *Dev. Dyn.* **198,** 254–64 (1993).

113. Matsumura, K., Ervasti, J. M., Ohlendieck, K., Kahl, S. D. & Campbell, K. P. Association of dystrophin-related protein with dystrophin-associated proteins in mdx mouse muscle. *Nature* **360,** 588–91 (1992).

114. Khurana, T. S. *et al.* Immunolocalization and developmental expression of dystrophin related protein in skeletal muscle. *Neuromuscul. Disord.* **1,** 185–94 (1991).

115. Pons, F., Nicholson, L. V. B., Robert, A., Voit, T. & Leger, J. J. Dystrophin and dystrophin-related protein (utrophin) distribution in normal and dystrophin-deficient skeletal muscles. *Neuromuscul. Disord.* **3,** 507–514 (1993).

116. Helliwell, T. R., Man, N. T., Morris, G. E. & Davies, K. E. The dystrophin-related protein, utrophin, is expressed on the sarcolemma of regenerating human skeletal muscle fibres in dystrophies and inflammatory myopathies. *Neuromuscul. Disord.* **2,** 177–84 (1992).

117. Winder, S. J. *et al.* Utrophin actin binding domain: analysis of actin binding and cellular targeting. *J. Cell Sci.* **108 (Pt 1,** 63–71 (1995).

118. Chung, W. & Campanelli, J. T. WW and EF hand domains of dystrophin-family proteins mediate dystroglycan binding. *Mol. Cell Biol. Res. Commun.* **2,** 162–71

119. Ervasti, J. M. & Campbell, K. P. A role for the dystrophin-glycoprotein complex as a transmembrane linker between laminin and actin. *J. Cell Biol.* **122,** 809–23 (1993).

120. Karpati, G. *et al.* Localization and quantitation of the chromosome 6-encoded dystrophin-related protein in normal and pathological human muscle. *Journal of neuropathology and experimental neurology* **52,** 119–128 (1993).

121. Mizuno, Y., Nonaka, I, Hirai, S. & Ozawa, E. Reciprocal expression of dystrophin and utrophin in muscles of Duchenne muscular dystrophy patients, female DMDcarriers and control subjects. *J. Neurol. Sci.* **119,** 43–52 (1993).

122. Law, D. J., Allen, D. L. & Tidball, J. G. Talin, vinculin and DRP (utrophin) concentrations are increased at mdx myotendinous junctions following onset of necrosis. *J. Cell Sci.* **107,** 1477–83 (1994).

123. Nghiem, P. P. *et al.* Sparing of the dystrophin-deficient cranial sartorius muscle is associated with classical and novel hypertrophy pathways in GRMD dogs. *Am. J. Pathol.* **183,** 1411–1424 (2013).

124. Wilson, L. A., Cooper, B. J., Dux, L., Dubowitz, V. & Sewry, C. A. Expression of utrophin (dystrophin-related protein) during regeneration and maturation of skeletal muscle in canine X-linked muscular dystrophy. *Neuropathol. Appl. Neurobiol.* **20,** 359–67 (1994).

125. Schatzberg, S. J. *et al.* Molecular analysis of a spontaneous dystrophin 'knockout' dog. *Neuromuscul Disord* **9,** 289–295 (1999).

126. Weir, A. P., Burton, E. A., Harrod, G. & Davies, K. E. A- and B-utrophin have different expression patterns and are differentially up-regulated in mdx muscle. *J. Biol. Chem.* **277,** 45285–45290 (2002).

127. Deconinck, a E. *et al.* Utrophin-dystrophin-deficient mice as a model for Duchenne muscular dystrophy. *Cell* **90,** 717–727 (1997).

128. Tinsley, J. M. *et al.* Amelioration of the dystrophic phenotype of mdx mice using a truncated utrophin transgene. *Nature* **384,** 349–53 (1996).

129. Prochniewicz, E., Henderson, D., Ervasti, J. M. & Thomas, D. D. Dystrophin and utrophin have distinct effects on the structural dynamics of actin. *Proc. Natl. Acad. Sci. U. S. A.* **106,** 7822–7 (2009).

130. Rybakova, I. N., Humston, J. L., Sonnemann, K. J. & Ervasti, J. M. Dystrophin and utrophin bind actin through distinct modes of contact. *J. Biol. Chem.* **281,** 9996– 10001 (2006).

131. Li, D. *et al.* Sarcolemmal nNOS anchoring reveals a qualitative difference between dystrophin and utrophin. *J. Cell Sci.* **123,** 2008–2013 (2010).

132. Marshall, J. L. *et al.* Sarcospan-dependent Akt activation is required for utrophin expression and muscle regeneration. *J. Cell Biol.* **197,** 1009–1027 (2012).

133. Durko, M., Allen, C., Nalbantoglu, J. & Karpati, G. CT-GalNAc transferase overexpression in adult mice is associated with extrasynaptic utrophin in skeletal muscle fibres. *J. Muscle Res. Cell Motil.* **31,** 181–93 (2010).

134. Nguyen, H. H., Jayasinha, V., Xia, B., Hoyte, K. & Martin, P. T. Overexpression of the cytotoxic T cell GalNAc transferase in skeletal muscle inhibits muscular dystrophy in mdx mice. *Proc. Natl. Acad. Sci. U. S. A.* **99,** 5616–21 (2002).

135. Xia, B. *et al.* Overexpression of the CT GalNAc transferase in skeletal muscle alters myofiber growth, neuromuscular structure, and laminin expression. *Dev. Biol.* **242,** 58–73 (2002).

136. Fairclough, R. J., Bareja, A. & Davies, K. E. Progress in therapy for Duchenne muscular dystrophy. *Exp. Physiol.* **96,** 1101–13 (2011).

137. Miura, P. & Jasmin, B. J. Utrophin upregulation for treating Duchenne or Becker muscular dystrophy: how close are we? *Trends Mol. Med.* **12,** 122–9 (2006).

138. Tinsley, J. M. *et al.* Daily treatment with SMTC1100, a novel small molecule utrophin upregulator, dramatically reduces the dystrophic symptoms in the mdx mouse. *PLoS One* **6,** e19189 (2011).

139. Moorwood, C., Soni, N., Patel, G., Wilton, S. D. & Khurana, T. S. A Cell-Based High-Throughput Screening Assay for Posttranscriptional Utrophin Upregulation. *J. Biomol. Screen.* **18,** 400–406 (2012).

140. Amenta, A. R. *et al.* Biglycan recruits utrophin to the sarcolemma and counters dystrophic pathology in mdx mice. *Proc. Natl. Acad. Sci. U. S. A.* **108,** 762–7 (2011).

141. Van Ry, P. M., Wuebbles, R. D., Key, M. & Burkin, D. J. Galectin-1 Protein Therapy Prevents Pathology and Improves Muscle Function in the mdx Mouse Model of Duchenne Muscular Dystrophy. *Mol. Ther.* **23,** 1285–97 (2015).

142. Cooper, D. N. & Barondes, S. H. Evidence for export of a muscle lectin from cytosol to extracellular matrix and for a novel secretory mechanism. *J. Cell Biol.* **110,** 1681– 91 (1990).

143. Van den Brûle, F. a *et al.* Differential expression of galectin-1 and galectin-3 during first trimester human embryogenesis. *Dev. Dyn.* **209,** 399–405 (1997).

144. van den Brûle, F. *et al.* Galectin-1 accumulation in the ovary carcinoma peritumoral stroma is induced by ovary carcinoma cells and affects both cancer cell proliferation and adhesion to laminin-1 and fibronectin. *Lab. Invest.* **83,** 377–386 (2003).

145. Clausse, N., van den Brûle, F., Waltregny, D., Garnier, F. & Castronovo, V. Galectin-1 expression in prostate tumor-associated capillary endothelial cells is increased by prostate carcinoma cells and modulates heterotypic cell-cell adhesion. *Angiogenesis* **3,** 317–25 (1999).

146. Camby, I. *et al.* Galectin-1 modulates human glioblastoma cell migration into the brain through modifications to the actin cytoskeleton and levels of expression of small GTPases. *J. Neuropathol. Exp. Neurol.* **61,** 585–596 (2002).

147. von Wolff, M., Wang, X., Gabius, H. J. & Strowitzki, T. Galectin fingerprinting in human endometrium and decidua during the menstrual cycle and in early gestation. *Mol. Hum. Reprod.* **11,** 189–194 (2005).

148. Odom, G. L., Gregorevic, P., Allen, J. M., Finn, E. & Chamberlain, J. S. Microutrophin delivery through rAAV6 increases lifespan and improves muscle function in dystrophic dystrophin/utrophin-deficient mice. *Mol. Ther.* **16,** 1539–45 (2008).

149. Cerletti, M. *et al.* Dystrophic phenotype of canine X-linked muscular dystrophy is mitigated by adenovirus-mediated utrophin gene transfer. *Gene Ther.* **10,** 750–7 (2003).

150. Sonnemann, K. J. *et al.* Functional substitution by TAT-utrophin in dystrophindeficient mice. *PLoS Med.* **6,** e1000083 (2009).

151. Chancellor, D. R. *et al.* Discovery of 2-arylbenzoxazoles as upregulators of utrophin production for the treatment of duchenne muscular dystrophy. *J. Med. Chem.* **54,** 3241–3250 (2011).

152. Guiraud, S. *et al.* Second-generation compound for the modulation of utrophin in the therapy of DMD. *Hum. Mol. Genet.* **24,** 4212–24 (2015).

153. Casar, J. C., McKechnie, B. a., Fallon, J. R., Young, M. F. & Brandan, E. Transient up-regulation of biglycan during skeletal muscle regeneration: Delayed fiber growth along with decorin increase in biglycan-deficient mice. *Dev. Biol.* **268,** 358–371 (2004).

154. Lechner, B. E., Lim, J. H., Mercado, M. L. & Fallon, J. R. Developmental regulation of biglycan expression in muscle and tendon. *Muscle Nerve* **34,** 347–55 (2006).

155. Amenta, A. R. *et al.* Biglycan recruits utrophin to the sarcolemma and counters dystrophic pathology in mdx mice. *Proc. Natl. Acad. Sci. U. S. A.* **108,** 762–767 (2011).

156. Hynes, R. O. Integrins: Bidirectional, allosteric signaling machines. *Cell* **110,** 673– 687 (2002).

157. Hynes, R. O. Integrins: versatility, modulation, and signaling in cell adhesion. *Cell* **69,** 11–25 (1992).

158. Giancotti, F. G. Integrin Signaling. *Science (80-.).* **285,** 1028–1033 (1999).

159. Ginsberg, M. H., Partridge, A. & Shattil, S. J. Integrin regulation. *Curr. Opin. Cell Biol.* **17,** 509–16 (2005).

160. Bezman, N. & Koretzky, G. a. Compartmentalization of ITAM and integrin signaling by adapter molecules. *Immunol. Rev.* **218,** 9–28 (2007).

161. de Melker, a a & Sonnenberg, a. Integrins: alternative splicing as a mechanism to regulate ligand binding and integrin signaling events. *Bioessays* **21,** 499–509 (1999).

162. Burkin, D. J. & Kaufman, S. J. The alpha7beta1 integrin in muscle development and disease. *Cell Tissue Res.* **296,** 183–90 (1999).

163. Song, W. K., Wang, W., Foster, R. F., Bielser, D. A. & Kaufman, S. J. H36-alpha 7 is a novel integrin alpha chain that is developmentally regulated during skeletal myogenesis. *J. Cell Biol.* **117,** 643–57 (1992).

164. von der Mark, H. *et al.* Alternative Splice Variants of 7 1Integrin Selectively Recognize Different Laminin Isoforms. *J. Biol. Chem.* **277,** 6012–6016 (2001).

165. Burkin, D. J. & Kaufman, S. J. β 1 integrin in muscle development and disease The α 7β. 183–190 (1999).

166. Bao, Z. Z., Lakonishok, M., Kaufman, S. & Horwitz, a F. Alpha 7 beta 1 integrin is a component of the myotendinous junction on skeletal muscle. *J. Cell Sci.* **106 (Pt 2,** 579–89 (1993).

167. Martin, P. T., Kaufman, S. J., Kramer, R. H. & Sanes, J. R. Synaptic integrins in developing, adult, and mutant muscle: selective association of alpha1, alpha7A, and alpha7B integrins with the neuromuscular junction. *Dev. Biol.* **174,** 125–39 (1996).

168. Velling, T. *et al.* Distinct alpha 7A beta 1 and alpha 7B beta 1 integrin expression patterns during mouse development: alpha 7A is restricted to skeletal muscle but alpha 7B is expressed in striated muscle, vasculature, and nervous system. *Dev. Dyn.* **207,** 355–71 (1996).

169. Legate, K. R., Montañez, E., Kudlacek, O. & Fässler, R. ILK, PINCH and parvin: the tIPP of integrin signalling. *Nat. Rev. Mol. Cell Biol.* **7,** 20–31 (2006).

170. Hannigan, G., Troussard, A. a & Dedhar, S. Integrin-linked kinase: a cancer therapeutic target unique among its ILK. *Nat. Rev. Cancer* **5,** 51–63 (2005).

171. Wu, C. PINCH, N(i)ck and the ILK: Network wiring at cell-matrix adhesions. *Trends Cell Biol.* **15,** 460–466 (2005).

172. McDonald, P. C., Fielding, A. B. & Dedhar, S. Integrin-linked kinase--essential roles in physiology and cancer biology. *J. Cell Sci.* **121,** 3121–3132 (2008).

173. Gheyara, A. L. *et al.* Deletion of integrin-linked kinase from skeletal muscles of mice resembles muscular dystrophy due to alpha 7 beta 1-integrin deficiency. *Am. J. Pathol.* **171,** 1966–77 (2007).

174. Vachon, P. H. Integrin signaling, cell survival, and anoikis: distinctions, differences, and differentiation. *J. Signal Transduct.* **2011,** 738137 (2011).

175. Boppart, M. D., Burkin, D. J. & Kaufman, S. J. Activation of AKT signaling promotes cell growth and survival in α7β1 integrin-mediated alleviation of muscular dystrophy. *Biochim. Biophys. Acta* **1812,** 439–46 (2011).

176. Ziober, B. L. *et al.* Alternative extracellular and cytoplasmic domains of the integrin α7 subunit are differentially expressed during development. *J. Biol. Chem.* **268,** 26773–26783 (1993).

177. Song, W. K., Wang, W., Sato, H., Bielser, D. A. & Kaufman, S. J. Expression of alpha 7 integrin cytoplasmic domains during skeletal muscle development: alternate forms, conformational change, and homologies with serine/threonine kinases and tyrosine phosphatases. *J. Cell Sci.* **106 (Pt 4,** 1139–52 (1993).

178. Collo, G., Starr, L. & Quaranta, V. A new isoform of the laminin receptor integrin alpha 7 beta 1 is developmentally regulated in skeletal muscle. *J. Biol. Chem.* **268,** 19019–24 (1993).

179. Velling, T. *et al.* Distinct Alpha(7a)Beta(1) and Alpha(7b)Beta(1) Integrin Expression Patterns During Mouse Development - Alpha(7a) Is Restricted to Skeletal Muscle But Alpha(7b) Is Expressed In Striated Muscle, Vasculature, and Nervous System. *Dev. Dyn.* **207,** 355–371 (1996).

180. Ziober, B. L., Chen, Y. & Kramer, R. H. The laminin-binding activity of the alpha 7 integrin receptor is defined by developmentally regulated splicing in the extracellular domain. *Mol. Biol. Cell* **8,** 1723–34 (1997).

181. van der Flier, A., Kuikman, I., Baudoin, C., van der Neut, R. & Sonnenberg, A. A novel beta 1 integrin isoform produced by alternative splicing: unique expression in cardiac and skeletal muscle. *FEBS Lett* **369,** 340–344 (1995).

182. Kaariainen, M. *et al.* Expression of alpha7beta1 integrin splicing variants during skeletal muscle regeneration. *Am J Pathol* **161,** 1023–1031 (2002).

183. Schöber, S. *et al.* The role of extracellular and cytoplasmic splice domains of alpha7integrin in cell adhesion and migration on laminins. *Exp. Cell Res.* **255,** 303–13 (2000).

184. Armulik, A. Splice variants of human beta 1 integrins: origin, biosynthesis and functions. *Front Biosci* **7,** d219–27 (2002).

185. Brakebusch, C., Hirsch, E., Potocnik, a & Fässler, R. Genetic analysis of beta1 integrin function: confirmed, new and revised roles for a crucial family of cell adhesion molecules. *J. Cell Sci.* **110 (Pt 2,** 2895–2904 (1997).

186. Belkin, a M. *et al.* Muscle beta1D integrin reinforces the cytoskeleton-matrix link: modulation of integrin adhesive function by alternative splicing. *J. Cell Biol.* **139,** 1583–95 (1997).

187. Belkin, A. M. *et al.* β1D integrin displaces the β1A isoform in striated muscles: Localization at junctional structures and signaling potential in nonmuscle cells. *J. Cell Biol.* **132,** 211–226 (1996).

188. Baudoin, C., Goumans, M. J., Mummery, C. & Sonnenberg, a. Knockout and knockin of the beta1 exon D define distinct roles for integrin splice variants in heart function and embryonic development. *Genes Dev.* **12,** 1202–1216 (1998).

189. Stephens, L. E. *et al.* Deletion of ??1 integrins in mice results in inner cell mass failure and peri-implantation lethality. *Genes Dev.* **9,** 1883–1895 (1995).

190. Heino, J., Ignotz, R. a, Hemler, M. E., Crouse, C. & Massagué, J. Regulation of cell adhesion receptors by transforming growth factor-beta. Concomitant regulation of integrins that share a common beta 1 subunit. *J. Biol. Chem.* **264,** 380–388 (1989).

191. Ignotz, R. A., Heino, J. & Massagué, J. Regulation of cell adhesion receptors by transforming growth factor-beta. Regulation of vitronectin receptor and LFA-1. *J. Biol. Chem.* **264,** 389–92 (1989).

192. Lenter, M. & Vestweber, D. The Integrin Chains beta(1) and alpha(6) Associate with the Chaperone Calnexin Prior to Integrin Assembly. *J Biol Chem* **269,** 12263–12268 (1994).

193. Salicioni, A. M., Gaultier, A., Brownlee, C., Cheezum, M. K. & Gonias, S. L. Low density lipoprotein receptor-related protein-1 promotes beta1 integrin maturation and transport to the cell surface. *J. Biol. Chem.* **279,** 10005–10012 (2004).

194. Hodges, B. L. *et al.* Altered expression of the alpha7beta1 integrin in human and murine muscular dystrophies. *J. Cell Sci.* **110 (Pt 2,** 2873–81 (1997).

195. Burkin, D. J., Wallace, G. Q., Nicol, K. J., Kaufman, D. J. & Kaufman, S. J. Enhanced expression of the alpha 7 beta 1 integrin reduces muscular dystrophy and restores viability in dystrophic mice. *J. Cell Biol.* **152,** 1207–18 (2001).

196. Burkin, D. J. *et al.* Transgenic expression of {alpha}7{beta}1 integrin maintains muscle integrity, increases regenerative capacity, promotes hypertrophy, and reduces cardiomyopathy in dystrophic mice. *Am. J. Pathol.* **166,** 253–63 (2005).

197. Boppart, M. D., Burkin, D. J. & Kaufman, S. J. Alpha7beta1-integrin regulates mechanotransduction and prevents skeletal muscle injury. *Am. J. Physiol. Cell Physiol.* **290,** C1660–5 (2006).

198. Rooney, J. E. *et al.* Severe muscular dystrophy in mice that lack dystrophin and alpha7 integrin. *J. Cell Sci.* **119,** 2185–95 (2006).

199. Heller, K. N. *et al.* AAV-mediated overexpression of human α7 integrin leads to histological and functional improvement in dystrophic mice. *Mol. Ther.* **21,** 520–5 (2013).

200. Heller, K. N. *et al.* Human α7 Integrin Gene (ITGA7) Delivered by AdenoAssociated Virus Extends Survival of Severely Affected Dystrophin/UtrophinDeficient Mice. *Hum. Gene Ther.* (2015). doi:10.1089/hum.2015.062

201. Wuebbles, R. D., Sarathy, A., Kornegay, J. N. & Burkin, D. J. Levels of α7 integrin and laminin-α2 are increased following prednisone treatment in the mdx mouse and GRMD dog models of Duchenne muscular dystrophy. *Dis. Model. Mech.* **6,** 1175– 84 (2013).

202. Liu, J., Milner, D. J., Boppart, M. D., Ross, R. S. & Kaufman, S. J. β1D chain increases α7β1 integrin and laminin and protects against sarcolemmal damage in mdx mice. *Hum. Mol. Genet.* **21,** 1592–603 (2012).

203. Falk, M., Ferletta, M., Forsberg, E. & Ekblom, P. Restricted distribution of laminin alpha1 chain in normal adult mouse tissues. *Matrix Biol.* **18,** 557–68 (1999).

204. Flintoff-Dye, N. L. *et al.* Role for the alpha7beta1 integrin in vascular development and integrity. *Dev. Dyn.* **234,** 11–21 (2005).

205. Gurpur, P. B., Liu, J., Burkin, D. J. & Kaufman, S. J. Valproic acid activates the PI3K/Akt/mTOR pathway in muscle and ameliorates pathology in a mouse model of Duchenne muscular dystrophy. *Am. J. Pathol.* **174,** 999–1008 (2009).

206. Li, X., Huang, P., Cui, J. J., Zhang, J. & Tang, C. Novel pyrrolyllactone and pyrrolyllactam indolinones as potent cyclin-dependent kinase 2 inhibitors. *Bioorg. Med. Chem. Lett.* **13,** 1939–42 (2003).

207. Lane, M. E. *et al.* A Novel cdk2-selective Inhibitor , SU9516 , Induces Apoptosis in Colon Carcinoma Cells A Novel cdk2-selective Inhibitor , SU9516 , Induces Apoptosis in Colon. 6170–6177 (2001).

208. Gao, N., Kramer, L., Rahmani, M., Dent, P. & Grant, S. The Three-Substituted Indolinone Cyclin-Dependent Kinase 2 1 , 3-dihydro-indol-2-one (SU9516) Kills Human Leukemia Cells via Down-Regulation of Mcl-1 through a Transcriptional Mechanism. **70,** 645–655 (2006).

209. Takagi, K., Sowa, Y., Cevik, O. M., Nakanishi, R. & Sakai, T. CDK inhibitor enhances the sensitivity to 5-fluorouracil in colorectal cancer cells. *Int. J. Oncol.* **32,** 1105–10 (2008).

210. Angelini, C. *et al.* Deflazacort in Duchenne dystrophy: study of long-term effect. *Muscle Nerve* **17,** 386–91 (1994).

211. Beenakker, E. A. C. *et al.* Intermittent prednisone therapy in Duchenne muscular dystrophy: a randomized controlled trial. *Arch. Neurol.* **62,** 128–32 (2005).

212. Fenichel, G. M. *et al.* A comparison of daily and alternate-day prednisone therapy in the treatment of Duchenne muscular dystrophy. *Arch. Neurol.* **48,** 575–9 (1991).

213. Merlini, L. *et al.* Early prednisone treatment in Duchenne muscular dystrophy. *Muscle Nerve* **27,** 222–7 (2003).

214. Reitter, B. Deflazacort vs. prednisone in Duchenne muscular dystrophy: trends of an ongoing study. *Brain Dev.* **17 Suppl,** 39–43 (1995).

215. Holmberg, J. & Durbeej, M. Laminin-211 in skeletal muscle function. *Cell Adh. Migr.* **7,** 111–21 (2013).

216. Lisi, M. T. & Cohn, R. D. Congenital muscular dystrophies: New aspects of an expanding group of disorders. *Biochim. Biophys. Acta - Mol. Basis Dis.* **1772,** 159– 172 (2007).

217. Monaco, A. P. *et al.* Isolation of candidate cDNAs for portions of the Duchenne muscular dystrophy gene. *Nature* **323,** 646–50 (1986).

218. Hoffman, E. P., Brown, R. H. & Kunkel, L. M. Dystrophin: the protein product of the Duchenne muscular dystrophy locus. *Cell* **51,** 919–928 (1987).

219. Fenichel, G. M. *et al.* Long-term benefit from prednisone therapy in Duchenne muscular dystrophy. *Neurology* **41,** 1874–7 (1991).

220. Beenakker, E. A. *et al.* Intermittent prednisone therapy in Duchenne muscular dystrophy: a randomized controlled trial. *Arch Neurol* **62,** 128–132 (2005).

221. Sali, A. *et al.* Glucocorticoid-treated mice are an inappropriate positive control for long-term preclinical studies in the mdx mouse. *PLoS One* **7,** 1–9 (2012).

222. Kwon, M. S. *et al.* Calreticulin couples calcium release and calcium influx in integrin-mediated calcium signaling. *Mol. Biol. Cell* **11,** 1433–43 (2000).

223. von der Mark, H. *et al.* Alternative splice variants of alpha 7 beta 1 integrin selectively recognize different laminin isoforms. *J. Biol. Chem.* **277,** 6012–6 (2002).

224. Mayer, U. *et al.* Absence of integrin alpha 7 causes a novel form of muscular dystrophy. *Nat. Genet.* **17,** 318–323 (1997).

225. Hayashi, Y. K. *et al.* Mutations in the integrin alpha7 gene cause congenital myopathy. *Nat. Genet.* **19,** 94–7 (1998).

226. Guo, C. *et al.* Absence of alpha 7 integrin in dystrophin-deficient mice causes a myopathy similar to Duchenne muscular dystrophy. *Hum. Mol. Genet.* **15,** 989–98 (2006).

227. Doe, J. a *et al.* Transgenic overexpression of the α7 integrin reduces muscle pathology and improves viability in the dy(W) mouse model of merosin-deficient congenital muscular dystrophy type 1A. *J. Cell Sci.* **124,** 2287–97 (2011).

228. Masuda, S., Hayashi, T., Hashimoto, T. & Taguchi, S. Correlation of dystrophinglycoprotein complex and focal adhesion complex with myosin heavy chain isoforms in rat skeletal muscle. *Acta Physiol. (Oxf).* **195,** 483–94 (2009).

229. Anderson, J. E., Weber, M. & Vargas, C. Deflazacort increases laminin expression and myogenic repair, and induces early persistent functional gain in mdx mouse muscular dystrophy. *Cell Transpl.* **9,** 551–64. (2000).

230. Liu, J., Burkin, D. J. & Kaufman, S. J. Increasing alpha 7 beta 1-integrin promotes muscle cell proliferation, adhesion, and resistance to apoptosis without changing gene expression. *Am. J. Physiol. Cell Physiol.* **294,** C627–40 (2008).

231. Monaco, A. P. *et al.* Isolation of candidate cDNAs for portions of the Duchenne muscular dystrophy gene. *Nature* **323,** 646–50

232. Dickson, G., Roberts, M. L., Wells, D. J. & Fabb, S. A. Recombinant micro-genes and dystrophin viral vectors. *Neuromuscul. Disord.* **12 Suppl 1,** S40–4 (2002).

233. Klietsch, R., Ervasti, J. M., Arnold, W., Campbell, K. P. & Jorgensen, A. O. Dystrophin-glycoprotein complex and laminin colocalize to the sarcolemma and transverse tubules of cardiac muscle. *Circ. Res.* **72,** 349–60 (1993).

234. Petrof, B. J., Shrager, J. B., Stedman, H. H., Kelly, a M. & Sweeney, H. L. Dystrophin protects the sarcolemma from stresses developed during muscle contraction. *Proc. Natl. Acad. Sci. U. S. A.* **90,** 3710–4 (1993).

235. Phelps, S. F. *et al.* Expression of full-length and truncated dystrophin mini-genes in transgenic mdx mice. *Hum. Mol. Genet.* **4,** 1251–8 (1995).

236. Decrouy, A. *et al.* Mini-dystrophin gene transfer in mdx4cv diaphragm muscle fibers increases sarcolemmal stability. *Gene Ther.* **4,** 401–8 (1997).

237. Bertoni, C. & Rando, T. A. Dystrophin gene repair in mdx muscle precursor cells in vitro and in vivo mediated by RNA-DNA chimeric oligonucleotides. *Hum. Gene Ther.* **13,** 707–18 (2002).

238. Bachrach, E. *et al.* Systemic delivery of human microdystrophin to regenerating mouse dystrophic muscle by muscle progenitor cells. *Proc. Natl. Acad. Sci. U. S. A.* **101,** 3581–6 (2004).

239. Liu, M. *et al.* Adeno-associated virus-mediated microdystrophin expression protects young mdx muscle from contraction-induced injury. *Mol. Ther.* **11,** 245–56 (2005).

240. Béroud, C. *et al.* Multiexon skipping leading to an artificial DMD protein lacking amino acids from exons 45 through 55 could rescue up to 63% of patients with Duchenne muscular dystrophy. *Hum. Mutat.* **28,** 196–202 (2007).

241. Fletcher, S. *et al.* Morpholino oligomer-mediated exon skipping averts the onset of dystrophic pathology in the mdx mouse. *Mol. Ther.* **15,** 1587–92 (2007).

242. Yin, H., Lu, Q. & Wood, M. Effective exon skipping and restoration of dystrophin expression by peptide nucleic acid antisense oligonucleotides in mdx mice. *Mol. Ther.* **16,** 38–45 (2008).

243. Lu, Q.-L. *et al.* The status of exon skipping as a therapeutic approach to duchenne muscular dystrophy. *Mol. Ther.* **19,** 9–15 (2011).

244. Swiderski, K. *et al.* Tranilast administration reduces fibrosis and improves fatigue resistance in muscles of mdx dystrophic mice. *Fibrogenesis Tissue Repair* **7,** 1 (2014).

245. Huang, P., Zhao, X. S., Fields, M., Ransohoff, R. M. & Zhou, L. Imatinib attenuates skeletal muscle dystrophy in mdx mice. *FASEB J.* **23,** 2539–48 (2009).

246. Percival, J. M. *et al.* Sildenafil reduces respiratory muscle weakness and fibrosis in the mdx mouse model of Duchenne muscular dystrophy. *J. Pathol.* **228,** 77–87 (2012).

247. Heier, C. R. *et al.* VBP15, a novel anti-inflammatory and membrane-stabilizer, improves muscular dystrophy without side effects. *EMBO Mol. Med.* **5,** 1569–85 (2013).

248. Anderson, J. E., McIntosh, L. M. & Poettcker, R. Deflazacort but not prednisone improves both muscle repair and fiber growth in diaphragm and limb muscle in vivo in the mdx dystrophic mouse. *Muscle Nerve* **19,** 1576–85 (1996).

249. Hartel, J. V, Granchelli, J. A., Hudecki, M. S., Pollina, C. M. & Gosselin, L. E. Impact of prednisone on TGF-beta1 and collagen in diaphragm muscle from mdx mice. *Muscle Nerve* **24,** 428–32 (2001).

250. Siegel, A. L. *et al.* Treatment with inhibitors of the NF-kappaB pathway improves whole body tension development in the mdx mouse. *Neuromuscul. Disord.* **19,** 131– 9 (2009).

251. Crosbie, R. H. *et al.* mdx muscle pathology is independent of nNOS perturbation. *Hum. Mol. Genet.* **7,** 823–9 (1998).

252. Wehling, M., Spencer, M. J. & Tidball, J. G. A nitric oxide synthase transgene ameliorates muscular dystrophy in mdx mice. *J. Cell Biol.* **155,** 123–31 (2001).

253. Tidball, J. G. & Wehling-Henricks, M. Expression of a NOS transgene in dystrophin-deficient muscle reduces muscle membrane damage without increasing the expression of membrane-associated cytoskeletal proteins. *Mol. Genet. Metab.* **82,** 312–20 (2004).

254. Cordier, L. *et al.* Rescue of skeletal muscles of gamma-sarcoglycan-deficient mice with adeno-associated virus-mediated gene transfer. *Mol. Ther.* **1,** 119–29 (2000).

255. Welser, J. V *et al.* Myotendinous junction defects and reduced force transmission in mice that lack alpha7 integrin and utrophin. *Am. J. Pathol.* **175,** 1545–54 (2009).

256. Blake, D. J., Weir, A., Newey, S. E. & Davies, K. E. Function and genetics of dystrophin and dystrophin-related proteins in muscle. *Physiol. Rev.* **82,** 291–329 (2002).

257. Lynch, G. S. *et al.* Contractile properties of diaphragm muscle segments from old mdx and old transgenic mdx mice. *Am. J. Physiol.* **272,** C2063–C2068 (1997).

258. López, J. R., Briceño, L. E., Sánchez, V. & Horvart, D. Myoplasmic (Ca2+) in Duchenne muscular dystrophy patients. *Acta científica Venez.* **38,** 503–4 (1987).

259. Carlson, C. G., Samadi, A. & Siegel, A. Chronic treatment with agents that stabilize cytosolic IκB-α enhances survival and improves resting membrane potential in MDX muscle fibers subjected to chronic passive stretch. *Neurobiol. Dis.* **20,** 719– 730 (2005).

260. Carlson, C. G. & Roshek, D. M. Adult dystrophic (mdx) endplates exhibit reduced quantal size and enhanced quantal variation. *Pflugers Arch.* **442,** 369–75 (2001).

261. Lyons, P. R. & Slater, C. R. Structure and function of the neuromuscular junction in young adult mdx mice. *J. Neurocytol.* **20,** 969–981 (1991).

262. Moshinsky, D. J. *et al.* SU9516: biochemical analysis of cdk inhibition and crystal structure in complex with cdk2. *Biochem. Biophys. Res. Commun.* **310,** 1026–1031 (2003).

263. Nagel, A., Lehmann-Horn, F. & Engel, A. G. Neuromuscular transmission in the mdx mouse. *Muscle Nerve* **13,** 742–9 (1990).

264. Canato, M. *et al.* Mechanical and electrophysiological properties of the sarcolemma of muscle fibers in two murine models of muscle dystrophy: col6a1-/- and mdx. *J. Biomed. Biotechnol.* **2010,** 981945 (2010).

265. Miles, M. T., Cottey, E., Cottey, A., Stefanski, C. & Carlson, C. G. Reduced resting potentials in dystrophic (mdx) muscle fibers are secondary to NF-κB-dependent negative modulation of ouabain sensitive Na+-K+ pump activity. *J. Neurol. Sci.* **303,** 53–60 (2011).

266. Yeung, E. W. *et al.* Effects of stretch-activated channel blockers on [Ca2+]i and muscle damage in the mdx mouse. *J. Physiol.* **562,** 367–80 (2005).

267. Whitehead, N. P., Yeung, E. W. & Allen, D. G. Muscle damage in mdx (dystrophic) mice: role of calcium and reactive oxygen species. *Clin. Exp. Pharmacol. Physiol.* **33,** 657–62 (2006).

268. Allen, D. G., Gervasio, O. L., Yeung, E. W. & Whitehead, N. P. Calcium and the damage pathways in muscular dystrophy. *Can. J. Physiol. Pharmacol.* **88,** 83–91 (2010).

269. Turner, P. R., Westwood, T., Regen, C. M. & Steinhardt, R. A. Increased protein degradation results from elevated free calcium levels found in muscle from mdx mice. *Nature* **335,** 735–8 (1988).

270. Bakker, A. J., Head, S. I., Williams, D. A. & Stephenson, D. G. Ca2+ levels in myotubes grown from the skeletal muscle of dystrophic (mdx) and normal mice. *J. Physiol.* **460,** 1–13 (1993).

271. Burkin, D. J. & Wuebbles, R. D. A Molecular Bandage for Diseased Muscle. *Sci. Transl. Med.* **4,** 139fs19–139fs19 (2012).

272. Engvall, E. & Wewer, U. M. The new frontier in muscular dystrophy research:

booster genes. *FASEB J.* **17,** 1579–1584 (2003).

273. Tinsley, J. *et al.* Expression of full-length utrophin prevents muscular dystrophy in mdx mice. *Nat. Med.* **4,** 1441–1444 (1998).

274. Moghadaszadeh, B. *et al.* Compensation for dystrophin-deficiency: ADAM12 overexpression in skeletal muscle results in increased α7 integrin, utrophin and associated glycoproteins. *Hum. Mol. Genet.* **12,** 2467–2479 (2003).

275. Jones, K. *et al.* GSK3β mediates muscle pathology in myotonic dystrophy. **122,** 4461–4472 (2012).

276. Patricelli, M. P. *et al.* Functional interrogation of the kinome using nucleotide acyl phosphates. *Biochemistry* **46,** 350–358 (2007).

277. Wang, M. *et al.* Identification of Map4k4 as a novel suppressor of skeletal muscle differentiation. *Mol. Cell. Biol.* **33,** 678–87 (2013).

278. Anastassiadis, T., Deacon, S. W., Devarajan, K., Ma, H. & Peterson, J. R. Comprehensive assay of kinase catalytic activity reveals features of kinase inhibitor selectivity. *Nat. Biotechnol.* **29,** 1039–45 (2011).

279. He, B. *et al.* Tetraspanin CD82 attenuates cellular morphogenesis through downregulating integrin ??6-mediated cell adhesion. *J. Biol. Chem.* **280,** 3346–3354 (2005).

280. Han, S. Y. *et al.* Tsp66E, the Drosophila KAI1 homologue, and Tsp74F function to regulate ovarian follicle cell and wing development by stabilizing integrin localization. *FEBS Lett.* **586,** 4031–4037 (2012).

281. Alessi, D. R. *et al.* The WNK-SPAK/OSR1 pathway: Master regulator of cationchloride cotransporters. *Sci. Signal.* **7,** re3–re3 (2014).

282. Acharyya, S. *et al.* Interplay of IKK/NF-kappaB signaling in macrophages and myofibers promotes muscle degeneration in Duchenne muscular dystrophy. *J. Clin. Invest.* **117,** 889–901 (2007).

283. Yáñez-Mó, M., Barreiro, O., Gordon-Alonso, M., Sala-Valdés, M. & SánchezMadrid, F. Tetraspanin-enriched microdomains: a functional unit in cell plasma membranes. *Trends in Cell Biology* **19,** 434–446 (2009).

284. Richardson, M. M., Jennings, L. K. & Zhang, X. a. Tetraspanins and tumor progression. *Clin. Exp. Metastasis* **28,** 261–270 (2011).

285. Wei, Q. *et al.* CD82 Restrains Angiogenesis by Altering Lipid Raft Clustering and CD44 Trafficking in Endothelial Cells. *Circulation* 1493–1504 (2014). doi:10.1161/CIRCULATIONAHA.114.011096

286. Chen, Y.-W. *et al.* Early onset of inflammation and later involvement of TGFbeta in Duchenne muscular dystrophy. *Neurology* **65,** 826–34 (2005).

287. Porter, J. D. *et al.* A chronic inflammatory response dominates the skeletal muscle molecular signature in dystrophin-deficient mdx mice. *Hum. Mol. Genet.* **11,** 263–72 (2002).

288. Cai, D. *et al.* IKKbeta/NF-kappaB activation causes severe muscle wasting in mice. *Cell* **119,** 285–98 (2004).

289. Kumamoto, T. *et al.* Proteasome expression in the skeletal muscles of patients with muscular dystrophy. *Acta Neuropathol.* **100,** 595–602 (2000).

290. Hasselgren, P.-O. Ubiquitination, phosphorylation, and acetylation--triple threat in muscle wasting. *J. Cell. Physiol.* **213,** 679–89 (2007).

291. Baldwin, A. S. Series introduction: the transcription factor NF-kappaB and human disease. *J. Clin. Invest.* **107,** 3–6 (2001).

292. Hacker, H. & Karin, M. Regulation and Function of IKK and IKK-Related Kinases. *Sci. STKE* **2006,** re13–re13 (2006).

293. Verma, I. M., Stevenson, J. K., Schwarz, E. M., Van Antwerp, D. & Miyamoto, S. Rel/NF-kappa B/I kappa B family: intimate tales of association and dissociation. *Genes Dev.* **9,** 2723–35 (1995).

294. Bakkar, N. *et al.* IKK/NF-kappaB regulates skeletal myogenesis via a signaling switch to inhibit differentiation and promote mitochondrial biogenesis. *J. Cell Biol.* **180,** 787–802 (2008).

295. Yang, Q. *et al.* AAV-based shRNA silencing of NF-κB ameliorates muscle pathologies in mdx mice. *Gene Ther.* **19,** 1196–204 (2012).

296. Grounds, M. D. & Torrisi, J. Anti-TNFalpha (Remicade) therapy protects dystrophic skeletal muscle from necrosis. *FASEB J.* **18,** 676–82 (2004).

297. Whitehead, N. P., Pham, C., Gervasio, O. L. & Allen, D. G. N-Acetylcysteine ameliorates skeletal muscle pathophysiology in mdx mice. *J. Physiol.* **586,** 2003–14 (2008).

298. Messina, S. *et al.* Lipid Peroxidation Inhibition Blunts Nuclear Factor-κB Activation, Reduces Skeletal Muscle Degeneration, and Enhances Muscle Function in mdx Mice. *Am. J. Pathol.* **168,** 918–926 (2006).

299. Chung, J. Y., Park, Y. C., Ye, H. & Wu, H. All TRAFs are not created equal: common and distinct molecular mechanisms of TRAF-mediated signal transduction. *J. Cell Sci.* **115,** 679–688 (2002).

300. Zapata, J. M., Lefebvre, S. & Reed, J. C. Targeting TRAfs for therapeutic intervention. *Adv Exp Med Biol* **597,** 188–201 (2007).

301. Bradley, J. R. & Pober, J. S. Tumor necrosis factor receptor-associated factors (TRAFs). *Oncogene* **20,** 6482–6491 (2001).

302. Hindi, S. M., Sato, S., Choi, Y. & Kumar, A. Distinct roles of TRAF6 at early and late stages of muscle pathology in the mdx model of duchenne muscular dystrophy. *Hum. Mol. Genet.* **23,** 1492–1505 (2014).

303. Malumbres, M. & Barbacid, M. Cell cycle, CDKs and cancer: a changing paradigm. *Nat. Rev. Cancer* **9,** 153–166 (2009).

304. Lazzaro, M. a, Albert, P. R. & Julien, J. P. A novel cdc2-related protein kinase expressed in the nervous system. *J. Neurochem.* **69,** 348–364 (1997).

305. Vitari, A. C., Deak, M., Morrice, N. A. & Alessi, D. R. The WNK1 and WNK4 protein kinases that are mutated in Gordon's hypertension syndrome phosphorylate and activate SPAK and OSR1 protein kinases. *Biochem. J.* **391,** 17 (2005).

306. Piechotta, K., Lu, J. & Delpire, E. Cation chloride cotransporters interact with the stress-related kinases Ste20-related proline-alanine-rich kinase (SPAK) and oxidative stress response 1 (OSR1). *J. Biol. Chem.* **277,** 50812–50819 (2002).

307. Moriguchi, T. *et al.* WNK1 regulates phosphorylation of cation-chloride-coupled cotransporters via the STE20-related kinases, SPAK and OSR1. *J. Biol. Chem.* **280,** 42685–93 (2005).

308. Yan, Y. *et al.* Nuclear factor-kappaB is a critical mediator of Ste20-like proline/alanine-rich kinase regulation in intestinal inflammation. *Am. J. Pathol.* **173,** 1013– 1028 (2008).

309. Singh, R. *et al.* Increases in nuclear p65 activation in dystrophic skeletal muscle are secondary to increases in the cellular expression of p65 and are not solely produced by increases in IkappaB-alpha kinase activity. *J. Neurol. Sci.* **285,** 159– 71 (2009).

310. Weber, M.-A., Nagel, A. M., Jurkat-Rott, K. & Lehmann-Horn, F. Sodium (23Na) MRI detects elevated muscular sodium concentration in Duchenne muscular dystrophy. *Neurology* **77,** 2017–24 (2011).

311. Landfeldt, E. *et al.* The burden of Duchenne muscular dystrophy: an international, cross-sectional study. *Neurology* **83,** 529–36 (2014).

312. Monici, M. C., Aguennouz, M., Mazzeo, a, Messina, C. & Vita, G. Activation of nuclear factor-kappaB in inflammatory myopathies and Duchenne muscular dystrophy. *Neurology* **60,** 993–997 (2003).

313. Auphan, N., DiDonato, J., Rosette, C. & Helmberg, A. Immunosuppression by Glucocorticoids: Inhibition of NF-kappaB Activity Through Induction of IkappaB Sy nthesis. *Sci. (New York, NY)* (1995). doi:10.1126/science.270.5234.286

314. Delfín, D. a *et al.* Improvement of cardiac contractile function by peptide-based inhibition of NF-κB in the utrophin/dystrophin-deficient murine model of muscular dystrophy. *J. Transl. Med.* **9,** 68 (2011).

315. Peterson, J. M. *et al.* Peptide-based inhibition of NF-κB rescues diaphragm muscle contractile dysfunction in a murine model of Duchenne muscular dystrophy. *Mol. Med.* **17,** 508–15 (2011).

316. Kornegay, J. N. *et al.* NBD delivery improves the disease phenotype of the golden retriever model of Duchenne muscular dystrophy. *Skelet. Muscle* **4,** 18 (2014).

317. Altamirano, F. *et al.* Increased resting intracellular calcium modulates NF-κBdependent inducible nitric-oxide synthase gene expression in dystrophic mdx skeletal myotubes. *J. Biol. Chem.* **287,** 20876–87 (2012).

318. Wei, Q. *et al.* CD82 restrains pathological angiogenesis by altering lipid raft clustering and CD44 trafficking in endothelial cells. *Circulation* **130,** 1493–504 (2014).